UT-IG Tech. Report #40

UPPERSLOPE OILSEEP STUDY

I. GEOLOGICAL AND GEOPHYSICAL RESULTS

II. GEOCHEMICAL AND STABLE ISOTOPE RESULTS

FINAL REPORT
DECEMBER, 1983

by

E. William Behrens

PART I.

UPPER SLOPE OIL SEEP STUDY

GEOLOGICAL AND GEOPHYSICAL RESULTS

FINAL REPORT

DECEMBER 1983

TABLE OF CONTENTS

LIST OF FIGURES

* Large scale copy also provided separately

Large scale copy of Track Chart also provided separately

INTRODUCTION

Although tectonic features in the upper slope of the northwest Gulf of Mexico result essentially from only vertical forces, faulting can be highly complex. Controlling forces include the upward force of diapirism; tensional forces across the crests of diapirs; compressional forces between diapirs; downward forces between diapirs resulting from material withdrawal; and downward forces of sediment loading and differential compaction. Thus the interrelationships between faulting and sedimentation are equally complex. Finally, understanding the geological relations of faults is important, because they may act as either seals or conduits for hydrocarbon migrations.

An area where faults have apparently acted as conduits for liquid as well as gaseous hydrocarbons has been discovered in the Green Canyon sector of the north central Gulf of Mexico. Direct evidence of oil migration is the occurrence of up to 8% extractable hydrocarbons in sediments cored at this locality. This is a report on the geology of the first well-documented oil seep actually sampled in the northern Gulf of Mexico.

Location

The area studied lies between latitudes 27° 35' and 28° 00' N and longitudes 91° 05'-25' W and includes water depths from about 200 to 1,000 m. Thus it lies about 220 km (120 n.mi.) south of Morgan City, Louisiana on the upper continental slope. The area lies to the west of the Mississippi Fan in the central slope province (Holland, 1970) which is characterized by such an abundance of diapirs that sedimentary sections occur essentially as isolated or semi-isolated intraslope troughs or basins (Martin, 1973).

Of 16 piston cores taken in the area, nine contained liquid crude oil macroscopically visible either to the unaided eye or as bright flourescence under ultraviolet light. The oil-bearing cores were from a more restricted area within latitudes 27° 43'-45' N and longitudes 91° 12'-22' W and water depths of about 540 to 630 m.

METHODS

The area was initially visited while collecting multichannel seismic reflection data. Parts of two 24 fold, CDP lines pass through the area. It was subsequently crossed irregularly during several coring cruises. After the discovery of the oil seep, a rectalinear grid of 36 north-south and 26 east-west lines were surveyed. All navigation was done with Loran C. High resolution (3.5kHz) reflection profiles were collected continuously on all cruises (1,355 km within the grid; 1,620 km total). A map showing tracklines is provided separately. Appendix A gives locations of lines in the survey grid. Sixteen piston cores were collected. Lengths were from 240 to 1,015 cm for a total of 100 m of cores. Bulk density, water content, and $CaCO_3$ content were determined every 20 cm where possible. Various sediment parameters are shown on core logs in Appendix B. Organic carbon, stable carbon isotope, and hydrocarbon and gas analyses were done on a variety of samples selected on the basis of visible oil or oil flourescence. A portion of the chemical analyses has been reported by (Anderson et al, 1983). A more complete report on the geochemistry accompanies this report.

OBSERVATIONS

High Resolution (3.5 kHz) Seismic Data

The geologic features mapped (Fig. 2) as well as the bathymetry (Fig.

1) are based almost entirely on these data. Large scale copies of these maps are provided separately.

Bathymetry The shelfbreak in this area occurs at about 150 m. The mudline is on the inner shelf signifying a large sediment supply (Stanley et al. 1983; profile G, Fig 3). From the shelfbreak to about 400 m the bottom slopes more or less evenly southward with a southward bulge of contours between 91° 10'-15' W (Fig. 1). In the northwest of this area two irregular banks project from the surrounding slope with relief of up to 200 m. From 400 to between 550 and 625 m the bottom slopes somewhat more steeply than to the north and less steeply than to the south. This zone of intermediate slope is delineated on the geologic map (Fig. 2) with dashed, vertical lines. It has distinctly more small scale relief than adjacent areas, especially in the central part of the area (longitudes 91° 12'-19' W).

For the next 100 to 300 m the bottom slopes much more steeply (up to 8°), often appearing as an escarpment in the upper parts (Fig. 3). In the southwestern part of the study area this slope extends to about 800 m and then becomes an irregular platform that drops off to the southwest and south at the limit of the study area. The eastern margin of this platform is the western margin of a prominent trough (Fig. 4) which gradually decreases in slope southsoutheastward from 800 to almost 1,100 m. To the east of the trough the steep slope is longest and most regular, extending between depths of 575 and 975 m.

Shallow Stratigraphy In the northern half of the area, the 3.5 kHz records commonly reflect penetration to 100 milliseconds or more displaying 75 to over 100 m of multiple, parallel to subparallel, draping reflections. An uppermost Unit (A) is mostly transparent (Fig. 5). It may have one

moderately strong reflection and occasionally a few weak reflections within it. This unit generally is 5 to 15 m thick but increases to as much as 25 m in pockets just below the shelfbreak. It thins to zero thickness in an upward bulging region shown with horizontal dashes on the geologic map (see also Fig. 6). The base of this unit is commonly the strongest reflection in the section. The next Unit (B) characteristically has 20 to 30 internal reflections and is underlain by a second, mostly transparent Unit (C). The bottom of Unit C (and commonly the bottom of the record) is a single, moderate to strong reflection. The entire section onlaps at the shelfbreak either at an angular (erosional) unconformity or against fault scarps.

Units B and C combined are thickest in the central part of the study area (Fig. 7). To the northnorthwest of the prominent trough, they exceed 80 m and eastward they thicken to over 100 m. These areas of maximum thickness are all north of the region of steepest slope which trends through the central part of the study area at about latitudes 27° 42'-43' N.

Within the prominent trough in the south-central part of the study area, there are commonly irregular bulges of transparent material between the strong reflection at the base of Unit A and the package of multiple reflections in Unit B. The resulting thickening of Unit B generally places the reflector at the base of Unit C beyond the extent of penetration of the 3.5 kHz source. In the lower part of Unit B, one or more reflections may increase manyfold in amplitude for short distances (Fig. 8). These increases are commonly close to faults and on structural highs.

Faults The distribution of faults is shown in Figure 2. All appear to be normal. Pairs or sets of faults bounding clear-cut, down-thrown blocks within a generally upwarped area are mapped as grabens cresting uplifts. There are three main sets. A set with minima of both displacement and

uplift occur in the central part of the area within the bulge of gently dipping strata between latitudes 27° 47'-49' N and longitudes 91° 13'-18'W. A second, more striking set (Fig. 8) extend from the eastern end of the above set southwestward into the zone of intermediate slope just north of the prominent trough in the southern third of the area. The trough itself is bounded by faults but is a larger feature more on the scale of the uplifts rather than the grabens within them. A third set of grabens occurs within the platform in the southwest part of the study area.

Wipe-Outs Two forms of disappearance of subsurface reflections occur in the 3.5 kHz records. In the more widespread type, signal is simply lost so that subsurface reflections partly or completely disappear but the bottom echo is unaffected or may weaken also. This type of wipe-out most commonly occurs associated with crestal grabens and from the zone of intermediate slope into the zone of maximum slope.

In the second type of wipe-out, the subbottom characteristics are the same as in the first type, but the bottom echo is strong and prolonged (Figs. 8 & 9). This type of echo is common at the shelfbreak, on the projecting banks in the northwest part of the study area, and at scattered points within the zone of intermediate slope.

Core Data

Core locations are shown in Figure 2 and Table 3 (Appendix C). The targets for most were wipe-out zones - usually associated with faults. Ten of the 16 cores taken contained at least trace flouresence; and 14 of the 16 had either oil, gas or both. Eight of the 16 also had carbonate concretions. These varied from unlithified, soft mud to rock hard enough to stop over 600 kg of core pipe and lead weight.

The matrix for the hydrocarbons is homogeneous to layered, clayey mud.

Most of the mud is olive grey, but some with higher organic content is dark grey and some surficial mud is lighter and browner. A brown/grey color change commonly associated with the Holocene - Pleistocene boundary occurs in six cores from 40 to 320 cm depths. This suggests a Holocene rate of deposition of 11.5 cm/1000 years at about 70% porosity which is consistent with other estimates for slope sedimentation rates (Behrens, 1980).

Undisturbed slope muds from piston cores in this area commonly range in porosity from near 80% at the core tops to near 70% at about 10 m. Fifteen of the 16 cores taken in this study had porosities distinctly below 70%, 13 had porosities below 65%, and 9 were below 60%. Low porosities commonly correlate with high carbonate contents.

$\delta^{13}C$ values for extractable bitumen ranges from -26 to -28, those for kerogen-like residue range from -22 to -36, and those for carbonate carbon range from normal marine values near zero to -27.

The oil itself occurs in four modes: 1) In large amounts it forms an interconnecting network of veins of gum-like texture. In smaller amounts it may be 2) disseminated as tiny droplets, 3) disseminated as linings on gas vugs, or 4) lining high angle fractures. The fractures have the attitudes of normal faults, but displacement is not apparent within the cores.

Multichannel Seismic Data

The multichannel reflection profile (Fig. 10a) through the study area reveals 4 large diapirs. The crests of diapirs are indicated by the center of arching of sedimentary strata and the center of complex structural disruption over the diapirs. With one exception, no strongly reflecting caprock or salt appears in the profiles. Thus, although the extents of the diapirs are considerably greater than those shown by the crestal points (open double circles in Fig. 2), they are not clearly defined by these data. From west to east across Figure 2, the first point is over a diapir

with a strongly reflecting surface at about 850 m subsurface (Fig. 10b). The diapir appears to have a steeply dipping southwest side and a more gently dipping southeast side. Within the southeast side a deep, large scale wipe-out similar to those in the 3.5 kHz records extends from within the diapir, through the capping reflector, and into the sedimentary section (Fig. 10a). On the surface, this is manifest at the second crestal point as a wipe-out with a strong, prolonged, bottom echo. The next diapir crest occurs in the center of the zone of intermediate slope within an area of simple wipe-out. Although no strong caprock or salt-like reflector is apparent, the nearest core (about 1300 m to the southsouthwest) has interstitial water of increasing salinity with depth and values exceeding 200 $^{o}/_{oo}$ below 100 cm (Fig. 11).

The crest of a diapir underlies the juncture of the intermediate and steepest slopes at about 91° 11'W. The smaller crestal point just to the southwest appears to be just a projecting nose or shoulder of this diapir. The last crestal point is at the upper margin of the intermediate slope and within a slightly arched zone from which stratigraphic Unit A appears to offlap (Fig. 6).

DISCUSSION

Diapir Evidence and Interpretation The geologic features in this study area appear to be due predominantly and perhaps exclusively to salt tectonics, largely in the form of diapirism. The diapiric structures are clearly indicated in the multichannel profiles. Salt involvement is indicated by a high impedance-contrast reflector beneath one structure (Fig. 10) and by high interstitial water salinity over another. The involvement of shale diapirism in parts of the study area cannot be disproven; but ill-defined, strong reflectors at one to four km depths are associated with

most of the diapiric structures.

Where multichannel data is not available the simplest and most direct evidence of diapirism is shoaling bathymetry. The most obvious examples of this in the study area are the two banks between latitudes 27° 50'-55' N and longitudes 91° 20'-25' W. Older materials (against which Units A, B, and C and even older units onlap) project well above the surrounding bottom on all sides. Little or no subsurface structure in the 3.5 kHz reflection profile suggests that all of the high frequency energy is reflected by either indurated sediments or a coarse lag of surface material.

The area between latitudes 27° 35'-41' N and longitudes 91° 14'-22' W has less relief but is still obviously raised above the surrounding bottom. The surficial strata are disturbed only by occasional wipe-outs and are downfaulted in the center of the structure. This is clearly graben faulting due to tension across the crest of a diapir. A core within this graben contained no oil but had gas and anomalously low porosity (61 - 68%).

Although the bathymetry through the center of the study area appears more subtle and complex, its relations to diapirism can be interpreted. In strike section, domal uplift can still be the simple indication of a diapir. However, in dip sections, vertical uplift tends to produce a decrease in slope on the updip side of the structure and an increase in slope on the downdip side (Fig. 12). In both sections, the tension produced above the uplift is apparent in a system of normal faults across the crest of the structure. In strike section these form the antithetical system of a graben (Fig. 8). However, in dip section, the downdip margin of the faulted zone appears uplifted relative to the steepened, downslope side. Thus the fault system is not as antithetical as in the strike direction. This may be because diapiric uplift prevails over tension at this point. Uplift at this point may also result from rotation at depth of the blocks

downfaulted in the upslope portion of the faulted, intermediate slope.

Through much of the study area the downslope sequence of gentle or flattened slope, faulted intermediate slope, and steep slope suggests diapiric control of this bathymetry. Indeed the multichannel profile demonstrates this correlation at one point (Figs. 2 & 10a).

To the east of longitude 91° 11.5' W the intermediate slope changes to a broad swale with only one or two faults on the swells or ridges bounding the swell. The multichannel profile shows that both ridges are underlain by diapirs.

The combination of bathymetry, shallow fault structure, and deep structure suggests that an elongate (perhaps 2 to 4 km wide), roughly east-west trending diapir extends from about 91° 22' W to at least the eastern side of the study area (91° 05' W or 28 km) approximately between latitudes 27° 43'-46' N. At about 91° 16' W this diapir bifurcates with a portion of it extending northeastward under the more northerly ridge. Grabenal faulting follows this ridge to about 91° 11' W. Eastnortheastward only a single, normal fault follows the arching. The diminishing degree of faulting to the northeast suggests that the diapir plunges in this direction.

The set of grabenal faults striking east-west between latitudes 27° 47.5'-49.5' N and longitudes 91° 11'-17' W suggest that this deeper diapir also bifurcates westward. A fault with as much as 75 m displacement at the surface extends from this graben system to the two banks of piercement diapirs to the westnorthwest and suggests a deep-rooted connection of these structures.

The pattern emerges that the diapirs in this area may form a network of structures (Fig. 13). Major components of this network are two slightly

arcuate east-west ridges, the more southerly one (subsequently referred to as the central diapir ridge - CDR) extending to about 27° 43' N and the more northerly one (the northern diapir ridge - NDR) to about 27° 48' N. The NDR is apparently deeper or smaller but extends to piercement diapirs to the northwest (northwestern diapirs - NWD) and arcs around the large, bathymetric bulge of shallower depths in the north central part of the study area. This bulge may, in turn, be underlain by one or more salt structures. The ridges are connected by a northeast-southwest trending diapir ridge (diagonal diapir ridge - DDR). Interestingly, yet another diapir (the southwestern diapir - SWD) occurs along the southwestern projection of the DDR (south of 27° 40' N).

Non-graben Faults and Diapir Growth

Faults in the deep sedimentary section between the CDR and the NWD (Fig. 2) appear to be growth faults. A series of poorly defined but high amplitude reflectors at depths of from 3.5 to 4.5 seconds (Fig. 10a) suggest that the upthrown blocks of these faults are held up or lifted by a series of shoulders that slope northwestward from the CDR and may actually connect it with the NWD at depths greater than 5 seconds (about 6.5 km subsurface).

Single, normal faults that occur along the eastern parts of the NDR and CDR are interpreted to result from uplift by peaks or shoulders on the larger diapiric masses. These upthrown blocks are on the downslope sides of the ridges suggesting, perhaps, downslope, asymmetric growth of the ridges. This interpretation is compatible with the asymmetry suggested by the faulting between the CDR and the NWD.

Some absolute and relative rates of growth are suggested by thickness changes of the surficial stratigraphic units. Units B and C thin over the CDR but drape more uniformly over the NDR; while Unit A thins or disappears

only over small parts of the southernmost part (downdip margin of the zone of intermediate slope) of the CDR but offlaps much of the eastern third of the NDR. Thus the NDR appears younger than the CDR.

Within the zone where Unit A was either not deposited or has been eroded, the NDR projects up to 56 m above a line of uniform dip interpolated between undisturbed points upslope and downslope from the ridge. Depostion rates suggest that Unit A represents the time since significant downslope transport associated with a low, glacial sea level stand (10,000 to 20,000 BP). Thus rates of uplift of at least 3 - 6 mm/year are indicated. The absence of Unit A would have to be due to much more recent, post early Holocene, erosion for uplift rates to exceed 1 cm/year.

Gas and Oil Seepage

The targets for coring were sites near faults where subsurface strata were wiped-out in the 3.5 kHz records. At most sites the bottom record was also prolonged. It is well known that gas attenuates sound in sediments drastically (e.g., Addy & Worzel, 1979). The abundance of gas in the cores studied suggests that its existence in this area causes the observed wipe-outs. The complex composition of the gas indicates thermal generation at depth rather than shallow, bacterial methane generation. Thus the migration of oil and gas can be considered together.

Although sampling was not sufficient to define the full extent of oil and gas seepage, it can be observed that the seepage occurs repeatedly within the intensively faulted intermediate slope zone that signifies the crest of the CDR. More specifically, the seepage seems to be related to the faults at the downslope (7 cores) and upslope (2 cores) margins. These faults appear to extend to at least 1.6 sec. depth (about 660 m subsurface). According to the CDP record (Fig. 10a) the top of salt may be there

or as deep as 3 sec. (about 1,800 m subsurface).

Strata in the basin northwest of the CDR display cycles attributed to glacioeustatic sea level fluctuations (Bouma, 1981) to at least 2.3 sec. and perhaps over 3 sec. depth. Thus lateral hydrocarbon migration through these formations to the faults would involve Pleistocene oil. This seems an unlikely source because of the very limited generation time available. Thus migration from a deeper source, along the diapir margin and thence up the crestal faults seems more probable. Water moving along this route could increase in salinity by contact with salt. Hypersaline interstial water in core 2-10 supports this route.

Associations Related to Seepage

The $\delta^{13}C$ of the carbon in the carbonate nodules found in several cores indicates that much of its source involves microbial oxidation of organic molecules to CO_2. Secondary $CaCO_3$ precipitation obviously reduces porosity. Comparison of $CaCO_3$ content to porosity shows the negative correlation in not only the oil bearing cores but also in those having only gas and some having neither oil nor gas (Fig. 14). This suggests that hydrocarbons may migrate completely through a sediment leaving no obvious organic remnants but leaving an altered carbonate-porosity relationship. Thus hydrocarbon seepage was probably even more widespread than that indicated by the present distribution of oil.

Whereas prolonged bottom echoes have commonly been correlated to rough or coarse-grained sediment textures (e.g., Damuth, 1978), secondary carbonate nodules may account for this characteristic of many gas wipe-outs in the seepage area. The high-amplitude, limited-extent reflectors within Units B and C may also represent secondary precipitation of carbonates. Sulfides are also known to occur as diagenetic precipitates associated with hydrocarbons (Sassen,1980); and their high density contrasts could

certainly account for these anomalously strong reflections.

Prominent Trough

The origin of one feature and its relationship to the oil seepage remain unexplained. The southsoutheastward trending trough in the south central part of the study area is bounded by normal faults (making it a graben) and merges into the steep, southfacing margin of the CDR. All of the oil bearing cores were taken along the CDR updip of this trough; and all but one (2-10) were updip of the fault zones bounding the trough.

The trough is roughly twice the size of diapir-crest grabens in width and extends well beyond the study area. As such, it forms part of a complex system of troughs and basins which make up 40% of the midslope region. Bathymetric ridges and highs make up another 40% of the same slope area. In view of the salt diapir origin demonstrated for many of the positive features, it seems reasonable to conclude that the depressions are areas of salt withdrawal at depth. The graben faults then, do not result from tension but simply from differential vertical movements between the two areas. The trough shape may be fortuitous or may result from glacier-like downslope movement of the salt on the attenuated transitional crust. The down slope dip of the sediments within the trough makes migration of fluids to the seep sites possible from whatever Tertiary and Mesozoic sources exist at depth.

SUMMARY OF CONCLUSIONS

In addition to the more obvious indications of diapirs such as pierce-ment structures and domal uplifts with crestal grabens, diapirs, especially diapir-ridges trending along slope, may be interpreted from other bathymetric and shallow seismic reflection manifestations. The downslope sequence of gentle, intermediate, and steep dips with normal faulting in

the intermediate slope zone is the surface expression of an important diapir in the upper portion of the northern Gulf of Mexico continental slope considered in this study. Above this diapir, thermally generated hydrocarbons, both oil and gas, occur in the near surface muds, especially at the faulted margins of the intermediate slope zone. The associated gas can be remotely sensed as wipe-outs of subsurface reflections especially those with strong, prolonged bottom echoes. These echo characteristics may be related to diagenetic effects of the hydrocarbons - specifically carbonate precipitation shown to result from microbial oxidation of the hydorcarbons by their similar stable carbon isotopic compositions.

Most if not all structure in the area appears related to a three dimensional network of salt structures which includes salt ridges. The ridges may be growing asymmetrically upward with steeper sides seaward at rates of less than 1 cm per year.

High salilnity interstitial water in at least one oil-bearing core suggests a migration pathway that involves contact with the salt and originates below the Pleistocene. Migration may be from a trough formed by salt withdrawl at depth.

References

Addy,S.K., and Worzel, J.L. 1979, Gas seeps and subsurface structure off Panama City, Florida: American Association Petroleum Geologists Bulletin, vol. 63, p. 668-675.

Anderson, R.K., Scalan, R.S., Parker, P.L., Behrens, E.W., 1983, Seep oil and gas in Gulf of Mexico slope sediment: Science, vol. 222, no. 4624, p. 619-621.

Behrens, E.W., 1980, On sedimentation rates and porosity: Marine Geology, vol. 35, M11-M16.

Bouma, Arnold H., 1981, Depositional sequences in clastic continental slope deposits, Gulf of Mexico: Geo-Marine Letters, vol.1, p. 115-121.

Damuth, J.E., 1978, Echo character of the Norwegian-Greenland sea: relationship to Quaternary sedimentation: Marine Geology, vol. 28, p. 1-36.

Holland, W.C., 1970, Bathymetric Maps Eastern Continental Margin, U.S.A., Sheet 3 of 3, Norhtern Gulf of Mexico: Amer. Assoc. Petrol. Geologists, Tulsa, 3 sheets.

Martin, R.G., 1973, Salt structure and sediment thickness, Texas-Lousiana continental slope : US Geol. Survey Open File Rept., 21 p.

Sassen, Roger. 1980, Biodegradation of crude oil and mineral deposition in a shallow Gulf Coast salt dome: Organic Geochemistry, vol. 2, p. 153-166.

Stanley, D.J., Addy, Sunit K., Behrens, E.W., 1983, The mudline: variability of its position relative to shelfbreak: SEPM Special Publication no. 33, p. 279-298.

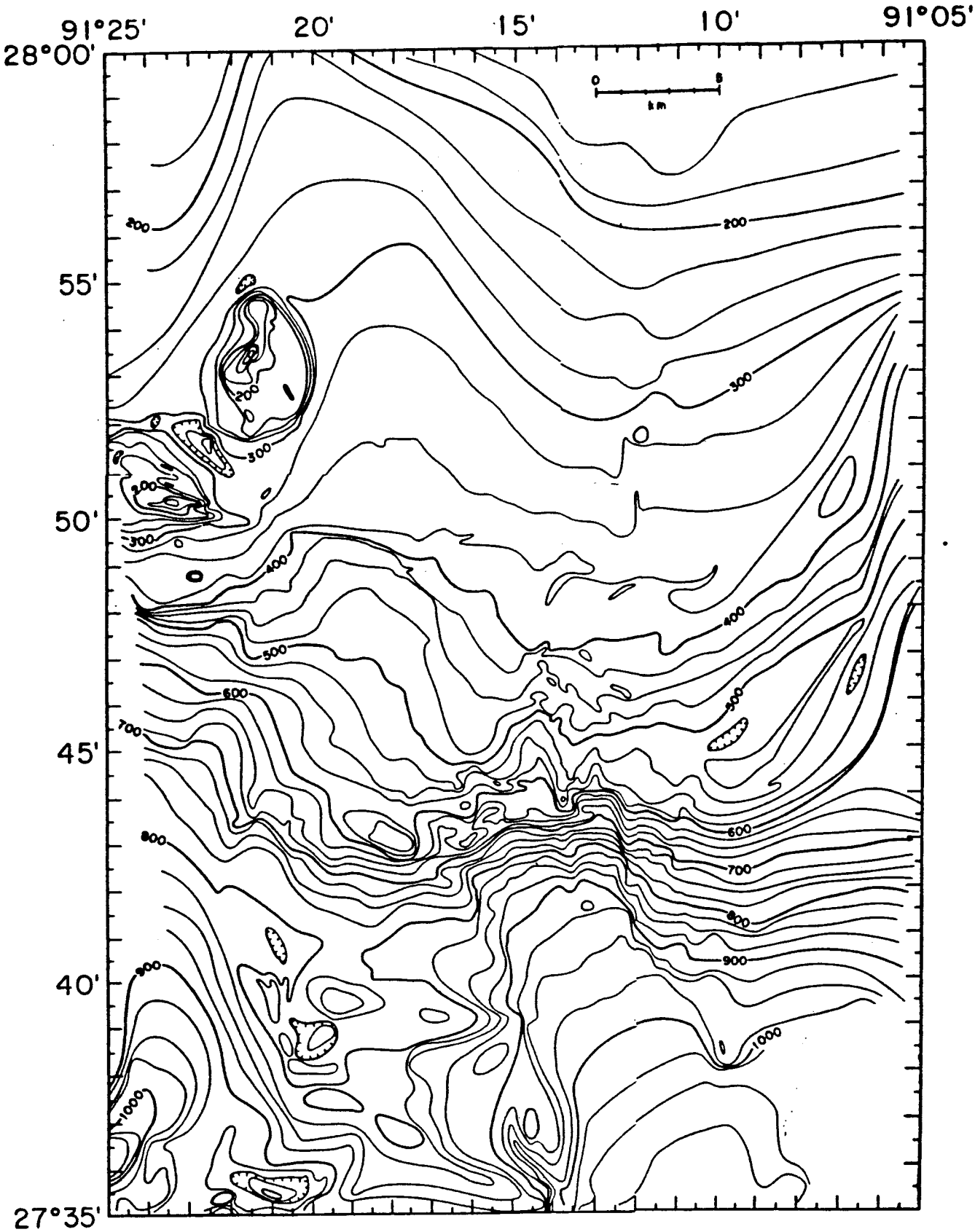

Figure 1. Bathymetric Map. Upper continental slope, northwest Gulf of Mexico. Contour Interval 25 meters. (Large-scale copy also included.)

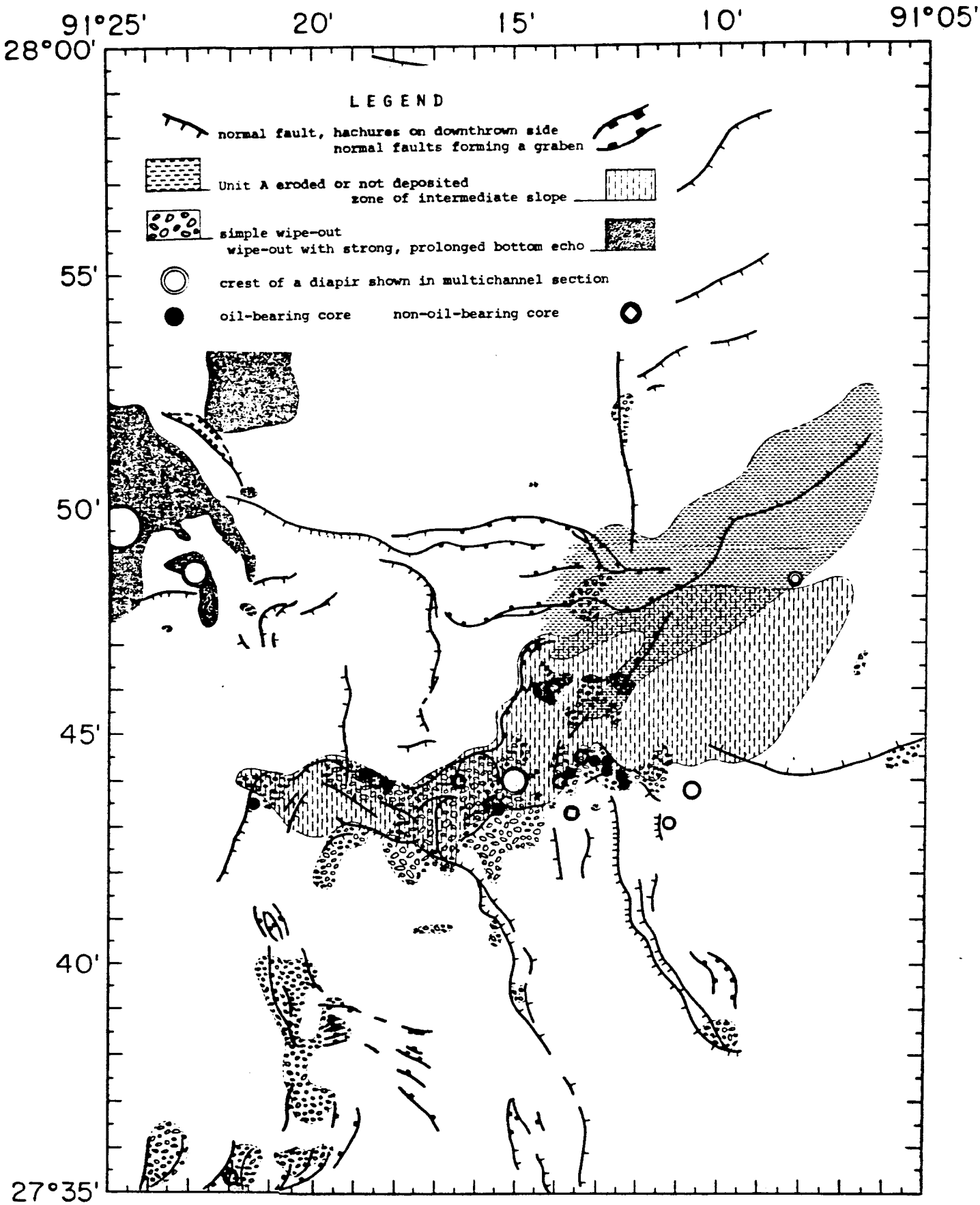

Figure 2. Geologic Map. (Large-scale copy also included.)

Fig. 3 Junction of the zones of intermediate and steep slopes over the central diapir ridge (CDR). North-South (dip) line at longitude 91°41.1' W, simple gas wipe-outs are indicated by g.

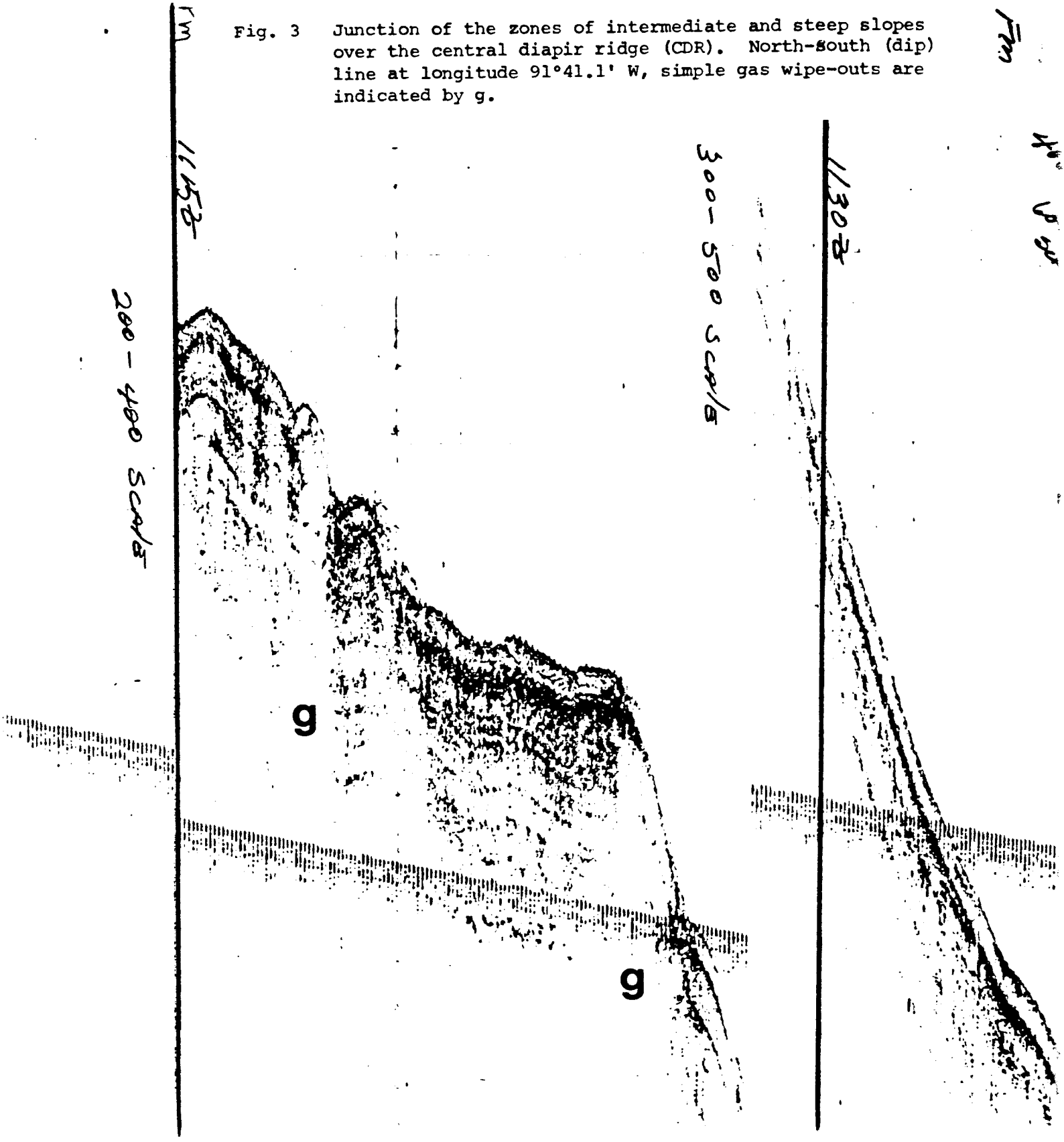

Fig. 4 Prominent trough extending downslope from the central diapir ridge (CDR). Slumped sediment may be from diapiric uplifts to the west or north.

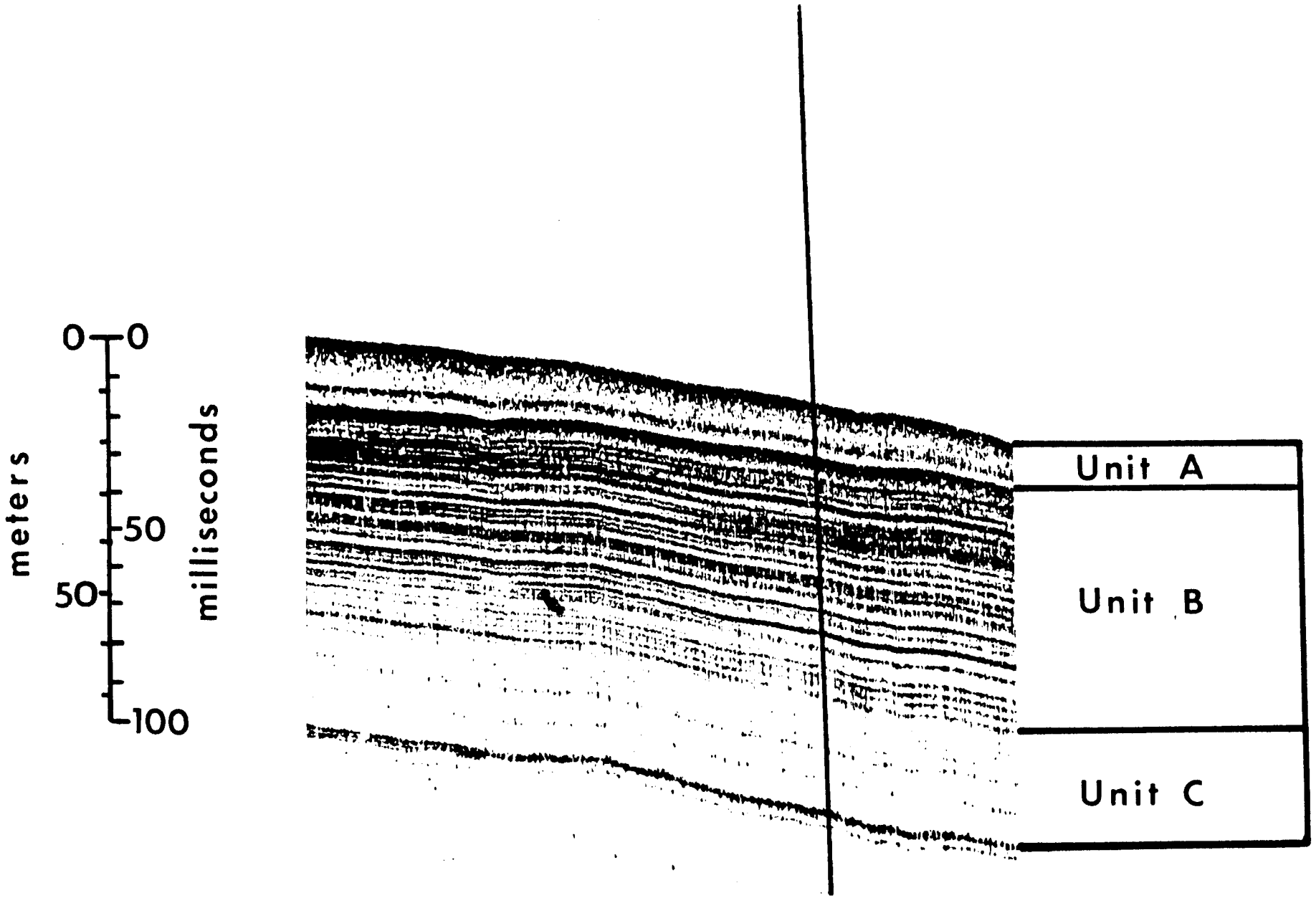

Fig. 5 Shallow stratigraphy of oil seep area as seen in 3.5 kHz reflection profiles.

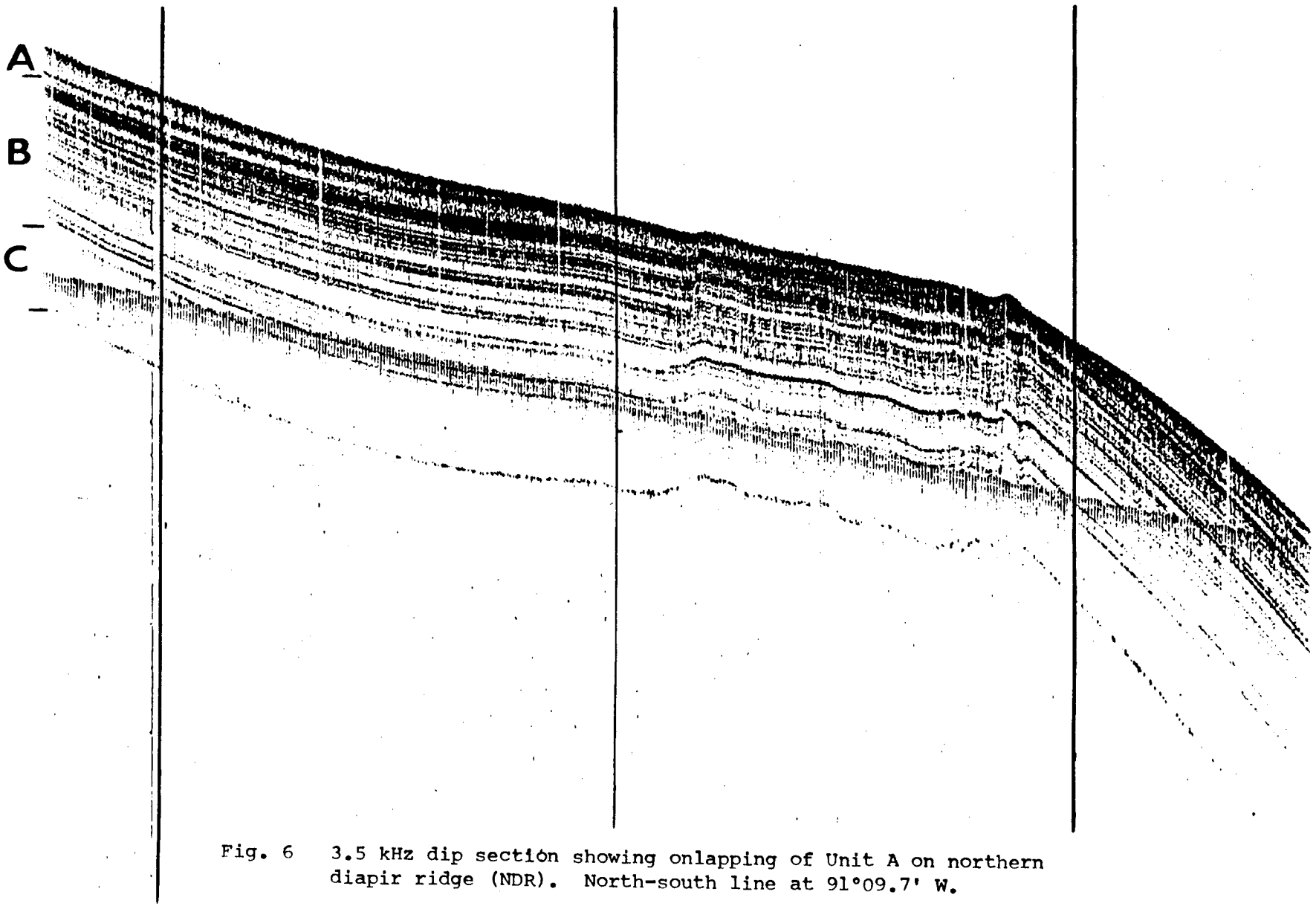

Fig. 6 3.5 kHz dip section showing onlapping of Unit A on northern diapir ridge (NDR). North-south line at 91°09.7' W.

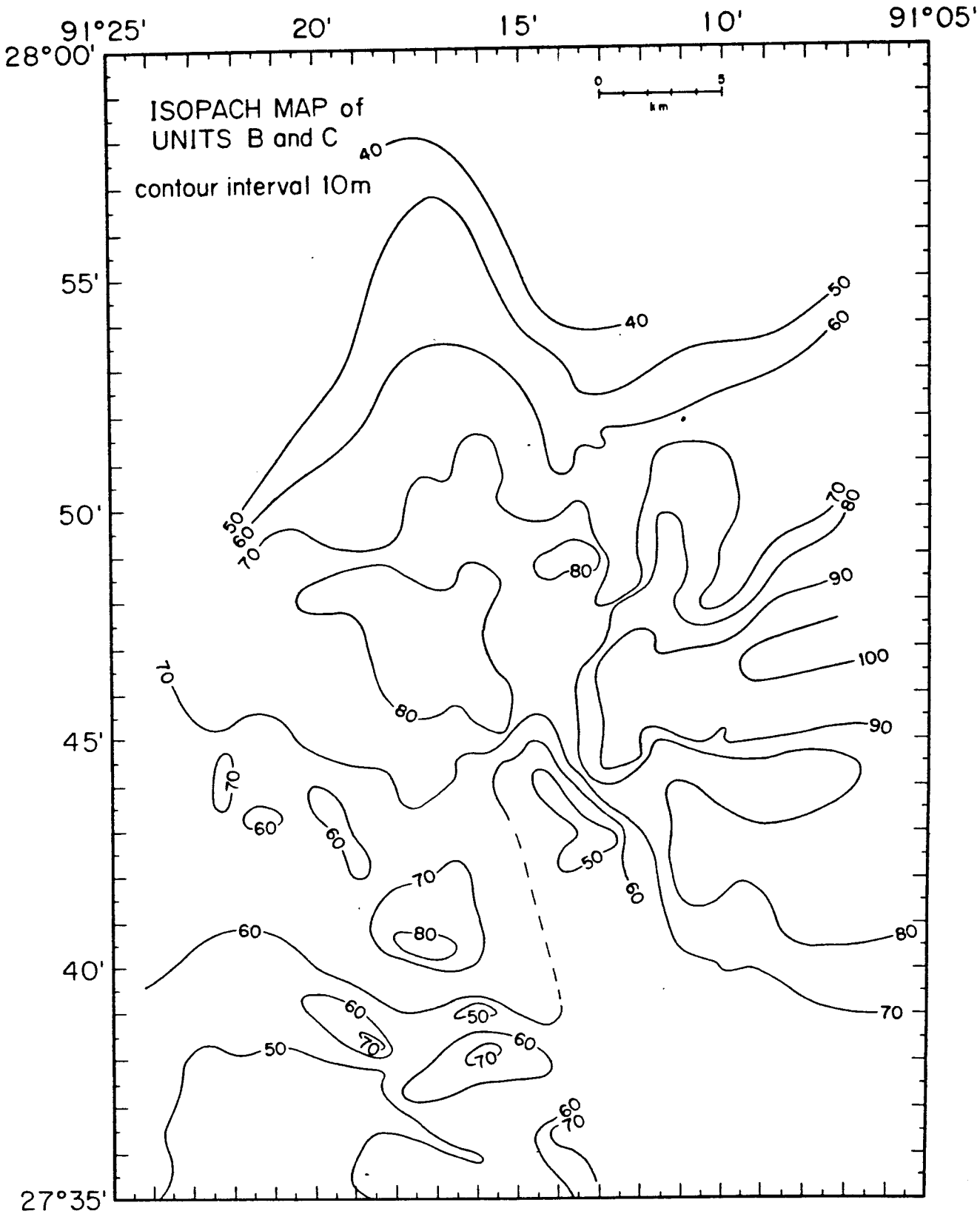

Figure 7. Isopach map of Units B and C. Thickest regions appear ponded upslope of the central diapir ridge (CDR). Thickening to the east suggests a Mississippi River source. (Large-scale copy also included.)

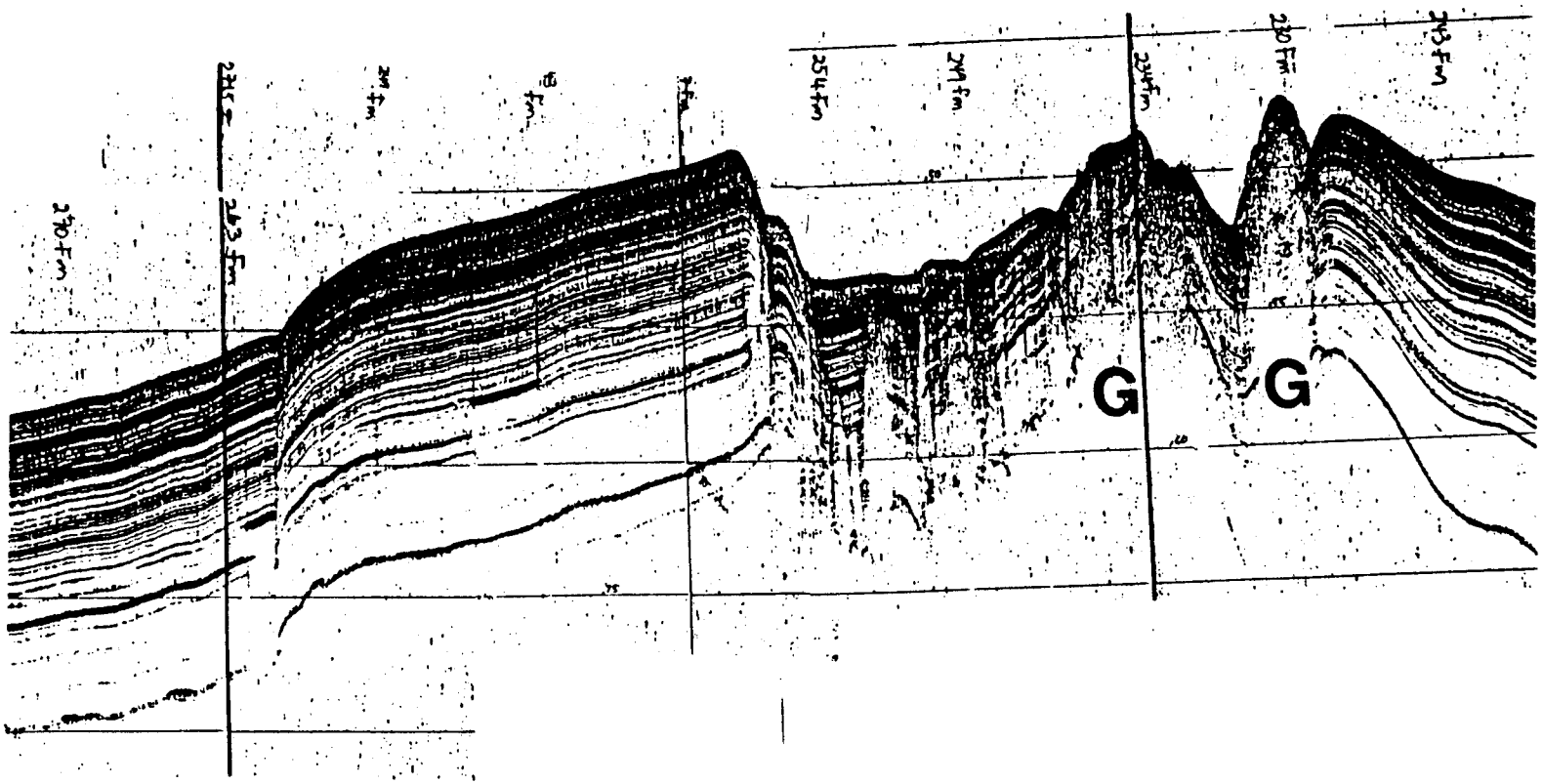

Fig. 8 East-west (strike) cross-section of diagonal diapir ridge (DDR) at latitude 27°46.1' N. Crestal graben area contains gas wipe-outs with prolonged bottom echoes (G). High amplitude reflectors (B) suggest diagenetic carbonate or sulfide precipitation related to hydrocarbon seepage.

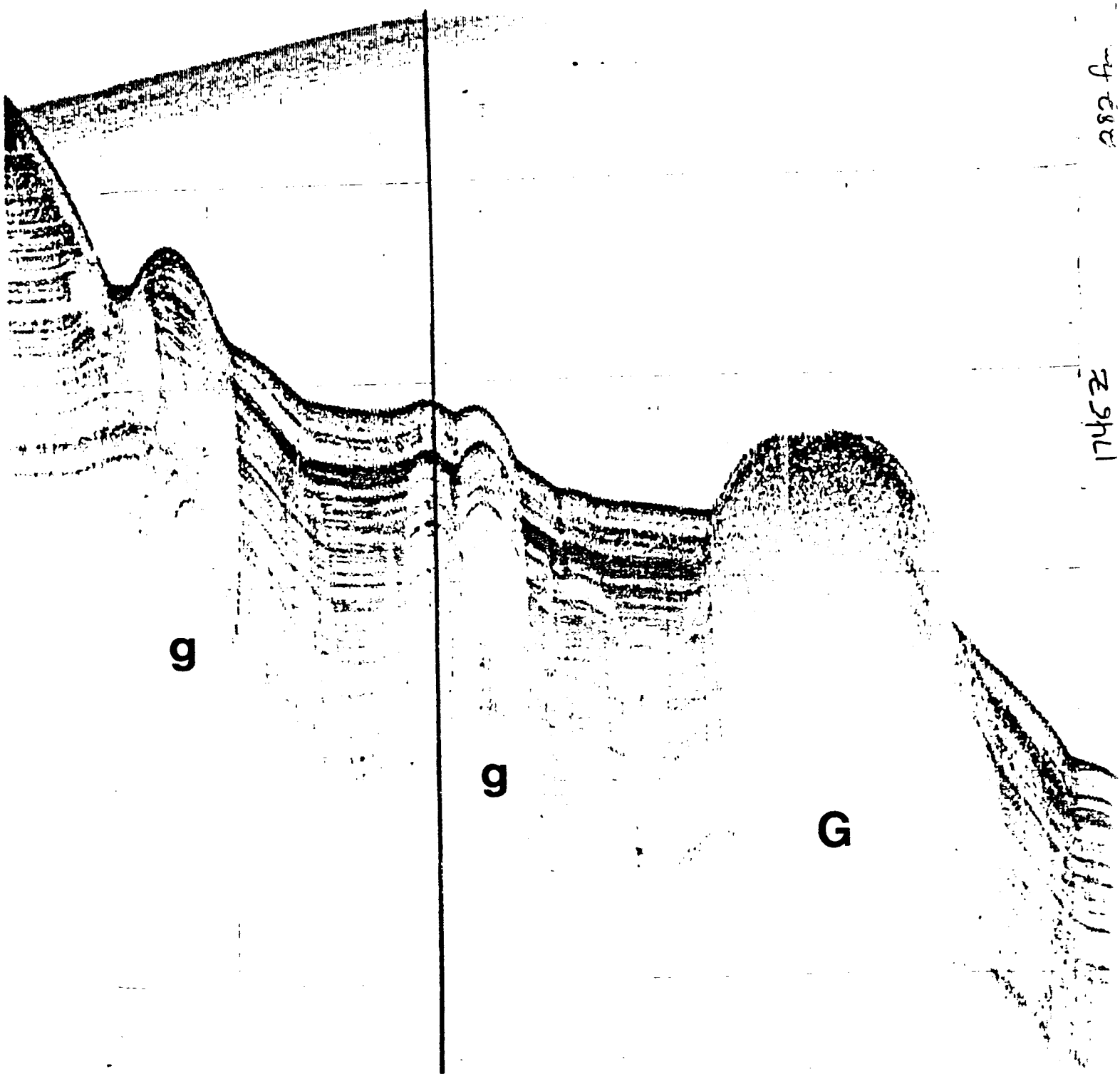

Fig. 9 Zone of intermediate slope with both simple wipe-outs (g) and wipe-out with strong, prolonged bottom echo (G).

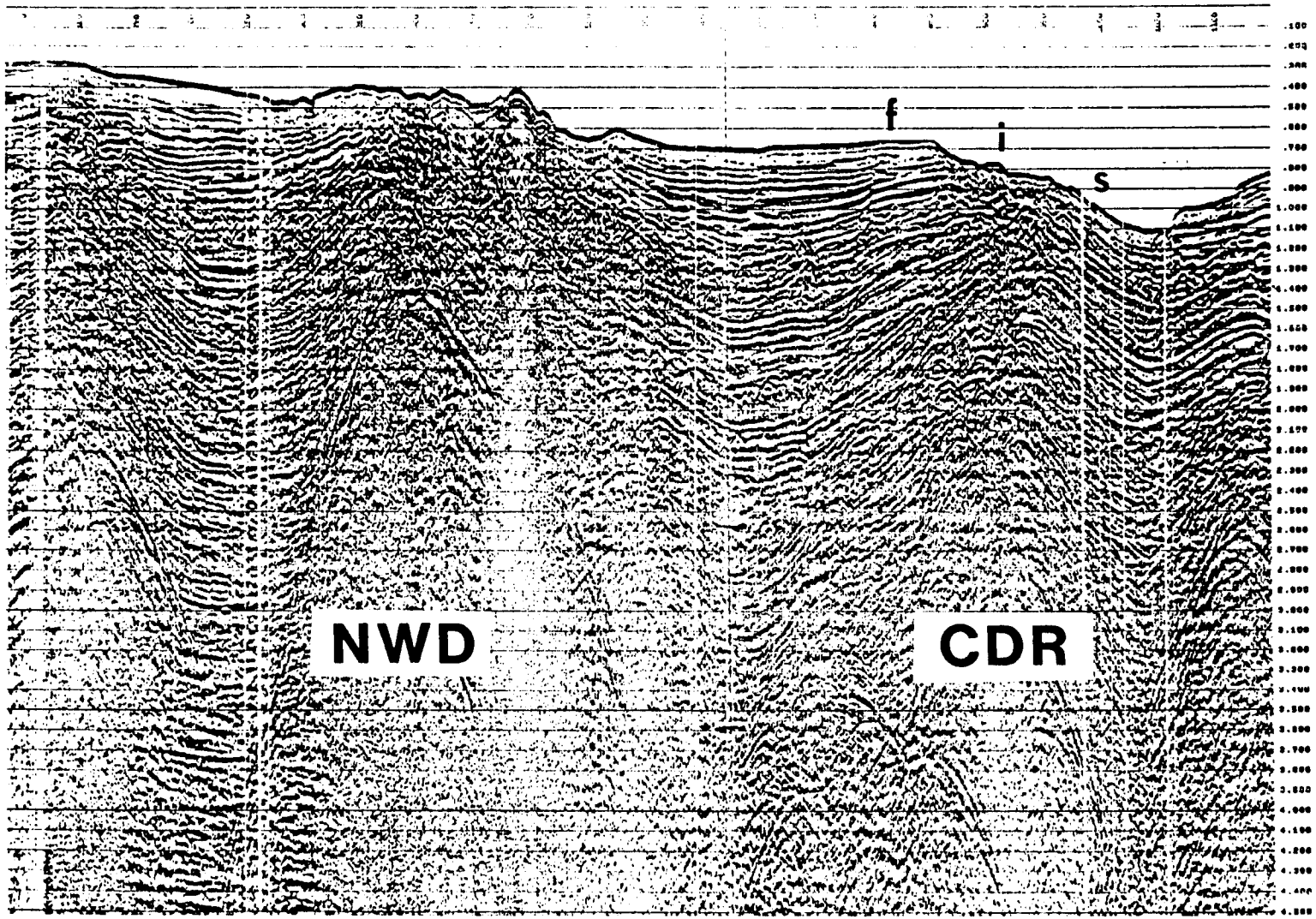

Figure 10a. Multichannel (24 fold) reflection profile. Diapir on the left (NWD) has strong caprock or salt reflector (see also Fig. 10b). A deep wipe-out possibly resulting from gas seepage is on its right (southeastern) flank. Diapir on the right (CDR) underlies oil seeps. f - flattened slope; i - intermediate (faulted) slope; s - steepened slope. This is line CS-32 with further processing of filtering, deconvolution, and rescaling with a relative amplitude (ABC) program.

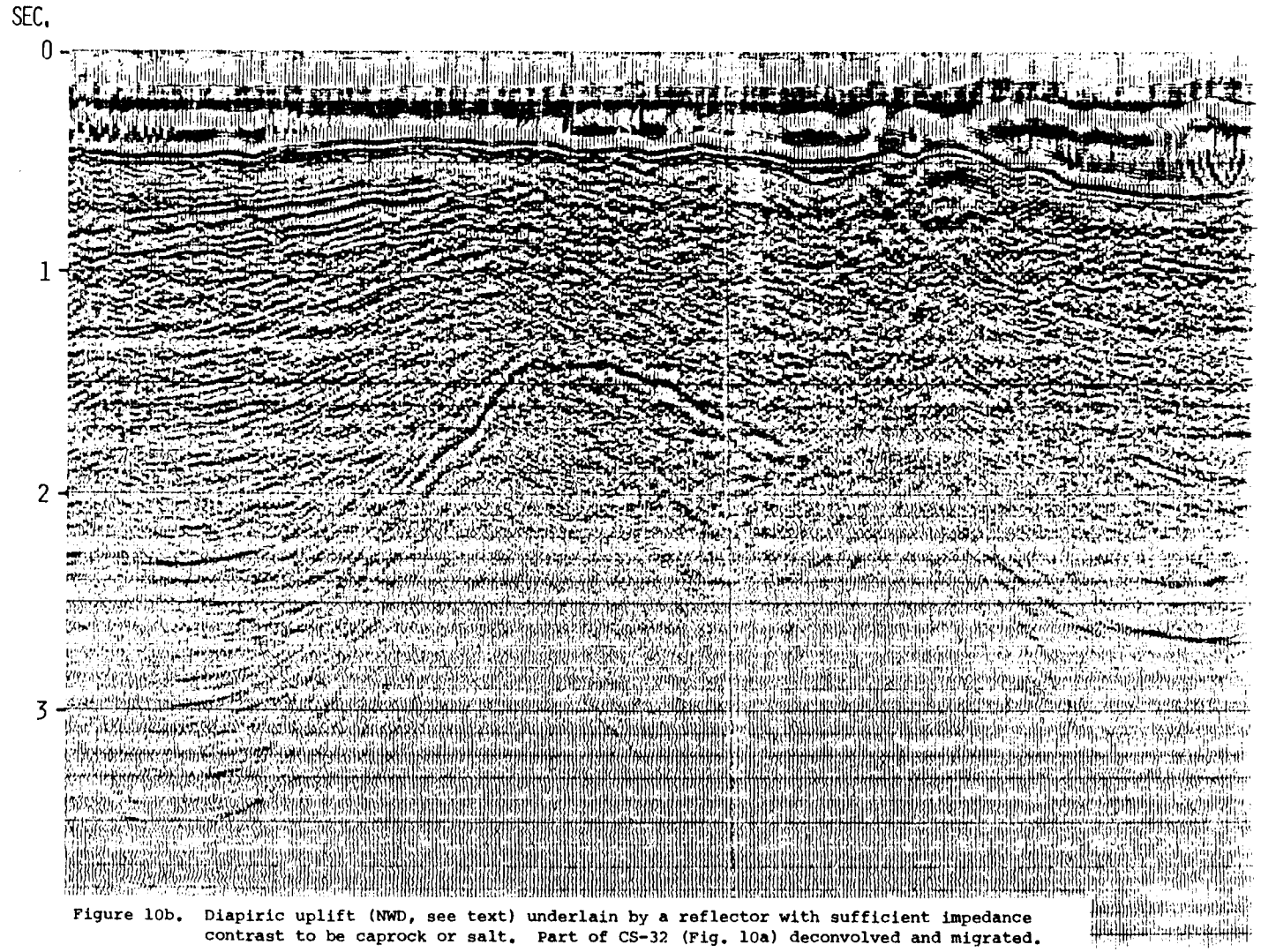

Figure 10b. Diapiric uplift (NWD, see text) underlain by a reflector with sufficient impedance contrast to be caprock or salt. Part of CS-32 (Fig. 10a) deconvolved and migrated.

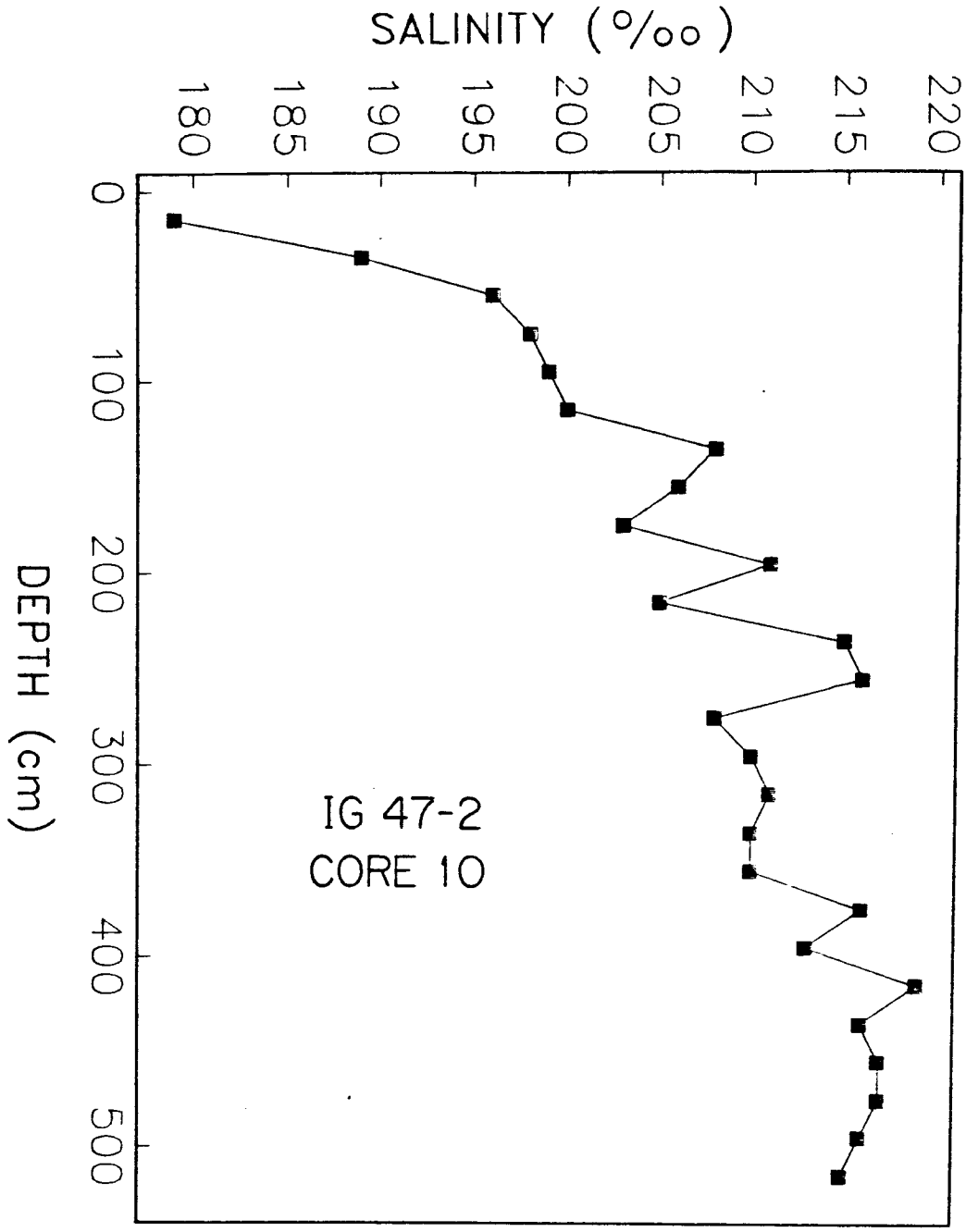

FIGURE 11. INTERSTITIAL WATER SALINITY IN CORE CONTAINING BOTH GAS AND OIL. CORE NEAR DOWNSLOPE MARGIN OF INTERMEDIATE SLOPE ZONE OVER CENTRAL DIAPIR RIDGE.

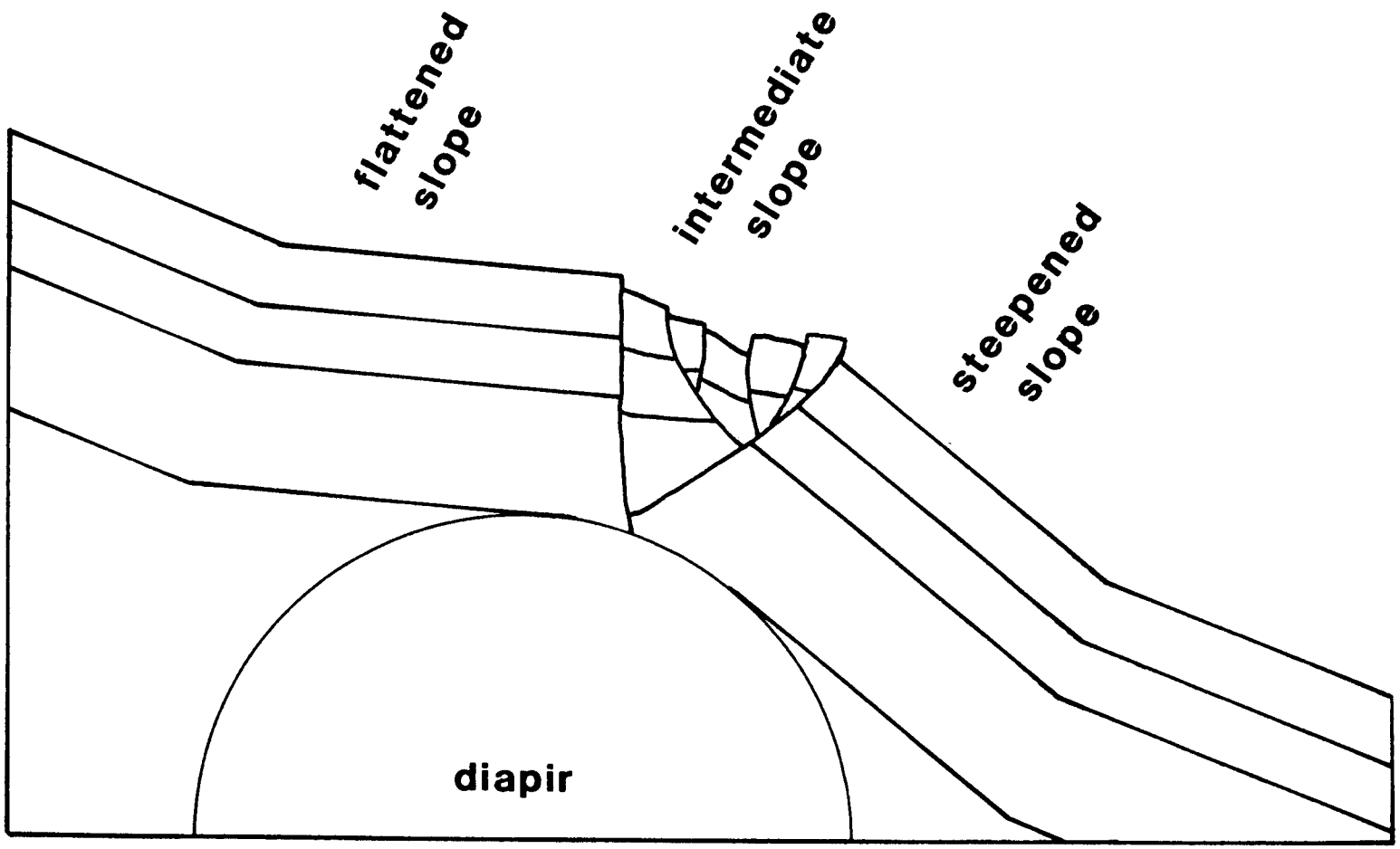

Figure 12. Diagrammatic illustration of diapir effect on bathymetry and shallow structure in dip section.

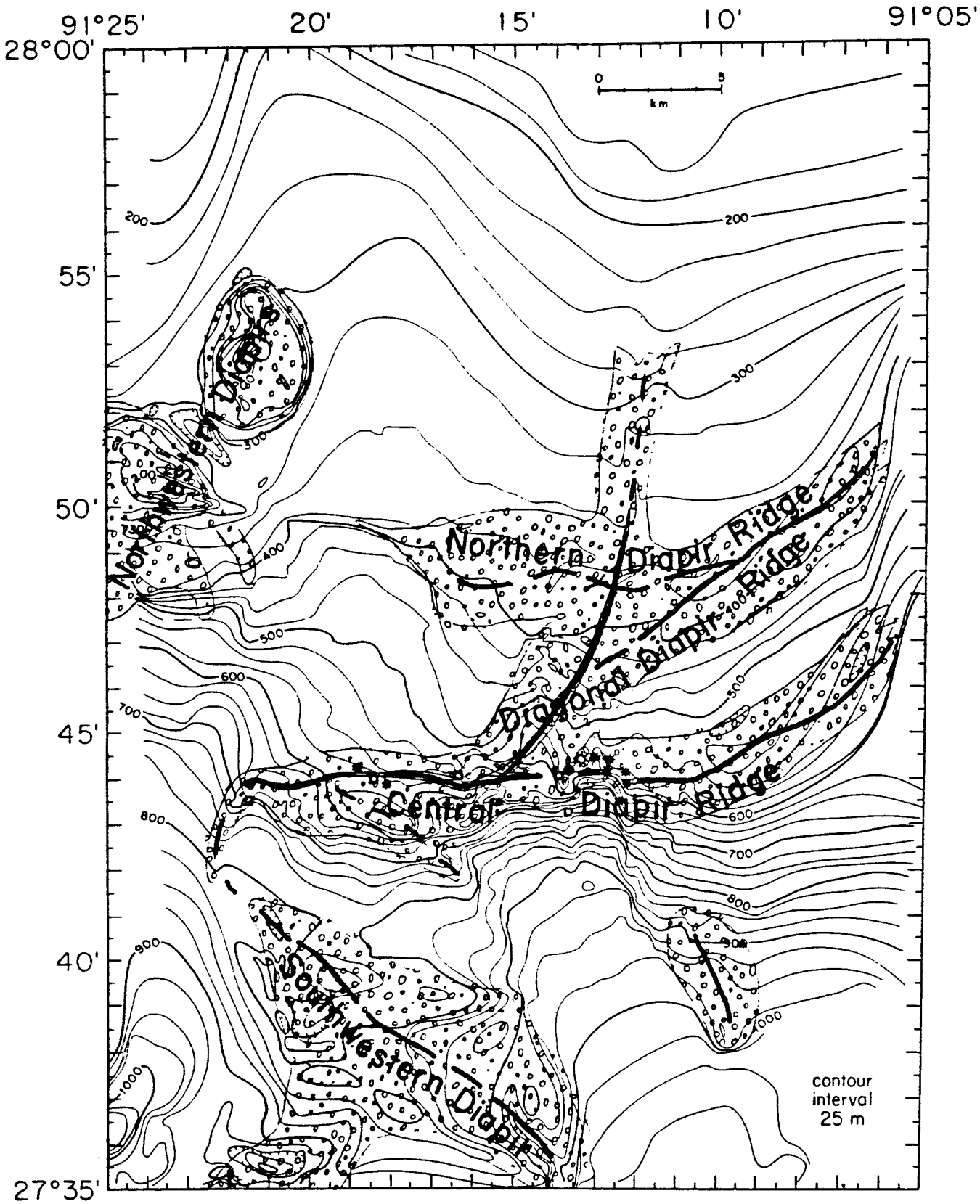

Fig. 13 Interpretation of diapir distribution network. Pattern shows interpreted extent of diapirs; heavy line shows interpreted crests of diapirs. ▫ - core with neither oil nor gas; ✲ - core with gas only; ● - core with oil only; ✱ - core with oil and gas.

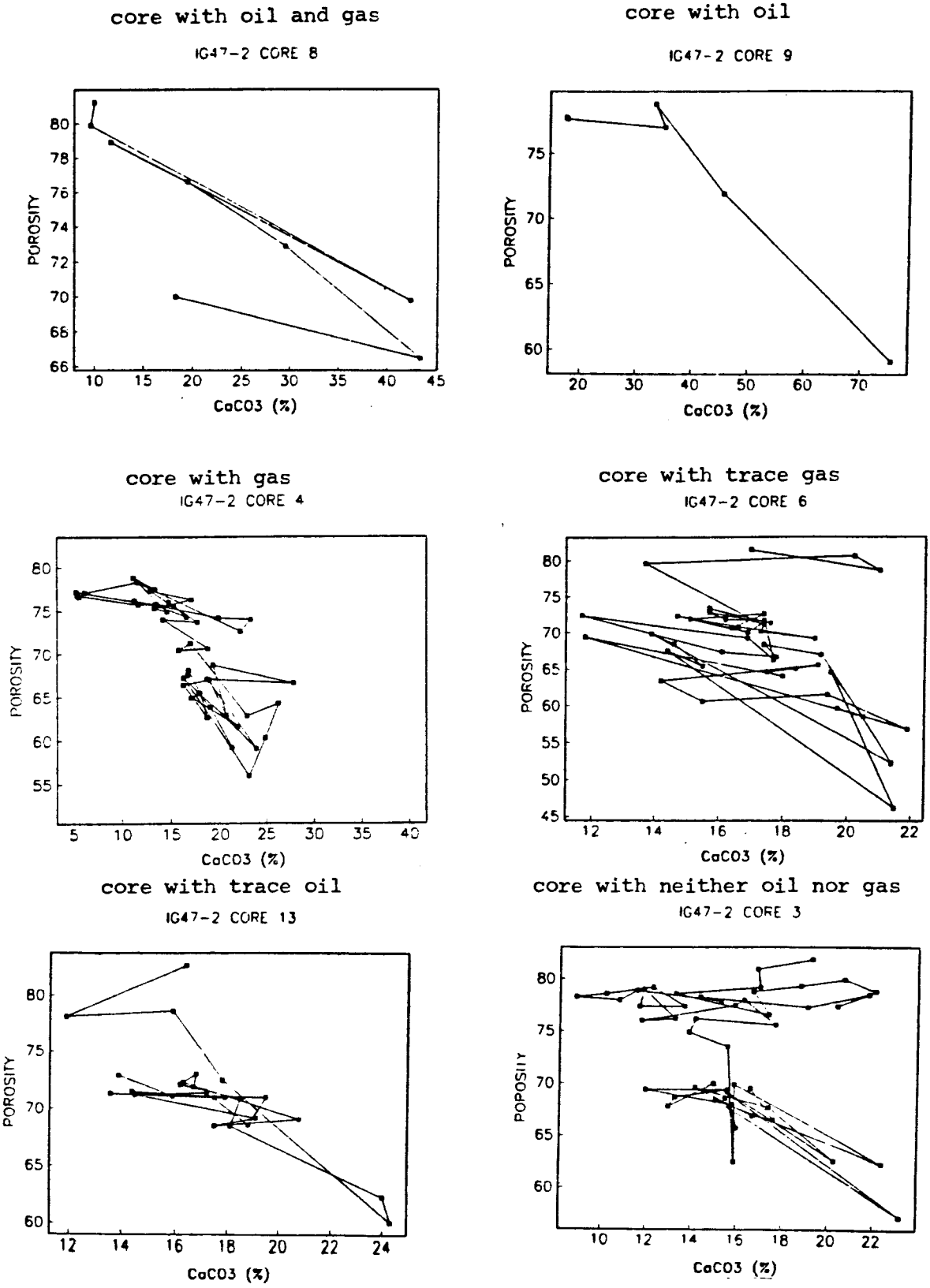

Figure 14. Carbonate - porosity relationships. Negative correlation suggests loss of porosity due to secondary carbonate precipitation related to hydrocarbon seepage.

Appendices Contents

APPENDIX A
LOCATIONS OF SURVEY LINES

Table 1 lists the beginning and ending points and line of latitude or longitude for lines surveyed with 3.5 kHz reflection profiles for this study. Table 2 lists dates surveyed and beginning and ending times. These can be used to locate the data on copies of the field recordings. The locations of other cruise tracks in the study area as well as these tabulated lines are also shown on a location map.

OIL SEEP SURVEY

Table 1

East/West Lines

LINE NUMBER	BEGINNING LONG.	LATITUDE	ENDING LONG.
1a	91°17.7'	28°00.0'	91°14.9'
1b	91°12.0'	27°59.9'	91°12.3'
1c	91°06.4'	28°00.0'	91°09.7'
2a	91°22.2'	27°53.1'	91°20.5'
2b	91°18.9'	27°53.1'	91°18.2'
2c1	91°17.0'	27°53.1'	91°15.2'
2c2	91°17.0'	27°53.1'	91°16.2'
2d	91°15.2'	27°53.2'	91°14.1'
2e	91°13.0'	27°53.1'	91°10.6'
2f	91°07.9'	27°53.0'	91°07.2'
3	91°24.4'	27°52.1'	91°18.4'
4	91°08.9'	27°51.6'	91°26.9'
5	91°23.8'	27°50.3'	91°08.8'
6	91°09.4'	27°49.5'	91°23.9'
7	91°23.9'	27°48.8'	91°08.6'
8	91°09.6'	27°47.8'	91°23.9'
9	91°23.4'	27°47.0'	91°08.5'
10	91°23.9'	27°46.1'	91°11.1'
11	91°08.4'	27°45.3'	91°23.7'
12E	91°13.1'	27°44.3'	91°08.8'
12W	91°16.1'	27°44.3'	91°23.6'
13a	91°11.9'	27°44.0'	91°14.1'
13E	91°18.6'	27°44.0'	91°14.5'
13W	91°18.7'	27°44.0'	91°22.5'
14E	91°11.3'	27°43.5'	91°23.0'
14W	91°21.4'	27°43.6'	91°23.6'
15a	91°11.9'	27°42.7'	91°10.8'
15	91°22.3'	27°42.7'	91°11.6'
16	91°17.1'	27°42.0'	91°11.9'
17	91°08.9'	27°41.5'	91°18.8'
18E	91°09.3'	27°41.0'	91°17.7'
18W	91°21.0'	27°41.0'	91°17.1'
19	91°13.7'	27°40.5'	91°08.3'
20	91°05.7'	27°40.0'	91°25.5'
21E	91°15.6'	27°39.5'	91°05.7'
21W	91°18.2'	27°39.5'	91°16.7'
22	91°12.8'	27°39.3'	91°22.6'
23	91°25.2'	27°38.4'	91°10.6'
24	91°24.8'	27°36.6'	91°09.2'
25E	91°22.1'	27°35.4'	91°20.2'
25W	91°24.6'	27°35.4'	91°21.5'
26	91°08.3'	27°35.2'	91°24.5'

North/South Lines

LINE NUMBER	BEGINNING LATITUDE	LONGITUDE	ENDING LATITUDE
1	27°40.1'	91°05.7'	28°00.0'
2	27°52.6'	91°06.6'	27°39.7'
3S	27°38.8'	91°08.6'	27°41.0'
3N	27°40.2'	91°08.6'	27°52.8'
4	27°59.9'	91°09.7'	27°36.5'
5	27°52.7'	91°10.6'	27°40.1'
6S	27°42.3'	91°11.2'	27°40.0'
6N	27°45.4'	91°11.2'	27°43.9'
7	27°36.2'	91°11.6'	27°59.8'
8	27°42.4'	91°11.7'	27°46.0'
9	27°41.1'	91°12.0'	27°45.7'
10	27°59.5'	91°12.3'	27°39.1'
11a	27°45.7'	91°12.6'	27°41.4'
11b	27°53.7'	91°12.5'	27°42.4'
12S	27°45.2'	91°12.9'	27°41.2'
12N	27°45.7'	91°12.8'	27°44.4'
13	27°35.2'	91°13.0'	27°52.8'
14S	27°41.6'	91°13.3'	27°43.7'
14Na	27°43.5'	91°13.3'	27°45.4'
14Nb	27°45.6'	91°13.3'	27°44.6'
15S	27°41.4'	91°13.6'	27°45.3'
15N	27°43.9'	91°13.6'	28°00.0'
16	27°46.9'	91°13.8'	27°41.6'
17	27°52.9'	91°14.1'	27°41.0'
18	27°44.4'	91°14.4'	27°47.7'
19	27°59.8'	91°14.8'	27°35.0'
20	27°41.0'	91°15.1'	27°53.2'
21	27°52.7'	91°15.6'	27°39.5'
22	27°52.7'	91°16.2'	27°40.6'
23	27°39.5'	91°16.7'	27°53.1'
24	27°41.6'	91°17.1'	27°52.7'
25	27°35.2'	91°17.6'	28°00.0'
26	27°51.7'	91°18.1'	27°43.9'
27	27°52.9'	91°18.5'	27°40.1'
28	27°41.8'	91°19.2'	27°44.9'
29	27°35.6'	91°19.6'	27°53.1'
30	28°00.0'	91°20.6'	27°58.0'
31	27°50.0'	91°21.0'	27°55.9'
32	27°55.7'	91°21.5'	27°41.2'
33	27°39.7'	91°22.5'	27°52.7'
34	27°60.0'	91°23.5'	27°35.4'
35a	27°43.8'	91°24.1'	27°49.2'
35b	27°44.3'	91°23.7'	27°46.9'
35c	27°48.1'	91°24.0'	27°48.8'
35d	27°49.5'	91°23.9'	27°49.9'
36	27°48.7'	91°24.6'	27°54.7'

Table 2

East/West Lines

LINE NUMBER	DATE	START TIME	END TIME
1a	1-13-83	0110Z	0125Z
1b	1-15-83	1830Z	1835Z
1c	1-15-83	1050Z	1115Z
2a	1-16-83	0035Z	0048Z
2b	1-15-83	0115Z	0120Z
2c1	1-15-83	0504Z	0511Z
2c2	1-16-83	0625Z	0632Z
2d	1-16-83	1010Z	1015Z
2e	1-14-83	0713Z	0730Z
2f	1-14-83	1120Z	1130Z
3	1-18-83	1740Z	1845Z
4	1-18-83	1450Z	1640Z
5	1-18-83	1245Z	1435Z
6	1-18-83	1105Z	1235Z
7	1-18-83	0905Z	1055Z
8	1-18-83	0720Z	0857Z
9	1-18-83	0530Z	0712Z
10	1-17-83	0630Z	0800Z
11	1-17-83	0435Z	0620Z
12E	1-17-83	0355Z	0425Z
12W	1-18-83	0415Z	0505Z
13a	1-17-83	1835Z	1855Z
13E	1-16-83	1632Z	1727Z
13W	1-18-83	2205Z	2230Z
14E	1-17-83	0820Z	0940Z
14W	1-18-83	2240Z	2340Z
15a	1-17-83	1800Z	1815Z
15	1-17-83	0950Z	1105Z
16	12-16-82	1340Z	1430Z
17	1-16-83	1305Z	1440Z
18E	12-16-82	1215Z	1325Z
18W	1-16-83	0410Z	0440Z
19	1-16-83	1150Z	1250Z
20	1-14-83	1326Z	1545Z
21E	1-15-83	0654Z	0800Z
21W	1-15-83	0310Z	0320Z
22	1-15-83	2120Z	2230Z
23	12-16-82	0845Z	1140Z
24	1-14-83	1615Z	1805Z
25E	1-14-83	2240Z	2255Z
25W	1-14-83	2110Z	2140Z
26	1-14-83	1835Z	2025Z

North/South Lines

LINE NUMBER	DATE	START TIME	END TIME
1	1-15-83	0805Z	1045Z
2	1-14-83	1135Z	1315Z
3S	12-16-82	1145Z	1210Z
3N	1-14-83	0940Z	1120Z
4	1-15-83	1120Z	1410Z
5	1-14-83	0735Z	0925Z
6S	1-17-83	1110Z	1130Z
6N	1-17-83	0805Z	0815Z
7	1-15-83	1430Z	1825Z
8	12-16-82	1435Z	1520Z
9	1-16-83	2340Z	0025Z
10	1-15-83	1835Z	2115Z
11a	12-16-82	1530Z	1610Z
11b	1-17-83	1630Z	1756Z
12S	1-16-83	2255Z	2335Z
12N	1-17-83	0031Z	0045Z
13	1-14-83	0455Z	0710Z
14S	1-16-83	1930Z	1950Z
14Na	1-16-83	2045Z	2105Z
14Nb	1-16-83	2110Z	2130Z
15S	12-16-82	1615Z	1707Z
15N	12-17-82	0210Z	0540Z
16	1-16-83	1825Z	1925Z
17	1-16-83	1015Z	1145Z
18	1-16-83	1730Z	1815Z
19	1-13-83	0130Z	0445Z
20	1-16-83	0820Z	1005Z
21	1-15-83	0515Z	0654Z
22	1-16-83	0635Z	0808Z
23	1-15-83	0320Z	0505Z
24	1-16-83	0445Z	0620Z
25	1-13-83	2155Z	0105Z
26	1-18-83	1850Z	2000Z
27	1-15-83	0125Z	0310Z
28	1-16-83	1445Z	1520Z
29	1-14-83	2300Z	0110Z
30	1-13-83	1830Z	2135Z
31	1-16-83	0115Z	0205Z
32	1-16-83	0210Z	0405Z
33	1-15-83	2235Z	0030Z
34	12-16-82	0430Z	0740Z
35a	1-18-83	2345Z	0045Z
35b	1-18-83	0505Z	0525Z
35c	1-18-83	0900Z	0904Z
35d	1-18-83	1235Z	1240Z
36	1-19-83	0040Z	0135Z

APPENDIX B
GRAPHIC CORE LOGS

This appendix contains graphical representations of 16 piston cores taken for this study. Six parameters are discussed briefly in the order they appear from left to right across the logs.

COLOR

Colors were noted immediately upon opening and splitting of the cores to avoid loss of ephemeral coloration especially due to the oxidation of metastable sulfides. Colors are described according to the Munsell System as used in the Rock Color Chart distributed by the Geological Society of America.

Hue is designated by a number-letter sequence that includes G - green, GY - green-yellow, Y - yellow, YR - yellow-red and R - red. Within each letter code there are 10 numerical divisions with 5 being the "pure" color and other numbers indicating gradations to the adjacent color.

Two other color characteristics are indicated by a fraction, e.g., 3/2. The numerator indicates lightness-darkness (1-darkest, 8-lightest), and the denominator indicates degree of coloration (0-no color (only black to white); 6-vivid color, no grayishness). Examples of frequently observed colors include:

5GY 4/1	dark greenish gray
5GY 6/1	greenish gray
5Y 2/1	olive black
5Y 3/2	dark olive gray
5Y 4/1	moderate olive dark gray
5Y 5/2	light olive gray
10Y 4/2	grayish olive
5YR 4/1	brownish gray
5YR 5/2	pale brown
10YR 4/2	dark yellowish brown
N1	black (no denominator)
N3	dark gray (no denominator)

$CaCO_3$

Calcium carbonate content was determined by weight loss upon acidification with HCl. The data is plotted in 5% bands, but analytical accuracy is probably better than 1%. The 30% reference line is the lower boundary of oozes.

SEDIMENTARY STRUCTURES

Structures were determined primarily by visual observation. X-radiographs were taken of all cores and were frequently consulted. A legend of structural symbols is on a separate page. The classification was largely based on and tailored for this core suite.

FORM OF OIL OCCURRENCE

Oil can be seen in many cores with the unaided eye in normal light. Smaller amounts can also be seen clearly by their flourescence under ultraviolet (UV) light. The UV flourescences may be either bright, slightly greenish yellow or darker orange. The macroscopic appearance of oil in the cores studied falls more or less into three forms:

I. Liquid Veins This is the form of the most abundant oil (usually several per cent extractable hydrocarbons). Cohesive, gum-like strings of oil weave irregularly through the mud. This form occurs in three cores (46-5, 2-9, and 2-12) in two of which the UV flourescence is yellow and in one (2-12) it is orange.

II. Disseminated Usually best viewed under UV light, the oil in this form may occur as specks or as separated, irregular shapes in trace to abundant amounts.

A. Gas-Associated Irregularly shaped, disseminated oil commonly occurs lining gas vugs. This occurs in six cores with yellow flourescence being twice as common as orange flourescence.

B. Not Gas-Associated This form is slightly less common (5 cores) and all occurrences flouresce yellow. Rarely this form tends to concentrate in horizontal layers.

III. Coating Fractures In two cores (2-5 and 2-7) oil occurs on smooth planes that form high angles (>45°) with horizontal bedding. The planes have attitudes of normal faults, but no control was available to detect displacement. In one core (2-12) the occurrence was similar, but the planes were not smooth but irregular like gas envelopes. Two of the cores had orange flourescence and one had yellow.

POROSITY

Porosity is calculated from weight loss of water upon oven drying. It is corrected for salt content assuming a grain density of quartz (2.65 g/cc) and a normal marine salinity (35 0/00) unless there were indications of abnormal conditions. The only case of this was the brine found in core 2-10.

COMMENTS

Holocene-Pleistocene boundary indications are all estimates based largely on a common color stratigraphy which has been correlated with this boundary in other studies.

LEGEND

Oil and Gas Occurrence

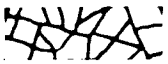 - I. Liquid veins

 - II. A. Disseminated (Gas-associated)

 - II. B. Disseminated (Not gas-associated)
(Density of symbols is a semiquantitative indication of abundance of oil)

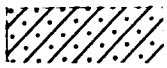 - III. Coating fractures

G - Abundant gas fracturing

g - Less abundant gas

Ultraviolet flourescence

o - Orange

y - Yellow

Carbonate Concretions

Secondary carbonate (identified by organic $\delta^{13}C$ values) is apparent in many cores as light gray or whitish nodules.

● ● ● - Indurated (rocky), nodular concretions

o o - Non-indurated, muddy concretions

Sedimentary Structures

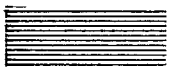 - Regularly laminated; distinct, horizontal, essentially undisturbed, generally less than 0.5cm thick

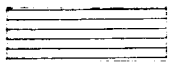 - Regularly layered; same as regular laminae except generally 0.5cm to 2cm thick

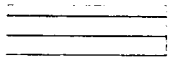 - Regularly bedded; same as regular laminae except generally thicker than 2cm

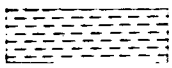 - Irregularly laminated; discontinuous or vague, partially disturbed but original horizontality still apparent

 - Irregularly layered; same as irregular laminae except generally thicker than 0.5cm

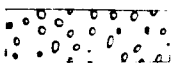 - Distinctly mottled; distinct, sharp boundaries, mostly isolated mottles

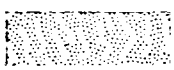 - Indistinctly mottled; indistinct boundaries and/or complex, multiple types of mottles

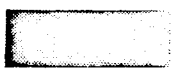 - Homogeneous; may have vague or rare mottles or irregular bedding; but is characterized chiefly by randomly oriented, irregular structures

 - Implosion of core liner or other coring artifacts

IG - 47

Core Number	Latitude N	Longitude W	Corrected Water Depth (m)	Gas	Oil
IG47-1-1	27°44.10'	91°12.40'	614	P	P
IG47-1-2	27°44.05'	91°16.32'	557		
IG47-2-1	27°35.31'	91°21.99'	937	P	
IG47-2-2	27°44.21'	91°18.60'	568	P	P
IG47-2-3	27°43.38'	91°13.51'	684		
IG47-2-4	27°44.56'	91°13.32'	553	P	
IG47-2-5	27°44.43'	91°12.93'	567	P	P
IG47-2-6	27°44.06'	91°13.70'	562	tr.	
IG47-2-7	27°44.02'	91°12.27'	554	P	P
IG47-2-8	27°44.27'	91°12.58'	550	P	P
IG47-2-9	27°44.21'	91°13.43'	567		P
IG47-2-10	27°43.44'	91°15.35'	642	P	P
IG47-2-11	27°44.09'	91°18.33'	574	tr.	
IG47-2-12	27°43.98'	91°18.10'	563	P	P
IG47-2-13	27°43.60'	91°21.44'	689		tr.
IG46-5	27°44.40'	91°12.70'	555	P	P

Appendix C

Carbonate - Porosity

In the absence of geochemical diagensis, porosity is largely a function of compaction and should have little, if any, correlation to carbonate content. However addition of secondary carbonate would be at the expense of porosity and thus would produce a negative correlation or negative slope on a scatter plot. Furthermore, undisturbed clayey muds at the depths sampled rarely, if ever, have porosities below 70%. The following plots are for core samples taken in depth increments of 20 cm where possible and plotted vs depth in Appendix B.

IG47-1 CORE 1

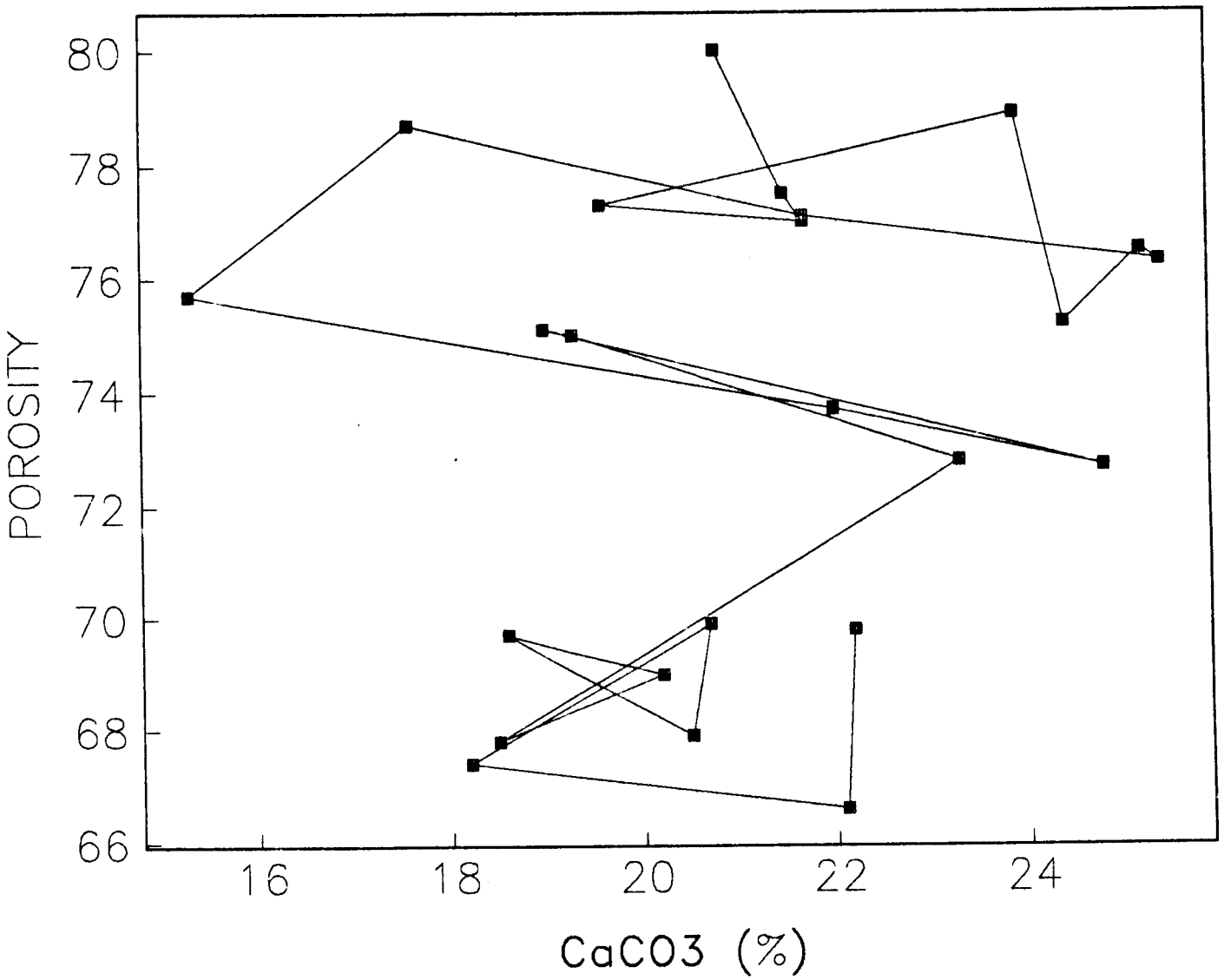

IG47-1 CORE 2

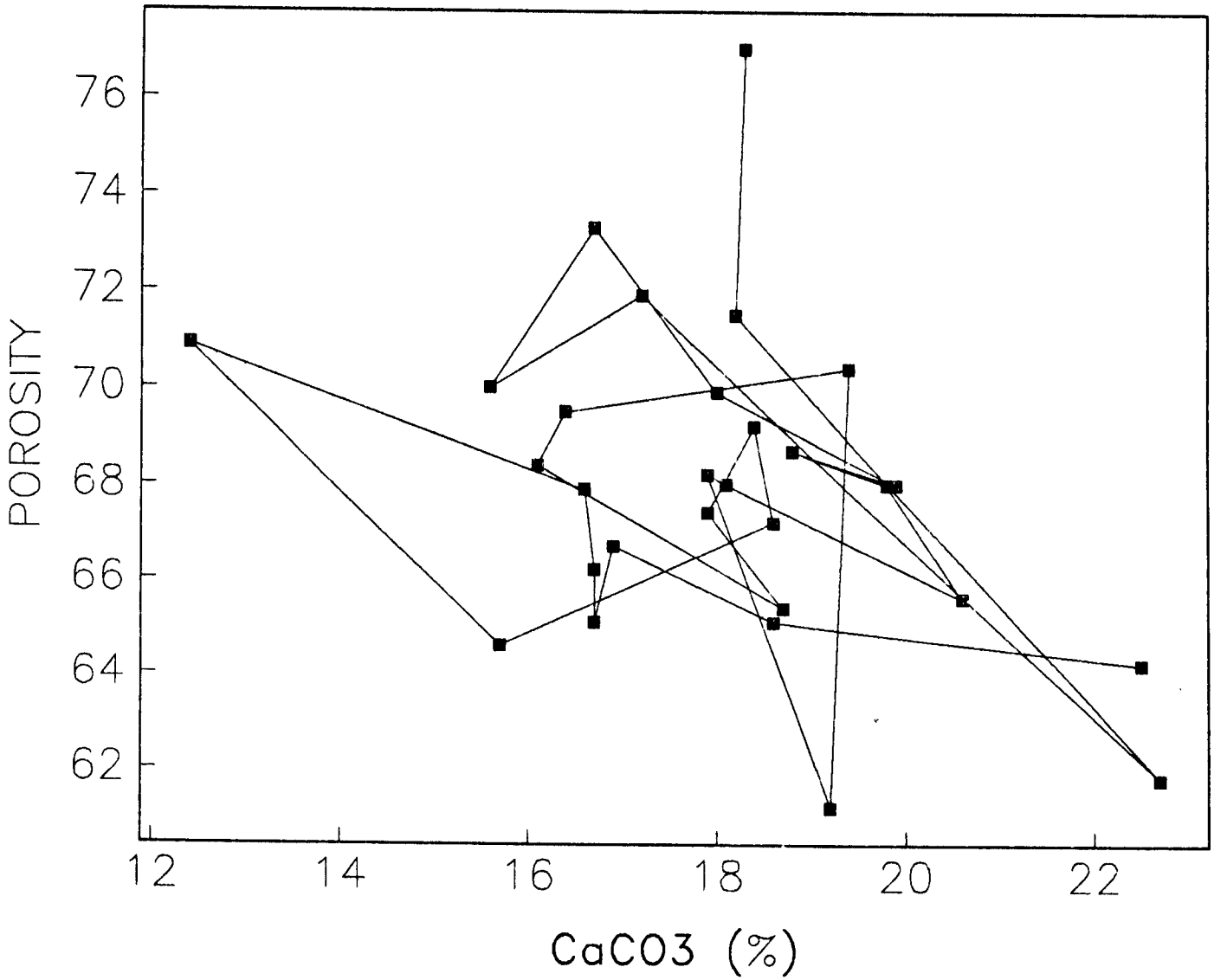

IG47-2 CORE 1

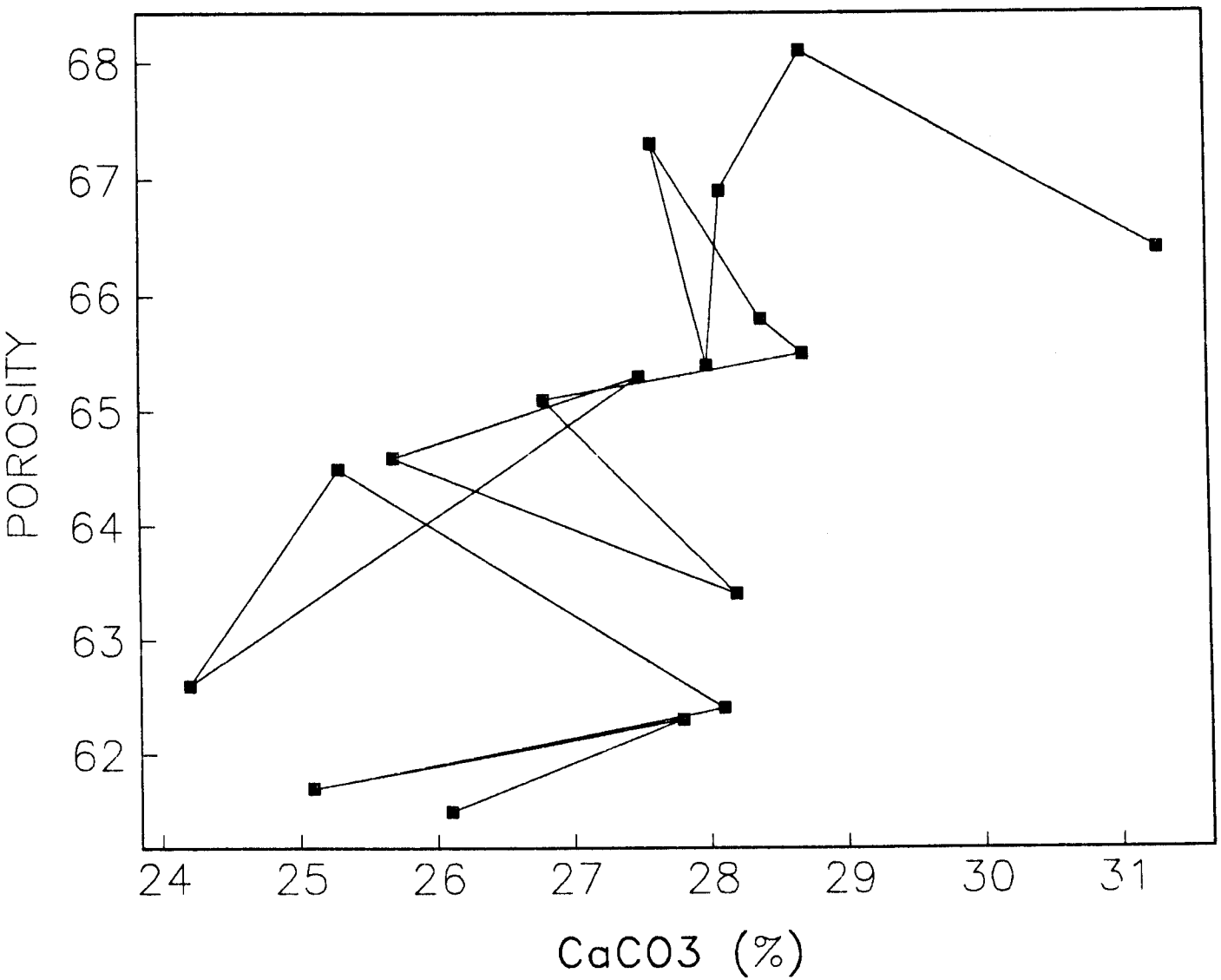

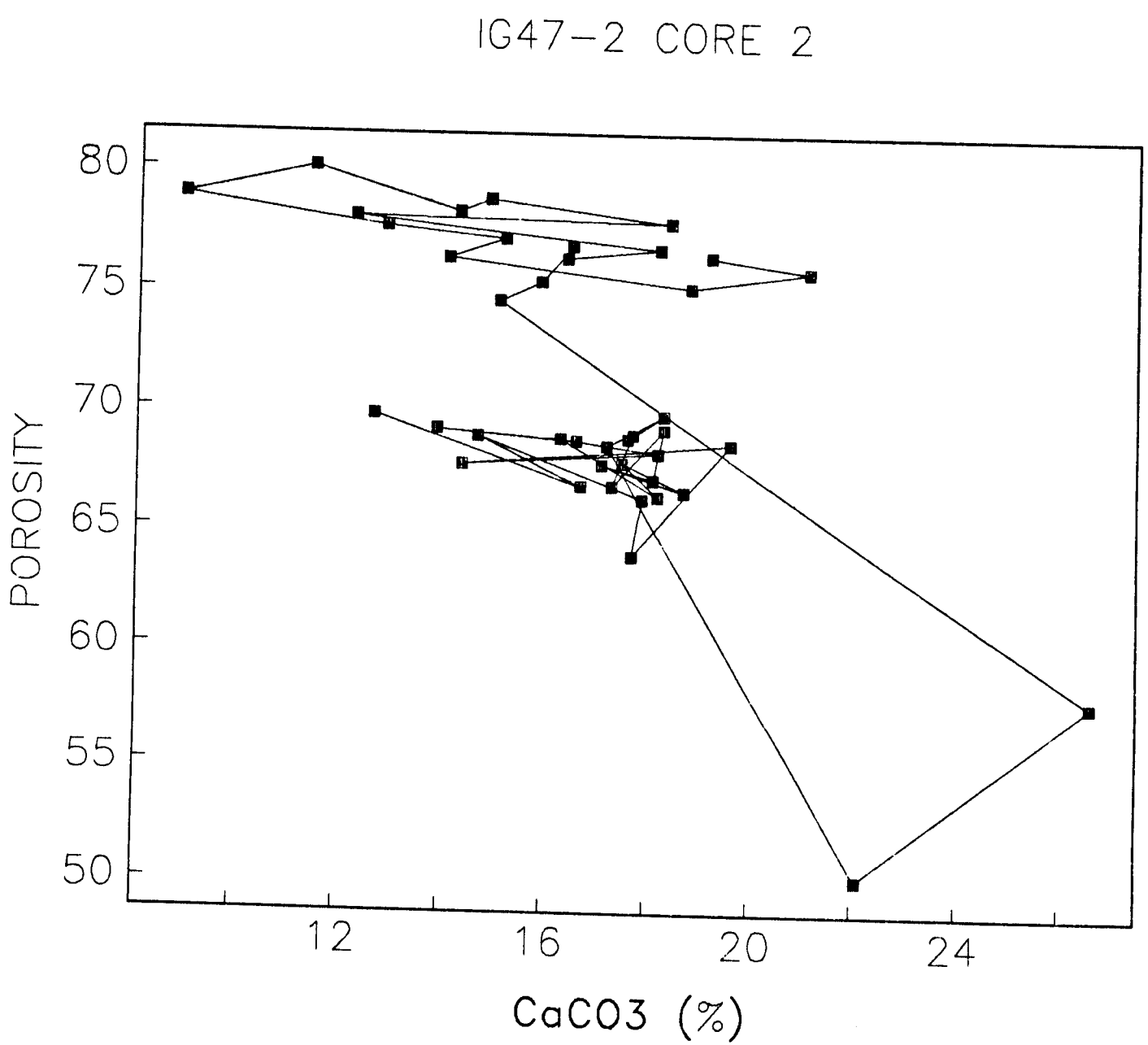
IG47-2 CORE 2
80
75
70
65
60
55
50
POROSITY
12
16
20
24
CaCO3 (%)

IG47-2 CORE 3

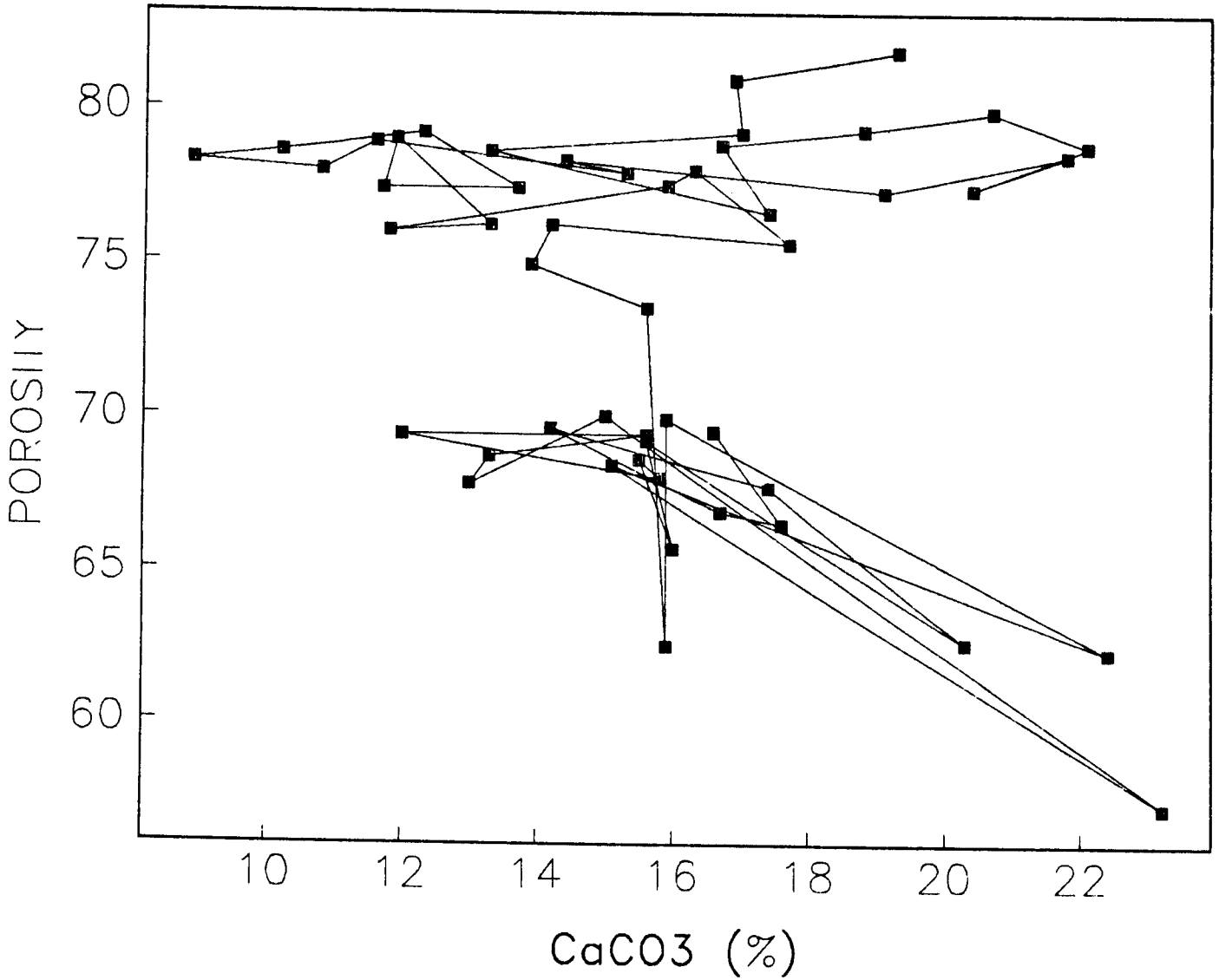

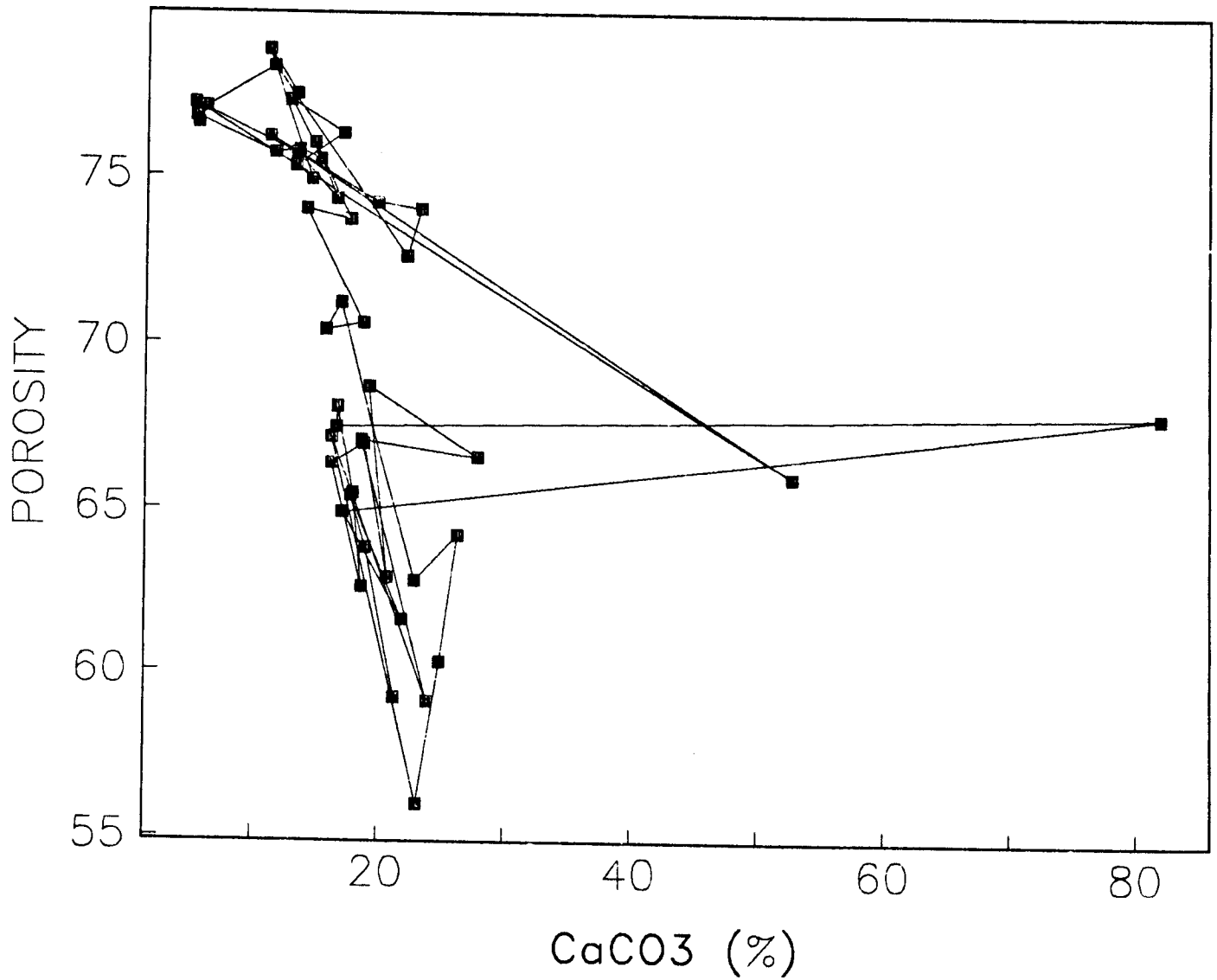
IG47-2 CORE 4
POROSITY
75
70
65
60
55
20
40
60
80
CaCO3 (%)

IG47-2 CORE 5

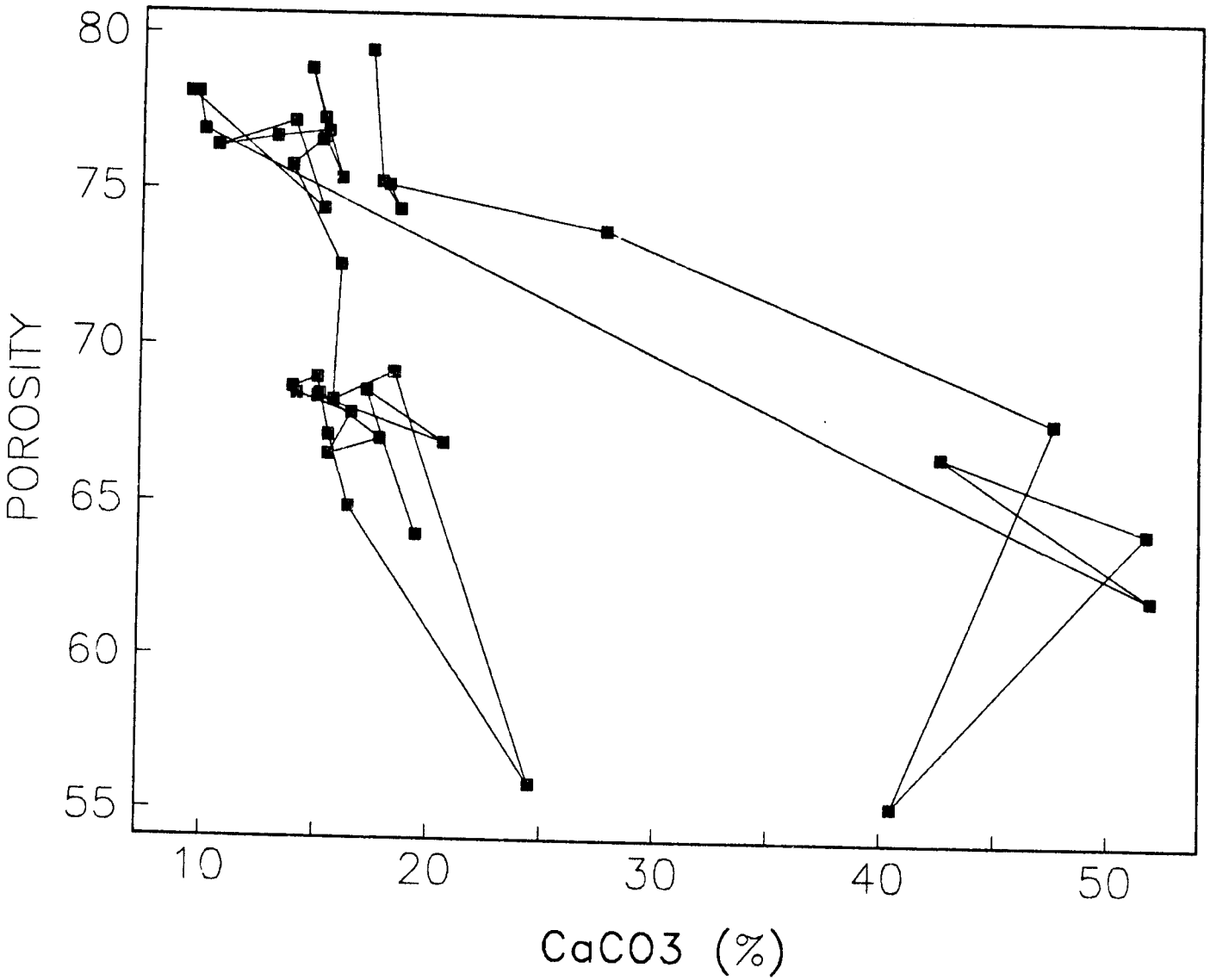

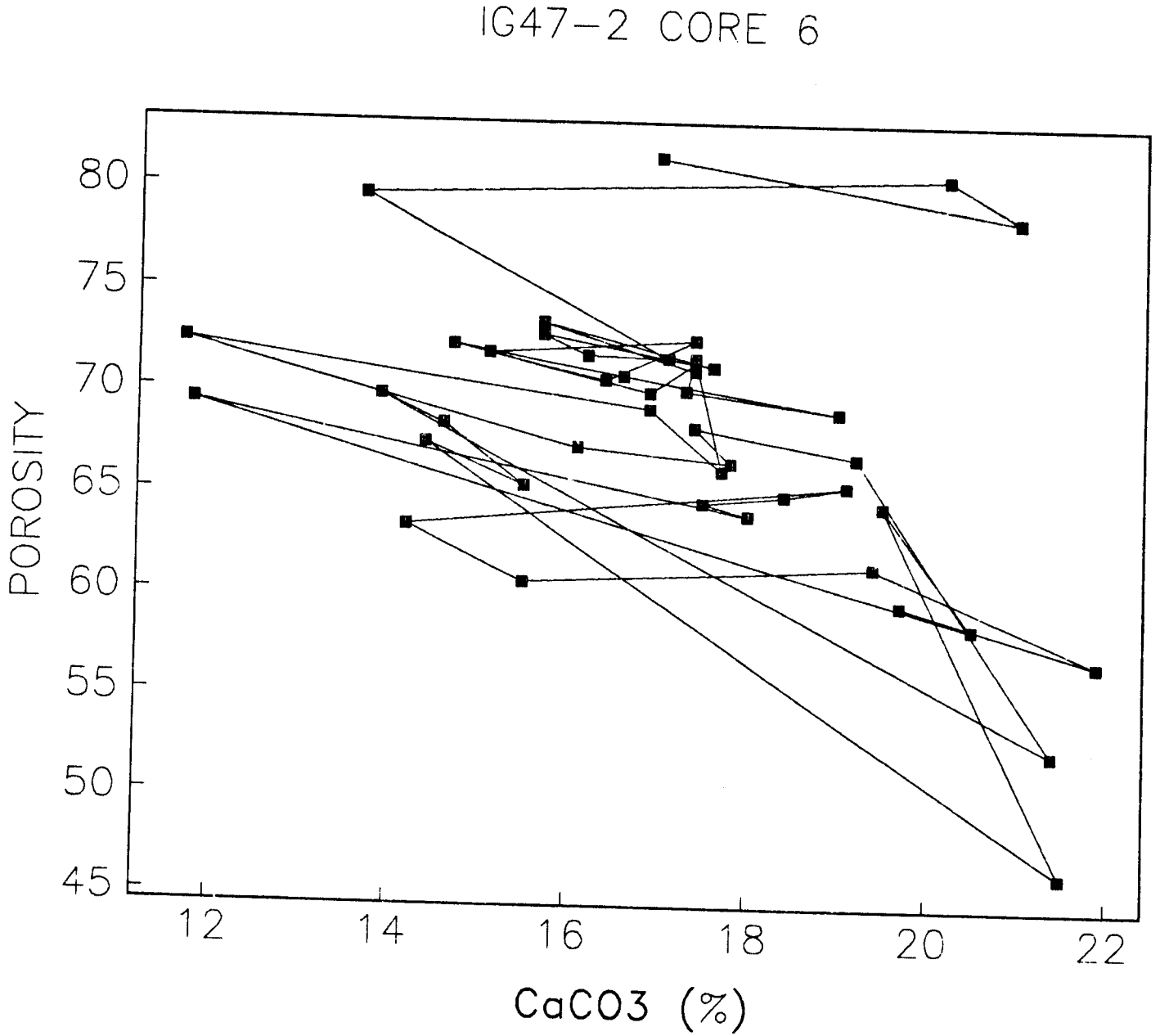
IG47-2 CORE 6
POROSITY
80
75
70
65
60
55
50
45
12
14
16
18
20
22
CaCO3 (%)

IG47-2 CORE 7

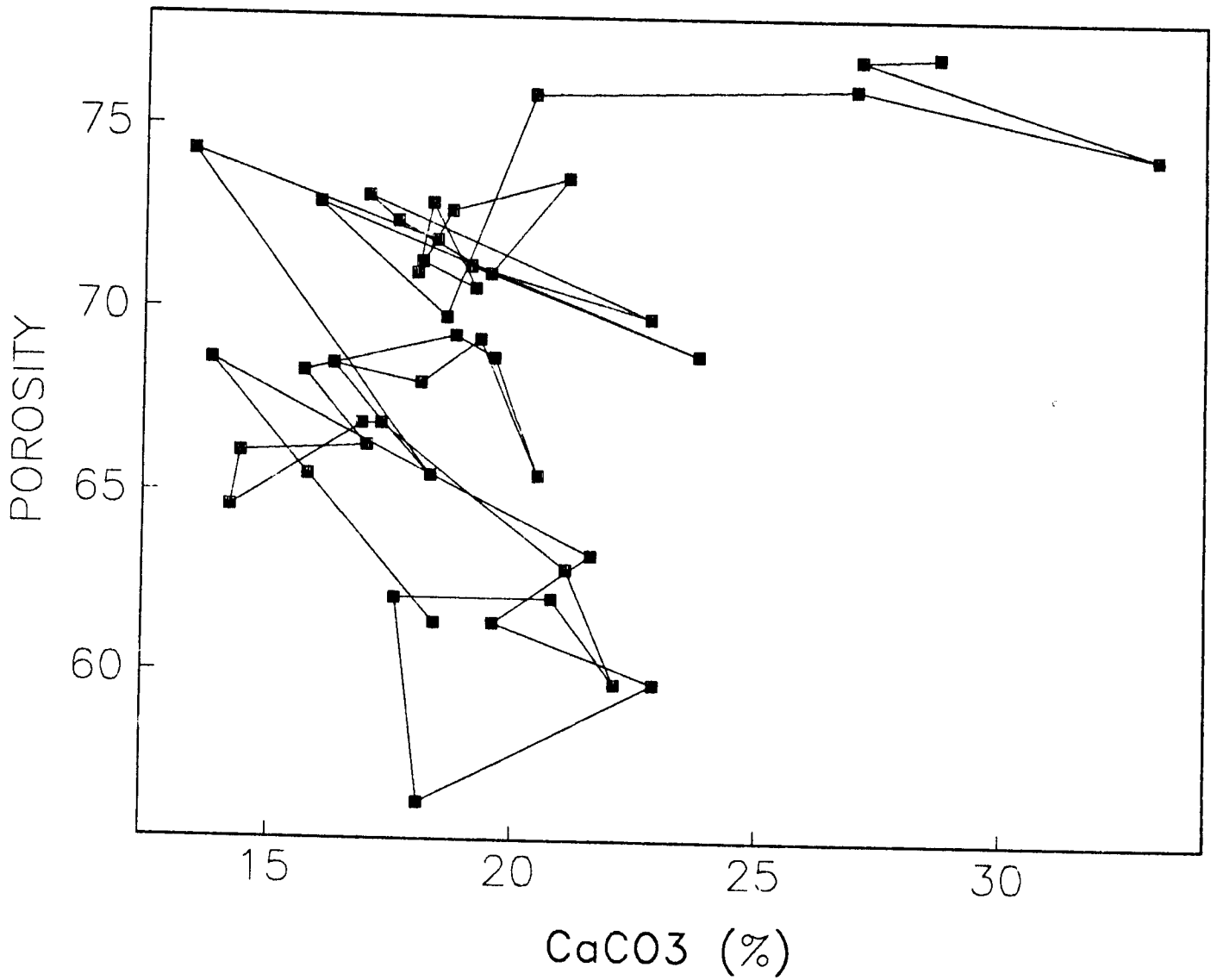

IG47-2 CORE 8

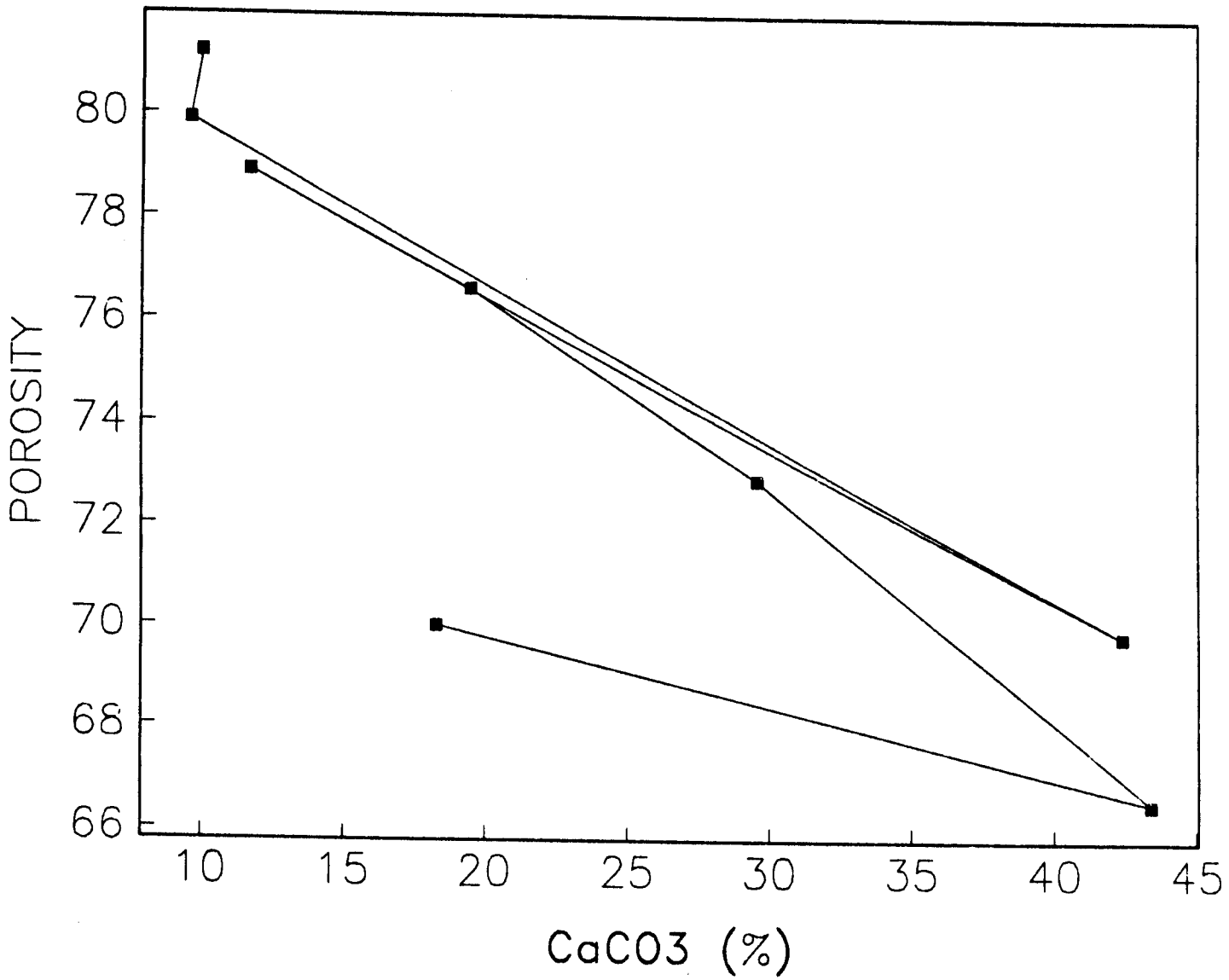

IG47-2 CORE 9

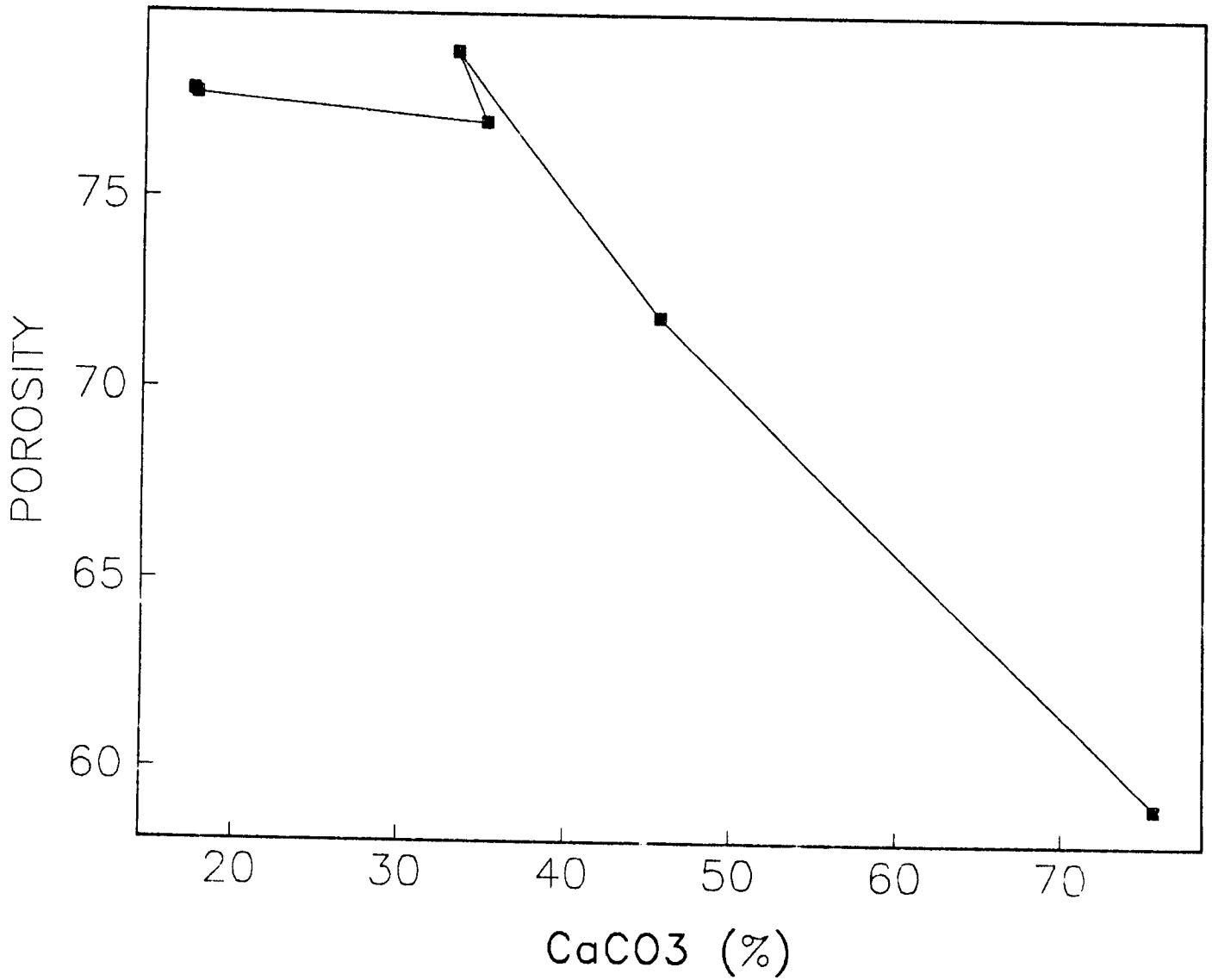

IG47-2 CORE 10

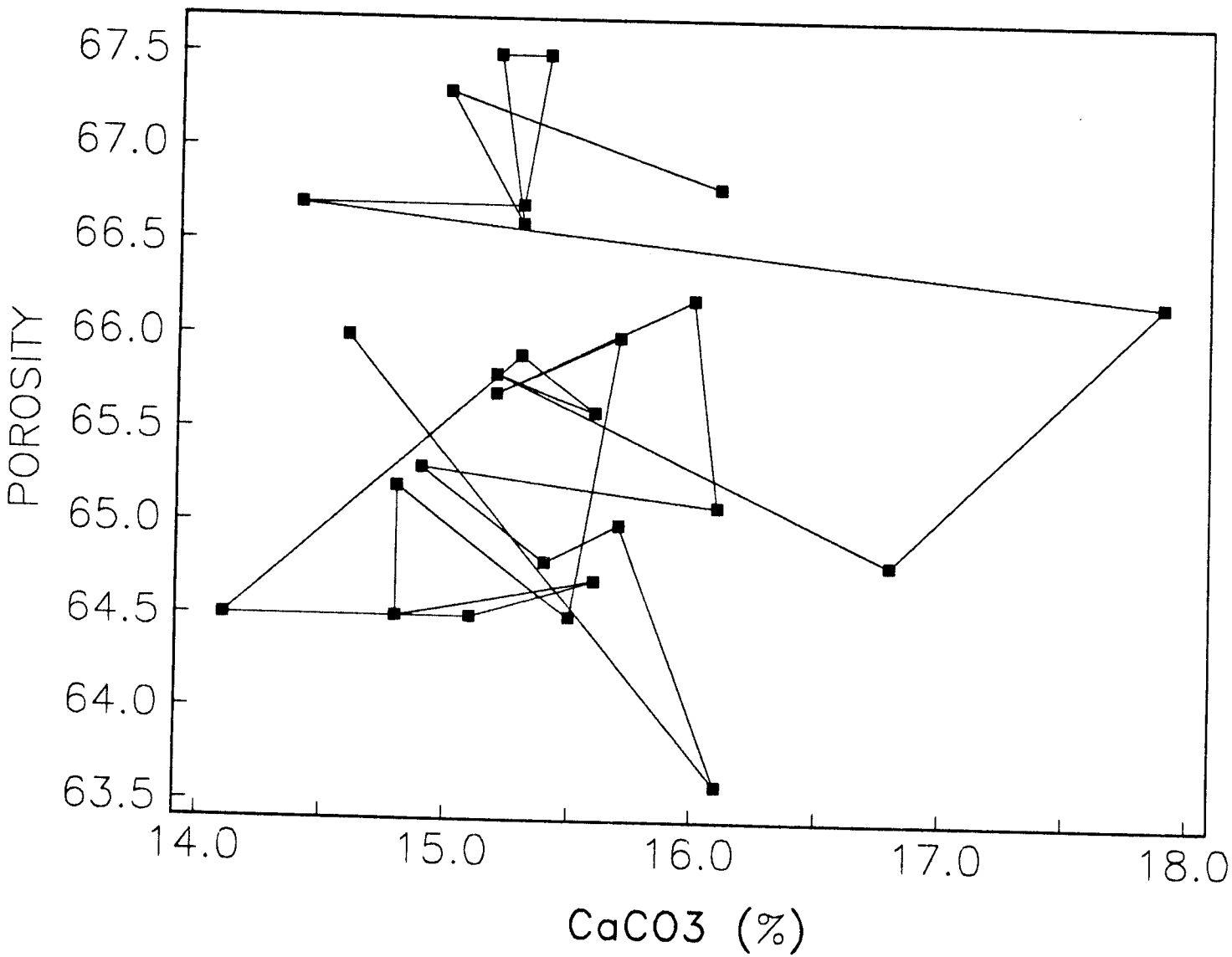

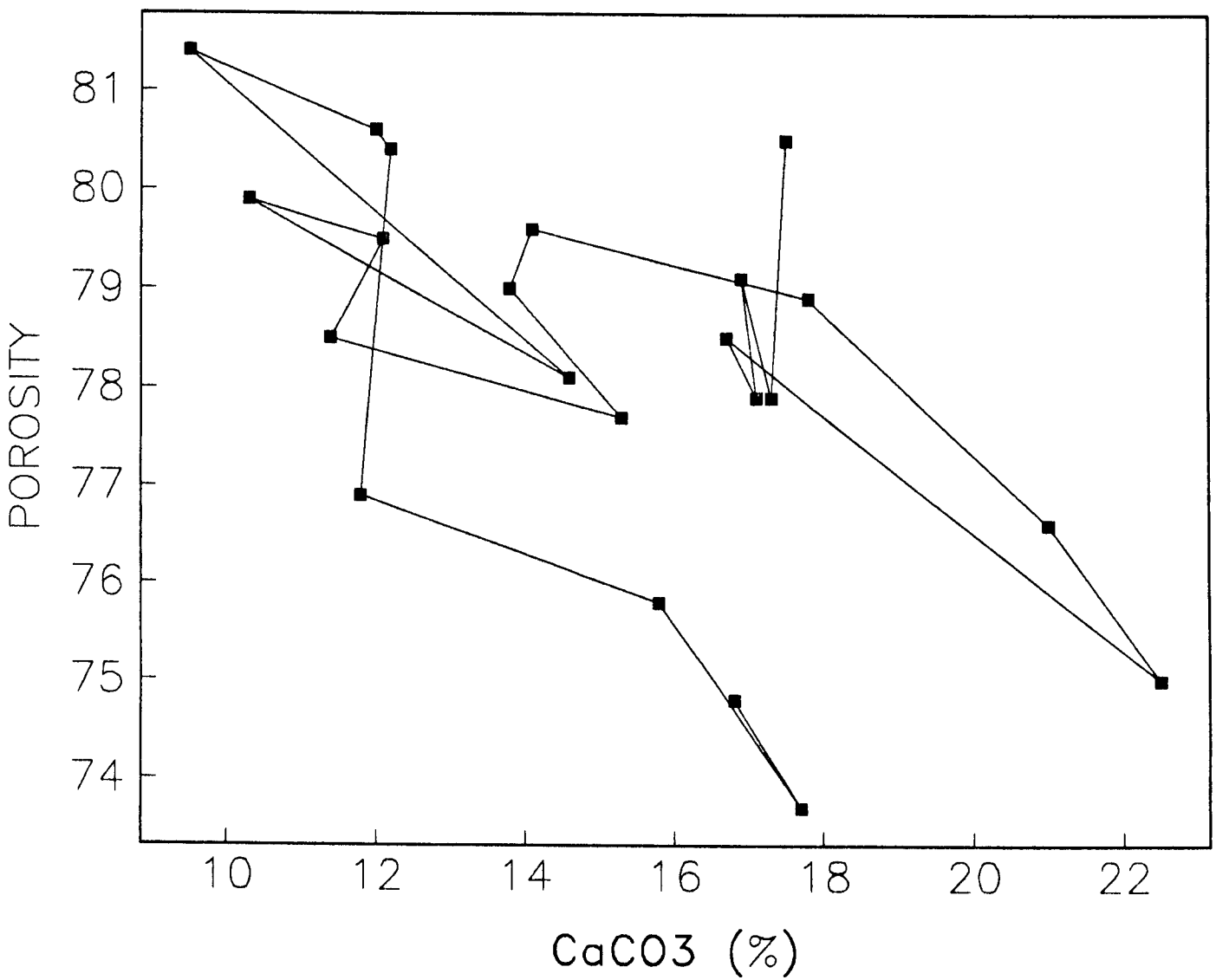
IG47-2 CORE 11
POROSITY
81
80
79
78
77
76
75
74
10
12
14
16
18
20
22
CaCO3 (%)

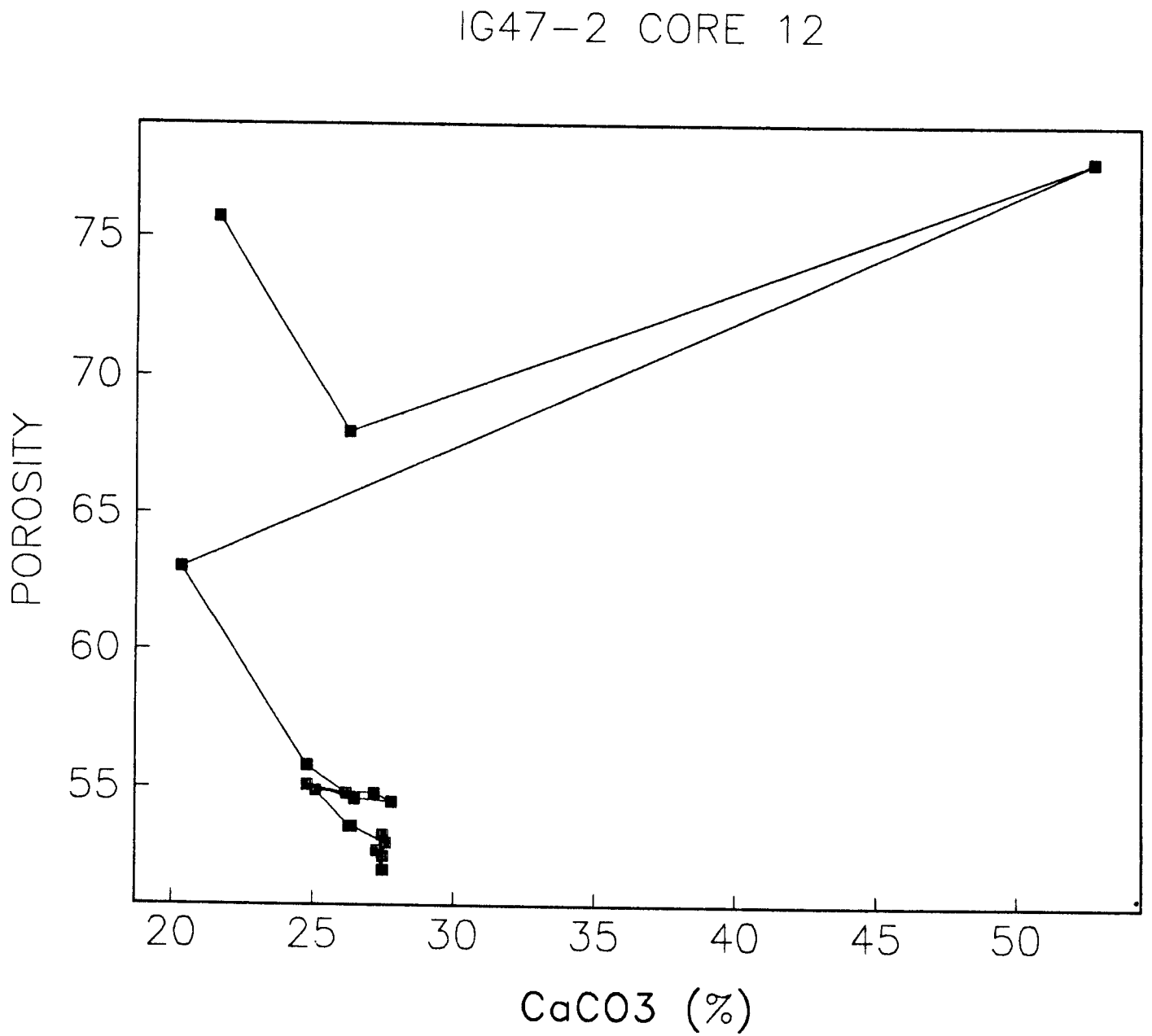
IG47-2 CORE 12
POROSITY
75
70
65
60
55
20
25
30
35
40
45
50
CaCO3 (%)

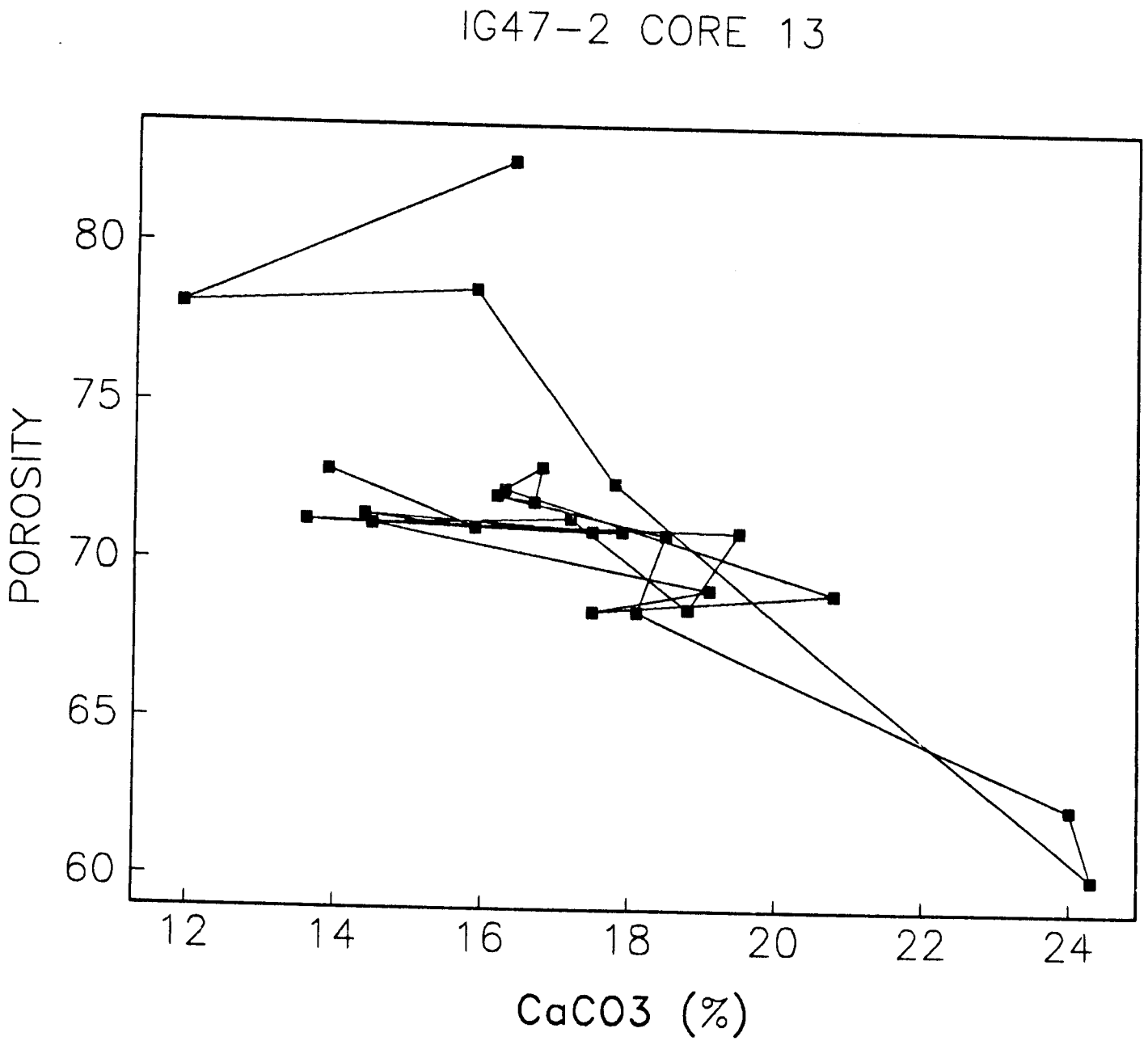
IG47-2 CORE 13
POROSITY
80
75
70
65
60
12
14
16
18
20
22
24
CaCO3 (%)

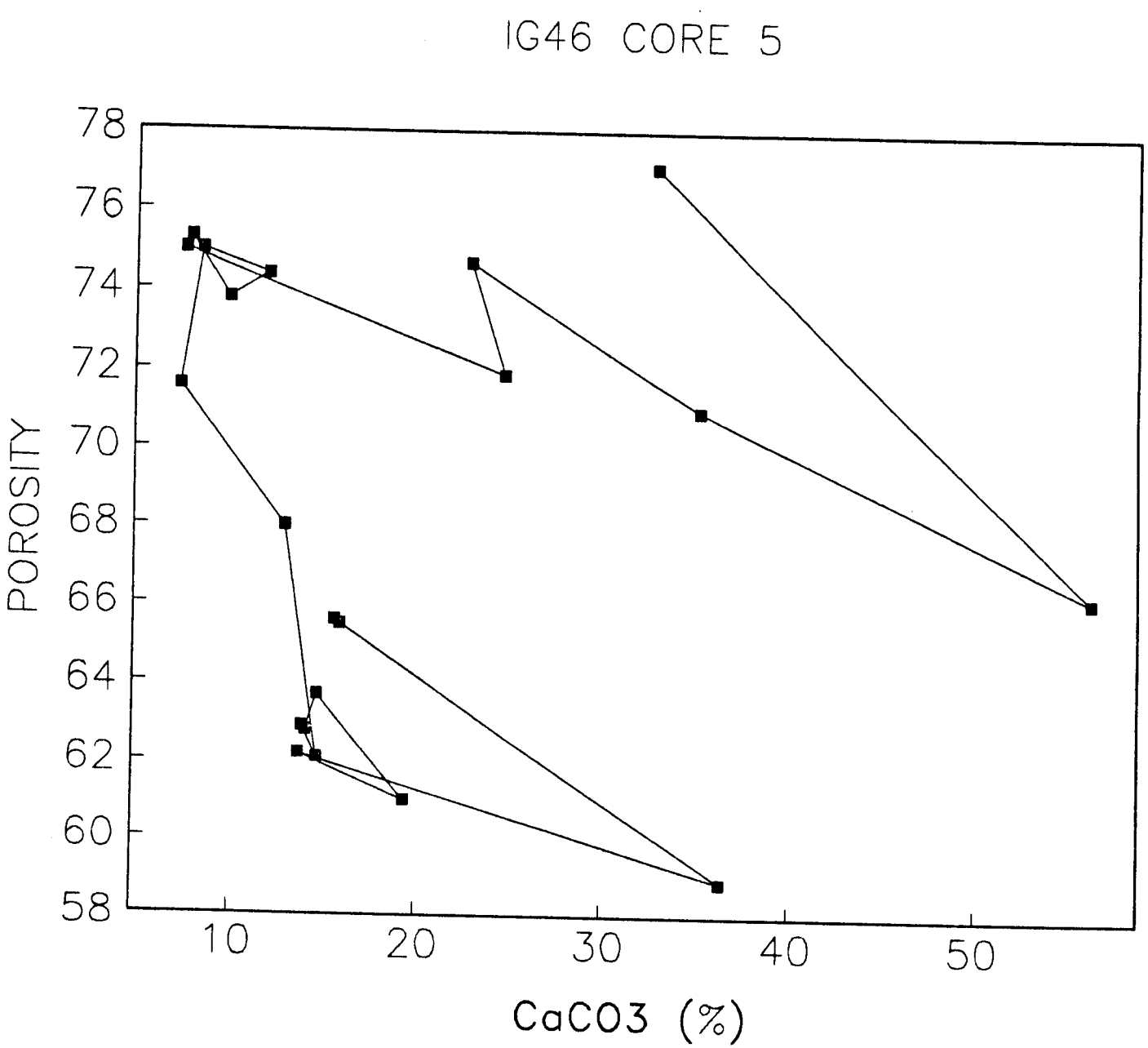
IG46 CORE 5
POROSITY
78
76
74
72
70
68
66
64
62
60
58
10
20
30
40
50
CaCO3 (%)

PART II.

UPPERSLOPE OILSEEP STUDY

GEOCHEMICAL AND STABLE ISOTOPE RESULTS

FINAL REPORT

DECEMBER, 1983

TABLE OF CONTENTS

LIST OF TABLES

LIST OF FIGURES

BACKGROUND

The report details an organic geochemistry and stable isotope survey of 13 cores which were taken on the slope of the northwestern Gulf of Mexico. The locations of the cores are given in Table C-1 and Figure C-1. The geological setting, geophysical data and selected physical-chemical data are tabulated in another section of the overall report. Nine (9) of the 13 cores had readily detected liquid petroleum, using a hand held ultraviolet light to locate fluoresence. Just prior to opening the plastic core liners to subsample the sediment it was noticed that gas spaces were present in several of the cores. It was decided to sample and analyze the gases rather than work up the 4 cores which showed no evidence of containing oil.

The study is divided into three parts: (1) isolation, fractionation and gas chromatographic analyses of liquid bitumen, (2) isolation and gas chromatographic analyses of hydrocarbon gases, and (3) stable isotope analyses of these various components. The methods used to do these three analyses, the data set generated and an interpretation is given in the following pages.

LIQUID BITUMEN: CHEMICAL CHARACTERIZATION

Methods

The cores were kept at ambient temperature on shipboard, and at 4°C in the Galveston laboratory. The plastic liners were split, the cores split and subsamples taken at the Galveston laboratory. Fluorescence of oil under UV light was used as a guide for subsampling, some consideration was given to even spacing of subsamples. The subsamples were taken to the Port Aransas laboratory for geochemical studies. There the samples were stored at -20°C until used.

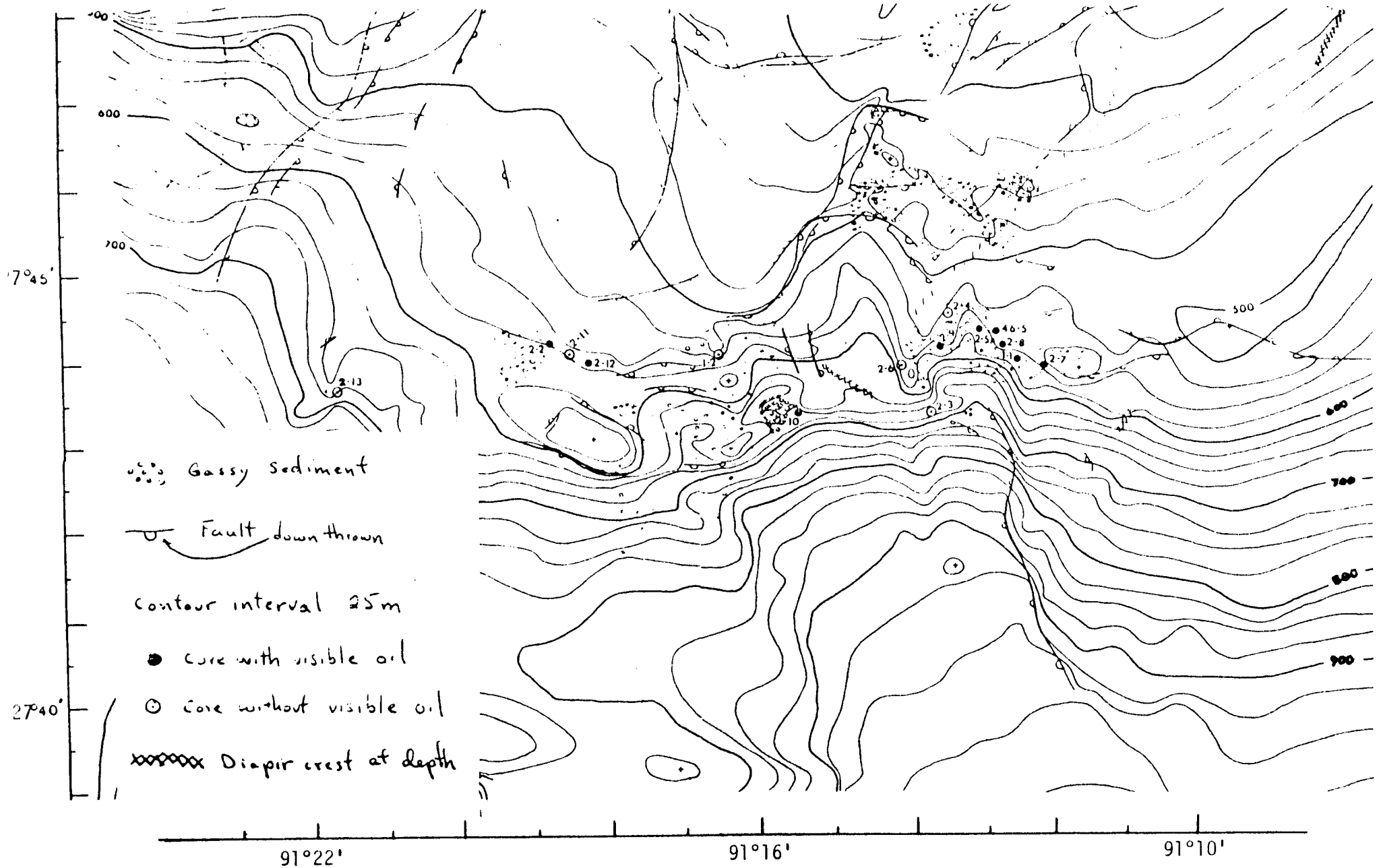

Figure C-1. Location of Cores.

Table C-1. Location of Cores

Core #	Latitude N	Longitude W	Core Length (cm)	Water Depth (m) uncorrected
IG46-5	27°44'.40	91°12.65		
IG47-1				
1.	27 44.10	91 12.40	485	600
2.	27 44.05	91 16.32	602	541
IG47-2-				
1.	27 35.31	91 21.99	378	918
2.	27 44.21	91 18.60	1001	552
3.	27 43.38	91 13.51	1015	669
4.	27 44.56	91 13.32	1150	538
5.	27 44.43	91 12.93	1006	554
6.	27 44.06	91 13.70	907	549
7.	27 44.02	91 12.27	966	541
8.	27 44.27	91 12.58	833	538
9.	27 44.21	91 13.43	311	552
10.	27 43.44	91 15.35	579	627
11.	27 44.09	91 18.33	479	560
12.	27 43.98	91 18.10	393	549
13.	27 43.60	91 21.44	521	673

Total bitumen, methanol-benzene soluble material, was recovered from the sediment subsamples by refluxing. Three extractions were usually adequate to remove all colored material from the sediment. The methanol-benzene extracts were taken to near dryness by roto-evaporation under vacuum at 50°C. Hexane was added and the remaining methanol and benzene removed by repeated roto-evaporation. A suitable aliquot of the total bitumen was separated into three fractions, corresponding to saturated, unsaturated and polar molecules, by silica gel chromotography. The solvents used to elute were hexane, benzene and methanol. The total bitumen and fractions were submitted to stable isotope analysis and selected saturated and unsaturated fractions to gas chromatography. All subsampling was quantitative so that the data can be expressed as percent. Care was taken to use distilled solvents, glassware cleaned in an oven and a contamination free laboratory.

The aliquots for gas chromatography were taken into a quantity of hexane, in microliters, being 10 times the weight of the sample in milligrams. Three microliters of this solution was injected giving a total weight of samples injected equal to 0.3 mg hydrocarbons for each sample. The chromatographic analysis was performed using a Perkin-Elmer Model 910 gas chromatograph (FID) with a 25 meter OV-101 wall-coated open tubular column of 0.25mm fused silica. Helium carrier gas flow rate was 3mm per minute with a make-up flow rate of 25 ml per minute; the temperature was programmed from 100 to 270°C at 7.5°C per minute. Data was recorded using a H-P Model 3352B integrator and appropriate supporting accessories.

Table C-2. Total Bitumen Content of IDA GREEN Cores.
(percent of dry sediment)

Depth	46-5	47-1-1	47-2-2	47-2-5	47-2-6	47-2-7	47-2-9	47-2-12	47-2-13
	4.02								0.02
	4.43	0.11				0.21	3.5		
50		0.06		0.23				1.46	
		0.10							
	4.26								
		0.10					6.8	0.2	
100	4.49			0.12		0.18			
		0.11							
	1.63	0.12						0.2	
		0.08					8.6		
150				0.09					
	2.33	0.12					7.2		
								0.1	
		0.07				0.08	6.4		
200	0.91		0.03	0.34					
		0.16							
		0.05					3.8	0.1	
250		0.07		0.11					
		0.11					2.0		
	0.79								
300		0.10		0.07		0.09			
		0.22						0.1	
		0.58							
		1.4							
350									
		0.24							
			0.05						
400		0.21							
	0.14	0.23							
									0.03
		0.06							
450		0.06							
		0.06				0.06			
			0.05						
		0.4							
500			0.08						
				0.09					
			0.08						
						0.06			
550									
						0.12			
600									
			0.03						
650									
				0.16					
700					0.03				
750			0.04						
						0.10			
800									
850				0.05					
					0.07	0.06			

Results

The total bitumen content of the 9 oil bearing cores are summarized in Table C-2. Four of the cores are rich in total bitumen with values greater than 1 percent. Cores 46-5 and 47-2-9 are very rich, with values up to 8.6 percent. The oil is not usually distributed in the cores in a homogeneous way. Several cores (47-1-1 and 47-2-12) have greater than 1 percent at specific depths, but fairly low values in the rest of the core. The visible (with UV light) oil occurrences have been classified as liquid veins, disseminated or as coating fractures. The distribution based on these visual observations are detailed in the Core Logs in Part I. Appendix B.

The results of the silica gel chromatography are given in Tables C-3 through C-9. No trends with regard to saturates, aromatics and NSO compound, with depth in core are obvious. Nor are any trends from core to core noted. Gravity (°API) determinations were made for core IG-46-5 with the following results:

10 cm	10.7 °API gravity
40	14.5
70	16.2
100	14.8
130	16.3
160	17.6

Sample 40-45 of core IG-46-5 contained 2.5 percent organic sulfur. This is consistent with the °API gravity data. Many samples were too low in bitumen content for silica gel analysis, and for stable carbon isotope analyses. In the case of IG47-2-12 the oil poor samples were pooled. It was decided to reserve the small samples for future chemical work rather

Table C-3. Composition of Bitumen. Core IG46-5

Interval (cm)	Bitumen (%)	Hexane[a] (%/ $\delta^{13}C$)	Benzene[b] (%/$\delta^{13}C$)	MeOH[c] (%/$\delta^{13}C$)	Carbonate ($\delta^{13}C$)	Residue[d] ($\delta^{13}C$)
10-15	4.0 -26.5	22.4 -26.8	51.3 -	27.1 -26.3	-12.4	-24.7
40-45	4.4 -26.7	25.7 -26.6	44.7 -26.4	20.3 -27.1	-27.5	-36.7
70-75	4.3 -26.3	36.4 -26.2	38.6 -26.3	17.4 -26.6	-22.7	-30.6
100-115	4.5 -26.4	34.8 -26.3	42.3 -26.2	17.6 -26.6	-9.6	-26.1
130-135	1.6 -	34.8 -26.3	44.3 -26.4	13.4 -26.3	-3.9	-24.5
160-165	2.3 -26.2	44.1 -26.2	45.0 -26.2	11.5 -26.2	-0.2	-25.2
190-195	0.91 -26.3	40.0 -26.4	38.0 -26.2	14.0 -26.6	+0.6	-24.2
280-285	0.79 -26.3	33.9 -26.4	42.0 -26.6	13.9 -26.6	-5.0	-26.0
410-415	0.14 -26.7	13.7 -26.7	23.0 -26.6	18.9 -27.0	-1.6	-25.7

[a,b,c]Refers to the hexane, benzene or methanol eluate of the total bitumen sample from silica gel chromatography

[d]Residue is the non-lipid organic matter remaining in the sediment after extraction.

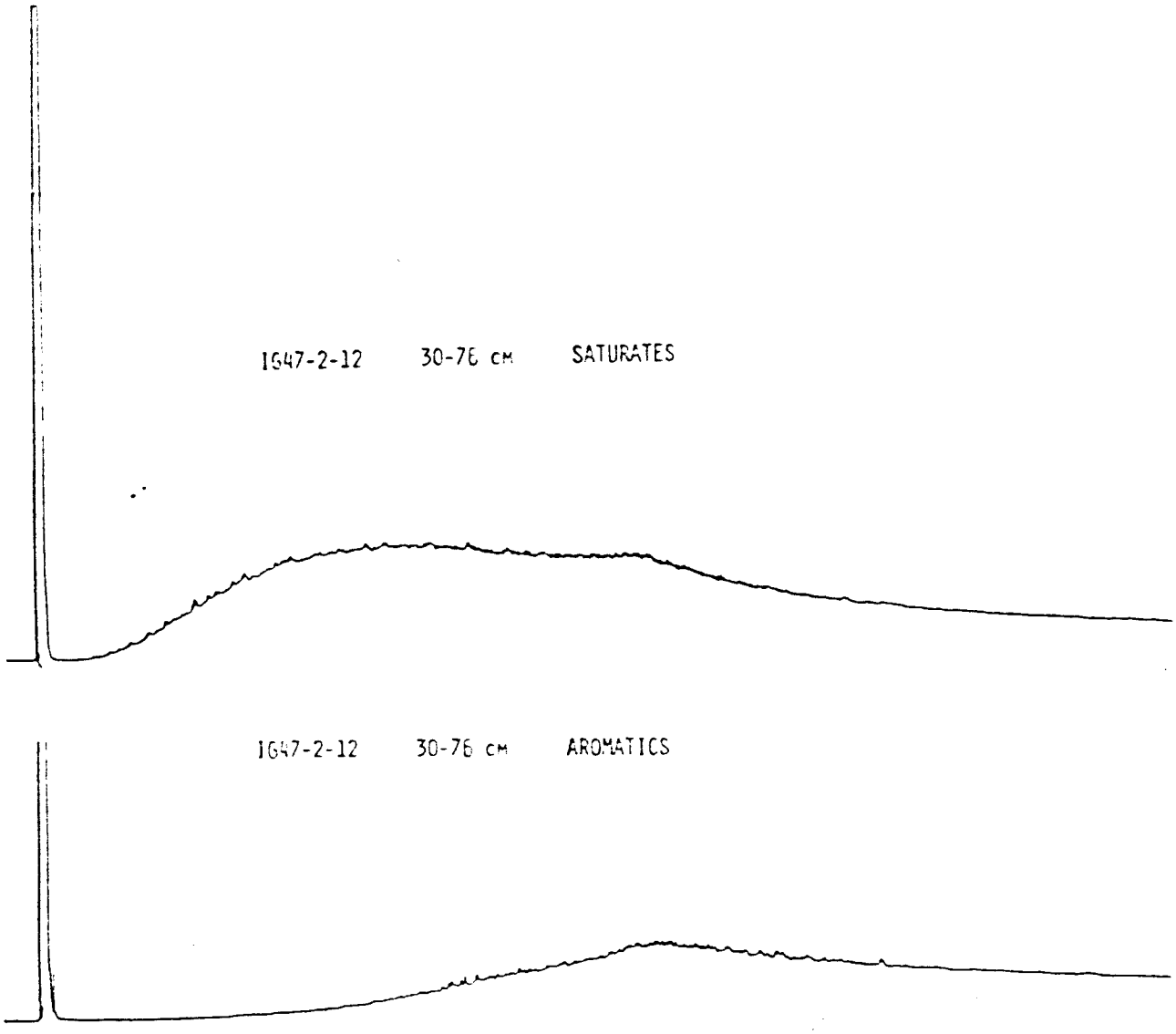

Figure C-2. GC of Bitumen Fractions,
Core IG47-2-12 (30-76cm).

Table C-4. Composition of Bitumen. Core IG47-1-1

Depth (cm)	Bitumen (%)	Hexane (%/$\delta^{13}C$)	Benzene (%/$\delta^{13}C$)	MeOH (%/$\delta^{13}C$)	Carbonate ($\delta^{13}C$)	Residue ($\delta^{13}C$)
0-40	0.11 -26.5	10.8	28.7	23.8	-0.5	-21.1
40-60	0.06 -26.7					-21.4
60-80	0.10 -26.5					-21.4
80-100	0.10 -26.7					-21.5
100-120	0.11 -26.5				-0.4	-21.8
120-140	0.12 -26.2					-21.5
140-160	0.08 -26.4					
160-180	0.12 -26.5				-2.1	
180-200	0.07 -27.5					
200-220	0.16 -27.6				-1.1	
220-240	0.05 -28.3					
240-260	0.07 -28.1				-5.4	-25.4
260-280	0.11 -					-25.6

Table C-4 (Cont.) Core IG47-1-1

Depth (cm)	Bitumen (%)	Hexane (%/$\delta^{13}C$)	Benzene (%/$\delta^{13}C$)	MeOH (%/$\delta^{13}C$)	Carbonate ($\delta^{13}C$)	Residue ($\delta^{13}C$)
280-300	0.10 -27.9				-17.00	-24.8
300-320	0.22 -26.9					-24.6
320-340	0.58 -26.5	25.0	34.2	21.1		-25.0
340-360	1.4 -26.4	29.2 -26.5	37.8 -26.5	18.3 -26.4	-5.4	-25.7
360-380	0.24 -26.7	26.7 -26.7	29.2 -27.2	28.1 -27.8		-25.8
380-400	0.21 -26.6	20.5	25.1	24.8		-25.5
400-420	0.23 -26.7	30.8	36.2	25.0	-16.2	-26.1
420-440	0.06 -27.6	17.9	19.8	52.6	-4.7	
440-460	0.06 -27.9	13.5	17.2	32.2		
460-478	0.06 -28.1	16.8	21.3	52.7	-7.7	-25.8
480	0.4 -26.9	39.2 -26.5	41.4 -26.7	16.4 -27.6	-23.9	-27.0

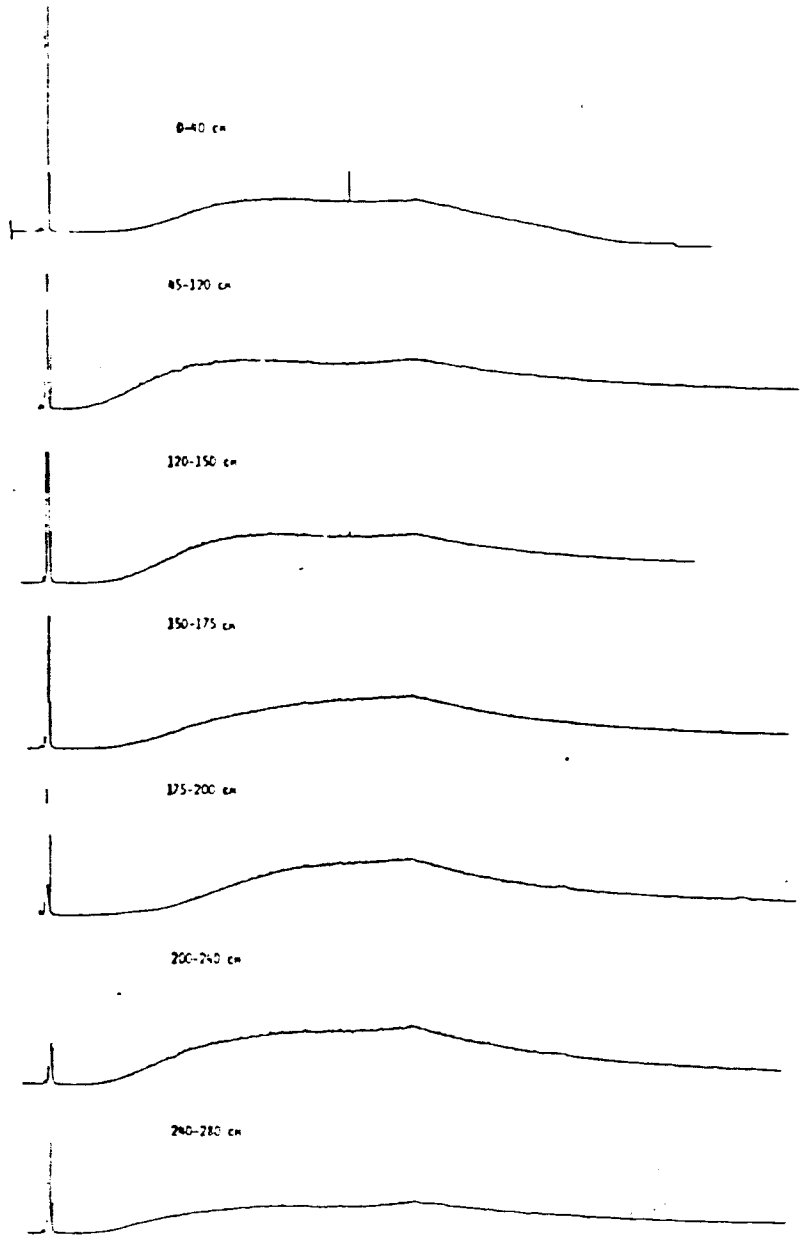

Figure C-3. GC of Bitumen Saturate Fractions, Core IG47-2-9.

Table C-5. Composition of Bitumen. Cores IG47-2-2 & IG47-2-5

Depth (cm)	Bitumen (%)	Hexane (%)	Benzene (%)	MeOH (%)
Core IG47-2-2				
200-240	0.03	15.0	26.5	47.2
380-400	0.05	43.6	23.6	29.9
490-510	0.05			
510-530	0.08			
530-550	0.08	34.2	20.9	29.5
640-660	0.03			
750-770	0.04			
Core IG47-2-5				
50-70	0.23	28.5	29.2	24.8
100-120	0.12			
150-170	0.09			
200-220	0.34	45.0	29.9	18.0
250-270	0.11			
290-310	0.07			
530-550	0.09			
680-700	0.16	35.1	25.6	26.8
850-870	0.05			

Table C-6. Composition of Bitumen. Core IG47-2-7

Depth (cm)	Bitumen (%)	Hexane (%/$\delta^{13}C$)	Benzene (%/$\delta^{13}C$)	MeOH (%/$\delta^{13}C$)	Carbonate ($\delta^{13}C$)	Residue ($\delta^{13}C$)
10-40	0.21 -26.4	14.8 -27.1	35.0 -26.4	23.8 -26.3	-0.4	-21.8
80-120	0.18 -27.8	12.7 -27.2	21.1 -26.8	17.0 -26.9	-3.5	-25.2
180-210	0.08 -28.6	21.2 -29.1	18.5 -28.7	27.8 -29.2	-16.1	-26.9
250-310	0.09 -26.8	29.1 -27.1	25.4 -26.8	30.4 -28.2	-12.2	-26.1
450-470	0.06 -28.6	13.2 -29.6	15.8 -28.4	60.2 -28.8	-3.0	-26.5
530-550	0.06 -27.4	22.1 -27.3	22.2 -27.2	23.6 -28.3	-1.4	-26.0
570-600	0.12 -27.2	24.0 -26.9	20.8 -26.8	23.3 -28.2	-1.3	-25.7
750-780	0.10 -27.6	21.8 -28.1	16.9 -28.0	16.9 -28.8	-0.2	-25.7
880-905	0.06 -27.9	19.6 -28.1	15.0 -28.0	24.7 -28.8	-0.5	-26.3

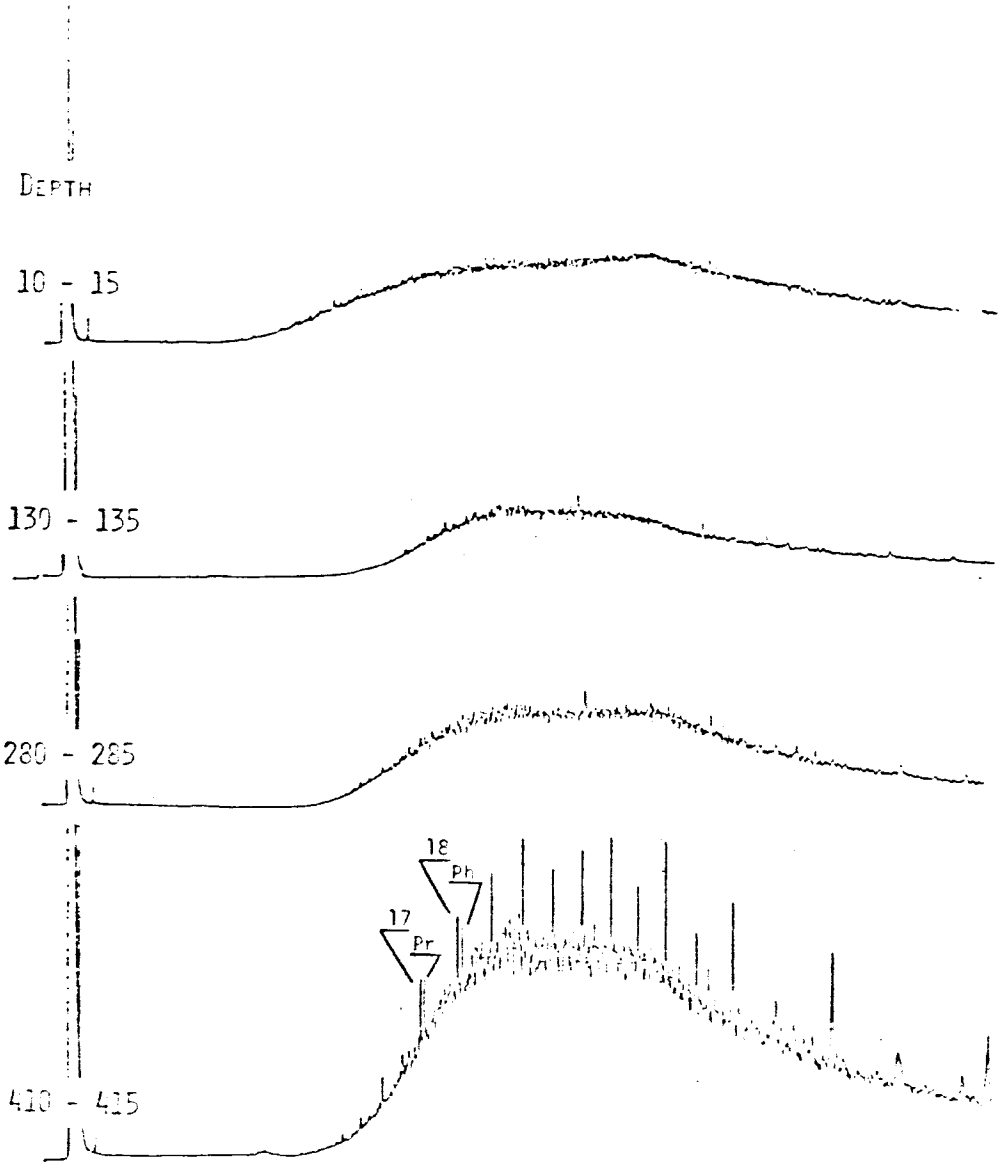

Figure C-4. GC of Bitumen Saturate Fractions,
Core IG46-5.

Table C-7. Composition of Bitumen. Core IG47-2-9

Depth (cm)	Bitumen (%/$\delta^{13}C$)	Hexane (%/$\delta^{13}C$)	Benzene (%/$\delta^{13}C$)	MeOH (%/$\delta^{13}C$)
0-40	3.5 -26.6	20.8 -26.9	58.5 -26.2	21.8 -
45-120	6.8 -	24.7 -26.7	49.8 -26.0	24.7 -26.5
120-150	8.6 -26.5	24.7 -26.8	58.9 -26.2	18.2 -26.6
150-175	7.2 -26.7	29.0 -26.7	50.6 -26.7	20.6 -26.9
175-200	6.4 -26.7	29.1 -26.7	45.9 -26.2	19.6 -27.0
200-240	3.8 -26.7	29.2 -26.7	35.7 -26.7	16.0 -
240-280	2.0 -	32.7 -26.6	42.2 -26.2	13.6 -27.7

Table C-8. Composition of Bitumen. Core IG47-2-12

Depth (cm)	Bitumen (%)	Hexane (%/$\delta^{13}C$)	Benzene (%/$\delta^{13}C$)	MeOH (%/$\delta^{13}C$)	Carbonate ($\delta^{13}C$)	Residue ($\delta^{13}C$)
30-76	1.46 -26.8	23.3 -26.6	40.1 -26.7	16.2 -27.0	sm -13.2[a] md -21.4 lg -23.0	-27.9
80-100	0.2 -26.8					
120-140	0.2 -26.8					
160-180	0.1 -27.0	48.1[b]	19.9	20.6		
220-240	0.1 -26.8					
310-330	0.1 -26.8					

[a]Carbonates in this sample were analyzed separately by grain size. sm = fines, md = lumps of about 1 mm diameter, lg = nodules of about 10 mm diameter.

[b]Extracts of all samples from 80 cm to 330 cm depth were combined for silica gel chromatography.

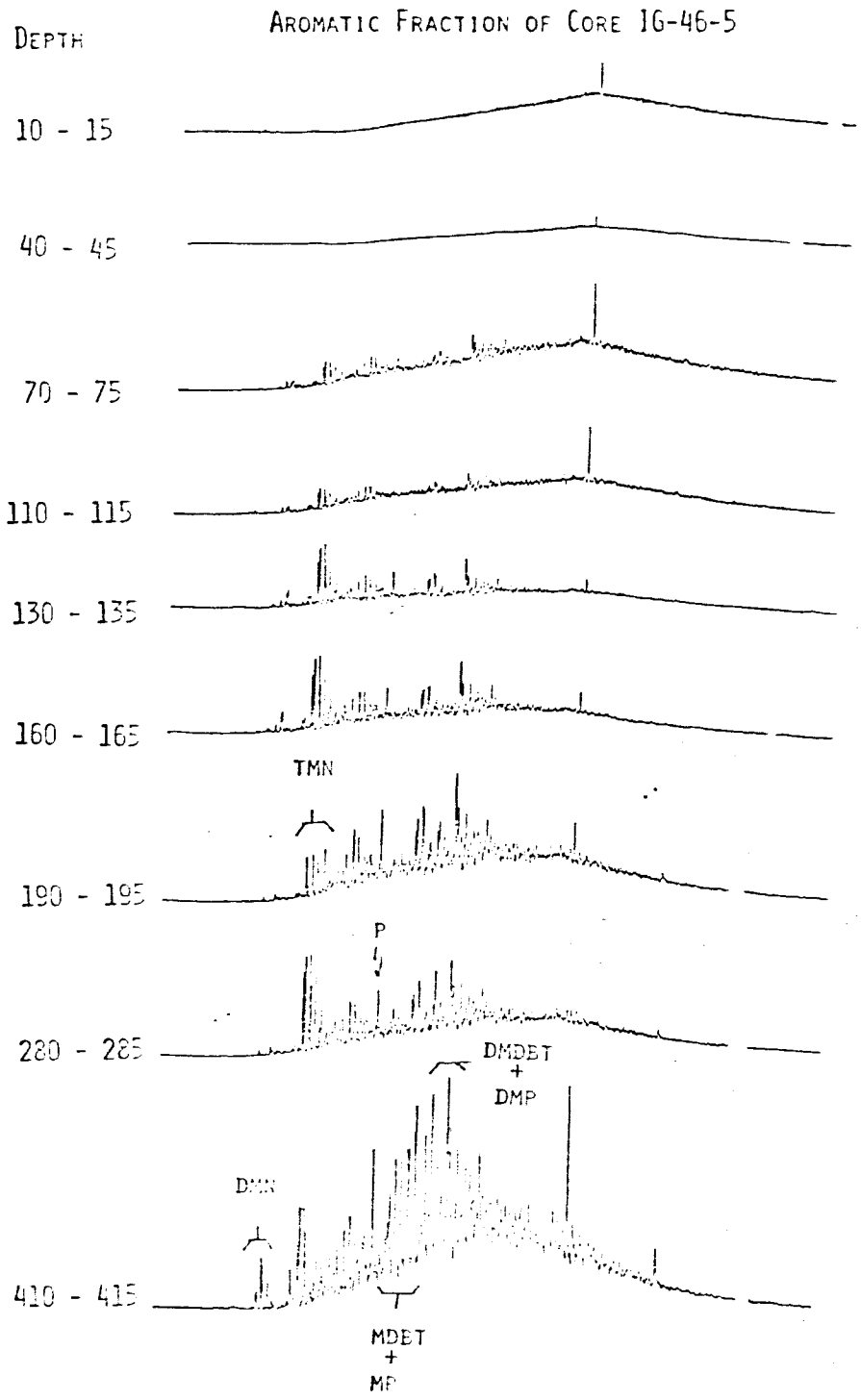
AROMATIC FRACTION OF CORE 1G-46-5
DEPTH
10 - 15
40 - 45
70 - 75
110 - 115
130 - 135
160 - 165
TMN
190 - 195
P
280 - 285
DMDBT
+
DMP
DMN
410 - 415
MDBT
+
MP

Figure C-5.

than burn them for isotope analyses.

A number of the saturated and aromatic fractions from the silica gel analyses were submitted to high resolution gas-liquid chromatography. Typical results are summarized in Figures C-2 to C-5. More detailed data analyses are given in Appendix II.

The GLC data indicate the the bitumen has been highly biodegraded. Saturated hydrocarbon peaks are missing in cores IG47-2-12 (Fig. C-2) and IG47-2-9 (Fig. C-3) although unresolved "humps" are still evident. Samples from the lower section of core IG46-5 (Figure C-4) show normal paraffin spikes on top of a large unresolved envelope. However, care must be used in this case because the sample with the spikes also has very low total bitumen content. The normal hydrocarbons may be partly baseline, modern biological hydrocarbons. On the other hand the presence of phytane suggests a petrogenic origin. This particular sample can be interpreted as being an immature oil. The aromatic fraction of core IG46-5 has a good deal of structure (Fig. C-5), especially in the deeper part of the core. The aromatics identified in Fig. C-5 are based on GLC retention times. It is remarkable, but not unexpected, that bacteria have been able to metabolize the aromatic hydrocarbons to this extent.

HYDROCARBON GASES: CHEMICAL CHARACTERIZATION

Methods

Gas spaces were observed in the core liners of cores IG47-2-(2,4,5,6,7,8,9,10,11,12) prior to opening them. Despite the fact that the cores were several days old it was decided to sample for gases. Gas samples were taken using Becton-Dickinson multiple sample needles to pierce

Table C-9. Concentration and isotopic composition of natural gas hydrocarbons in core IG47-2-7.

Depth (m)	Methane (ppm/$\delta^{13}C$)	Ethane (ppm/$\delta^{13}C$)	Propane (ppm/$\delta^{13}C$)	Iso-butane (ppm)	Butane (ppm)	Iso-pentane (ppm)	Pentane (ppm)	Other Data
1.1	5,900	142	tr	1100	nd	nd	nd	
2.3	273,000 -56.5	608	nd	99	nd	nd	nd	
3.7	105,000 -54.2	290	tr	92	nd	nd	nd	
5.7	196,000 -44.7	4,400	561	273	775	538	nd	
7.4	645,000 -61.9	9,980	1,440	397	3,080	1,130	331	
7.6	663,000 -61.8	10,600	1,510	334	2,880	906	290	δD_{SMOW} of C_1 = -170
9.2	659,000 -59.7	22,300 -28.6	9,630 -24.5	1,800	3,770	774	280	δD_{SMOW} of C_1 = -196
10.5	439,000 -61.0	14,200	5,830	1,104	3,525	963	456	Gases from 7.4 to 10.5 were pooled to measure these: $\delta^{13}C$ of C_2 = -28.5 $\delta^{13}C$ of CO_2 = -16.8 δD of C_2 = -101

*parts per million of component as volume of total recovered gas; the lower value is $\delta^{13}C_{PDB}$ of that component; tr stands for trace, nd stands for not detected.

Table C-10. Concentration and isotopic composition of natural gas hydrocarbons in cores IG47-2-12 and IG47-2-6.

Depth (m)	Methane (ppm/$\delta^{13}C$)	Ethane	Propane	Iso-butane (ppm)	Butane (ppm)	Iso-pentane (ppm)	Pentane (ppm)	Other Data
	IG47-2-12							
0.8	343,000 -48.1	32,000 -28.6	83,600 -24.5	21,000	3,680	257	tr	‡ δD of C_1 = -172
1.5	45,500 -30.5	4,340	11,400 -24.5	9,320 (n+i -25.7)	5,240	3,850	2,100	† δD of C_3 = -104
3.6	18,700 -53.7	9,890	25,800	13,100	5,530	2,660	1,360	† δD of C_4 = -101
	IG47-2-6							
7.7	486,000 -61.9	749						δD of C_1 = -197

*parts per million of component as volume of total recovered gas; the lower value is del $^{13}C_{PDB}$ of that component; tr stands for trace, nd stands for not detected.

‡ Samples 0.8 and 1.5 were combined for this number.

† Samples 0.8, 1.5 and 3.6 were combined for this number.

Table C-11. Composition of Hydrocarbons in Cores IG47-2-10 and IG47-2 (4,5,8,9,11)

Component	Core 2-10	
	2.3 m	4.0 m
Methane	312000	417000
Ethane	6020	6610
Propane	782	1050
Iso-Butane	1980	2970
n-Butane	368	903
Iso-Pentane	1280	2620
n-Pentane	Tr	225
Neo-Pentane	244	

Core	4	5	8	8	9	11
Depth (m)	8.3	11	4.8	9	1	1
Components						
Methane	414000	117000	197000	147000	2290	452
Ethane	278	127	141	330		
Iso-Butane		194				

the core liner and 20 ml, evacuated, B-D blood collection tubes (Vacutainers) to collect the gas. The gas samples were returned to the Port Aransas lab for GC and isotope analyses. The composition of the gases were measured by gas chromatography. A Hewlett-Packard Model 5710 GC with FID, a 1/8 inch by 2 meter packed column of Poropak-Q (Waters Assoc., Inc.) was used with a Hewlett-Packard Model 3352B data acquisition system. The GC was temperature programmed from 80°C to 160°C at 16°C per minute. The sample size injected was 0.5 ml. A thermal conductivity detector was used for non-condensible gases (air, CO_2).

Results

Several of the subsamples had high levels of hydrocarbons. Core IG47-2-7 gases were as high as 66 percent methane and 2 percent ethane. Gases from C_1 to C_5 were present in several samples (Tables C-9, C-10 and C-11). There is no doubt that petrogenic hydrocarbon gases are present in these cores. The compositional data suggests that gas hydrates are associated with these cores. Since our cores were taken, Jim Brooks at Texas A&M University has recovered gas hydrates in cores taken in a nearby area. No general study was done of the level of CO_2 in the cores, but it was detected in fair abundance in core IG47-2-7 and is probably present in the others. This analytical data support the suggestion that anomalous seismic reflections in the study area are due to gases and gas hydrates.

STABLE ISOTOPE CHARACTERIZATION

Methods

Mass spectrometry for stable isotope analysis was carried out on the various fractions using methods which are standard in our laboratory and which are similar to industry methods. Carbon isotope compositions are expressed relative to the Pee Dee belemnite (PDB) and hydrogen isotope compositions relative to Standard Mean Ocean Water (SMOW). Del ^{13}C values are reproducible to better than 0.2 per mil. Reproducibility of del D values is $\pm$ 5.0 per mil. Carbon dioxide for mass spectrometry was prepared from organic matter by a sealed tube method using pyrex tubes with copper oxide at 590°C. This method is reliable but it does require contact between the organic matter and the copper oxide. Hydrogen gas for del D was prepared in two steps; organic matter was oxidized in the sealed tube and then water from that reaction was converted to H_2 by reaction with uranium metal at 775°C.

Carbonate samples were converted to CO_2 with phosphoric acid. Individual hydrocabon gases were isolated by a combination of differential adsorption on silica-gel and packed column gas chromatography. The individual hydrocarbon peaks were diverted to a furnace and burned to CO_2 and H_2O. The CO_2 was recovered for del ^{13}C. The H_2O was recovered and converted to H_2 in the uranium furnace for del D analyses.

Results

The stable isotope data supports some rather firm conclusions regarding the source and biogeochemical reactions that the various carbon compounds have undergone in the study site. The major conclusions are that the liquid and gaseous hydrocarbons are petrogenic.

Most of the bitumen samples had del ^{13}C values of -26.5 $\pm$ 1 although values as negative as -28.6 were encountered. This is in the range for Gulf coast oils as well as the Challenger Knoll oil (Tables C-3 to 9). This uniformity of del ^{13}C suggests that the oils may be from a common source. No trends of del ^{13}C with depth in core or among cores was obvious. The hexane, benzene and methanol eluates had del ^{13}C values which were close to each other for a given sample and close to the total bitumen. The saturated fraction (hexane) was not usually more negative than the total bitumen, probably because the normal paraffins had been removed by microbes.

The del ^{13}C data for carbonates is given in Tables C-3, C-4, C-6 and C-8. Two types of carbonate carbon are present, normal marine carbonate with del ^{13}C ranging from -2 to +2, and a biogenic carbonate carbon with del values up to -27.5 (Tables C-3, C-4, C-6 and C-12). This negative carbon is thought to be the result of microbial oxidation of hydrocarbons. The single del for CO_2 from the core gases was -16.8 (Table C-9). In some cases, IG47-2-7 (C-6) negative carbonate is present although the bitumen level approaches baseline. This situation suggests that ^{13}C depleted carbonate in marine sediments may indicate a previous hydrocarbon presence. The carbonates were extensive in some cores, IG46-5 and IG47-2-9, pointing to major microbial activity.

The del ^{13}C values of several of the residue (kerogen) samples are remarkable. For example, samples IG46-5, 40-45 cm and 70-75 cm (Table C-3) have del values of -36.7 and -30.6. This cannot be due to a large fractionation in some unknown reaction, because there is no correspondingly heavy carbon. It can only be due to the microbial oxidation of ^{13}C

depleted gases. The light carbonate represents the CO_2 produced and the light residue must represent the bacterial cells that remain. This process has operated to produce a substantial amount of a unique carbon reservoir.

The isotopic data (Tables C-9 and C-10) supports the chemical data in the conclusion that much of the gas is petrogenic rather than biogenic. Del for the methane ranges from -30.5 to -61.9. Sample IG47-2-12, 0.8 m (Table C-10) shows a textbook relationship for natural gas with methane, ethane, and propane at -48.1, -28.6, and -24.5. The del D values of methane further support this conclusion. The del D values of ethane, propane and butanes represent some of the few such data in the literature and they are consistent with a petrogenic source.

SUMMARY

The 13 cores from about 100 square miles contain liquid and gaseous hydrocarbons in abundance. The liquid is highly biodegraded. Carbonate and kerogen residues indicate that extensive microbial oxidation of liquid and gas hydrocarbons is taking place in the sediment. The evidence is that the oil and gas are petrogenic and have migrated upward. The ultimate source of the material is not known.

APPENDIX I

Core Logs

note: See Part I. Appendix B

APPENDIX II

Liquid Hydrocarbon: GLC Data and OEP Values

IG47-1-(0-40 CM)

NO. OF CARBONS	REL. WT. PCNT.	SMOOTH WT. PCNT.	OEP VALUE
16	.660		
17	2.159		
18	3.616	3.164	1.110
19	4.499	3.451	1.628
20	1.637	3.617	1.944
21	5.054	4.712	1.401
22	6.213	6.454	1.226
23	9.163	7.735	1.260
24	7.479	8.338	1.190
25	8.960	8.814	1.037
26	9.829	8.937	.995
27	8.868	8.198	1.180
28	5.215	7.206	1.588
29	8.817	6.555	2.033
30	3.431	6.147	2.397
31	8.532	5.566	2.382
32	3.152		
33	2.714		

ISOPRENOIDS (RELATIVE TO N-ALKANES)

16	0
18	0
PRISTANE	2.159
PHYTANE	1.913

RATIOS

N-C-17 / PRISTANE	=	1.000	
N-C-18 / PHYTANE	=	1.890	
PRISTANE / PHYTANE	=	1.128	
AVG. OEP VALUE (25-35)	=	1.659	(7)

IG47-1-1(100-120 CM)

NO. OF CARBONS	REL. WT. PCNT.	SMOOTH WT. PCNT.	OEP VALUE
17	1.246		
18	3.285		
19	3.216	3.122	.923
20	3.211	3.299	1.015
21	3.431	3.479	1.029
22	3.645	3.671	1.152
23	4.428	3.714	1.536
24	2.212	4.733	1.224
25	5.994	7.865	.626
26	17.134	10.305	.518
27	8.067	9.377	.808
28	3.616	7.911	1.893
29	12.640	8.280	2.882
30	4.916	8.975	3.078
31	14.458	8.367	3.767
32	2.106		
33	6.396		

ISOPRENOIDS (RELATIVE TO N-ALKANES)

16	0
18	0
PRISTANE	0
PHYTANE	2.096

RATIOS

N-C-17 / PRISTANE	=	R	
N-C-18 / PHYTANE	=	1.567	
PRISTANE / PHYTANE	=	0	
AVG. OEP VALUE (25-35)	=	1.939	(7)

IG47-1-1-(160-180 CM)

NO. OF CARBONS	REL. WT. PCNT.	SMOOTH WT. PCNT.	OEP VALUE
16	1.542		
17	3.657		
18	4.883	4.263	.974
19	4.757	4.386	1.040
20	3.718	4.129	1.019
21	3.578	4.198	.814
22	5.539	4.365	.752
23	3.918	4.314	1.043
24	2.907	4.788	1.706
25	8.156	6.074	1.950
26	5.330	7.264	2.052
27	11.380	7.708	2.616
28	3.197	7.724	3.589
29	12.783	7.771	4.531
30	2.424	7.868	5.408
31	13.778	7.457	5.888
32	1.907		
33	6.547		

ISOPRENOIDS (RELATIVE TO N-ALKANES)

16	0
18	0
PRISTANE	2.514
PHYTANE	2.724

RATIOS

N-C-17 / PRISTANE	=	1.455	
N-C-18 / PHYTANE	=	1.793	
PRISTANE / PHYTANE	=	.923	
AVG. OEP VALUE (25-35)	=	3.719	(7)

IG47-1-1(240-260 CM)

NO. OF CARBONS	REL. WT. PCNT.	SMOOTH WT. PCNT.	OEP VALUE
17	1.264		
18	1.594		
19	2.101	2.191	1.081
20	2.618	2.875	1.275
21	4.346	3.558	1.570
22	2.920	4.216	1.853
23	6.608	4.940	2.076
24	3.503	5.820	2.180
25	9.350	7.063	2.195
26	5.339	8.626	2.373
27	14.924	9.855	2.678
28	5.380	10.266	3.016
29	15.914	9.891	3.569
30	3.279	8.931	4.417
31	13.217	7.497	5.512
32	1.326		
33	6.317		

ISOPRENOIDS (RELATIVE TO N-ALKANES)

16	0
18	0
PRISTANE	1.247
PHYTANE	1.843

RATIOS

N-C-17 / PRISTANE	=	1.013	
N-C-18 / PHYTANE	=	.865	
PRISTANE / PHYTANE	=	.677	
AVG. OEP VALUE (25-35)	=	3.394	(7)

IG47-1-1(280-300 CM)

NO. OF CARBONS	REL. WT. PCNT.	SMOOTH WT. PCNT.	OEP VALUE
15	1.080		
16	1.297		
17	1.971	1.865	1.044
18	2.353	2.158	.998
19	2.341	2.280	1.159
20	1.871	2.482	1.466
21	3.561	2.914	1.650
22	2.526	3.567	1.648
23	5.318	4.620	1.620
24	4.527	6.357	1.575
25	10.235	8.521	1.377
26	9.809	9.855	1.330
27	12.265	9.701	1.751
28	4.293	9.217	2.828
29	14.973	8.929	3.927
30	2.957	8.173	4.495
31	11.769	6.847	4.804
32	1.762		
33	5.090		

ISOPRENOIDS (RELATIVE TO N-ALKANES)

16	0
18	0
PRISTANE	1.809
PHYTANE	1.838

RATIOS

N-C-17 / PRISTANE	=	1.089	
N-C-18 / PHYTANE	=	1.280	
PRISTANE / PHYTANE	=	.984	
AVG. OEP VALUE (25-35)	=	2.930	(7)

IG47-1-1(360-380 CM)

NO. OF CARBONS	REL. WT. PCNT.	SMOOTH WT. PCNT.	OEP VALUE
14	1.867		
15	4.817		
16	4.300	4.681	1.300
17	5.768	5.056	1.200
18	4.894	5.118	1.047
19	4.702	5.986	1.130
20	6.346	8.370	1.802
21	16.832	9.585	2.434
22	4.819	7.365	2.061
23	3.006	4.570	1.271
24	3.231	4.401	1.059
25	6.049	6.286	.902
26	9.987	7.665	.891
27	8.399	6.807	1.330
28	1.698	4.875	2.625
29	5.722	3.624	3.772
30	1.339	2.905	3.161
31	3.105	2.321	2.345
32	1.436		
33	1.682		

ISOPRENOIDS (RELATIVE TO N-ALKANES)

16	1.559
18	3.325
PRISTANE	7.075
PHYTANE	3.185

RATIOS

N-C-17 / PRISTANE	=	.815
N-C-18 / PHYTANE	=	1.537
PRISTANE / PHYTANE	=	2.221
AVG. OEP VALUE (25-35)	=	2.147 (7)

IG47-1-1(380-400 CM)

NO. OF CARBONS	REL. WT. PCNT.	SMOOTH WT. PCNT.	OEP VALUE
14	1.404		
15	2.722		
16	5.428	5.251	1.120
17	8.374	6.461	1.330
18	5.663	6.482	1.252
19	6.038	6.276	1.039
20	6.650	6.261	1.012
21	6.561	5.963	1.194
22	4.221	5.486	1.477
23	6.525	5.395	1.811
24	3.457	6.340	1.837
25	9.896	8.105	1.275
26	10.794	8.691	.921
27	6.775	7.449	.994
28	4.146	6.297	1.642
29	8.881		
30	2.463		

ISOPRENOIDS (RELATIVE TO N-ALKANES)

16	1.827
18	3.073
PRISTANE	10.146
PHYTANE	5.164

RATIOS

N-C-17 / PRISTANE	=	.825	
N-C-18 / PHYTANE	=	1.097	
PRISTANE / PHYTANE	=	1.965	
AVG. OEP VALUE (25-35)	=	1.208	(4)

IG47-1-1(400-420 CM)

NO. OF CARBONS	REL. WT. PCNT.	SMOOTH WT. PCNT.	OEP VALUE
14	2.738		
15	6.419		
16	6.223	6.476	1.279
17	8.122	6.739	1.322
18	5.385	6.358	1.296
19	6.235	6.059	1.174
20	5.763	6.076	1.162
21	6.826	6.105	1.268
22	5.004	6.081	1.415
23	7.423	6.044	1.542
24	4.508	5.940	1.626
25	7.290	5.781	1.676
26	4.134	5.514	1.754
27	6.759	5.101	1.978
28	2.719	4.693	2.325
29	6.369	4.397	2.619
30	2.141		
31	5.943		

ISOPRENOIDS (RELATIVE TO N-ALKANES)

16	2.359
18	3.566
PRISTANE	10.674
PHYTANE	5.542

RATIOS

N-C-17 / PRISTANE	=	.761	
N-C-18 / PHYTANE	=	.972	
PRISTANE / PHYTANE	=	1.926	
AVG. OEP VALUE (25-35)	=	2.070	(5)

IG47-1-1(420-440)

NO. OF CARBONS	REL. WT. PCNT.	SMOOTH WT. PCNT.	OEP VALUE
14	2.738		
15	6.419		
16	6.223	6.476	1.279
17	8.122	6.739	1.322
18	5.385	6.358	1.296
19	6.235	6.059	1.174
20	5.763	6.076	1.162
21	6.826	6.105	1.268
22	5.004	6.081	1.415
23	7.423	6.044	1.542
24	4.508	5.940	1.626
25	7.290	5.781	1.676
26	4.134	5.514	1.754
27	6.759	5.101	1.978
28	2.719	4.693	2.325
29	6.369	4.397	2.619
30	2.141		
31	5.943		

ISOPRENOIDS (RELATIVE TO N-ALKANES)

16	2.359
18	3.566
PRISTANE	10.674
PHYTANE	5.542

RATIOS

N-C-17 / PRISTANE	=	.761	
N-C-18 / PHYTANE	=	.972	
PRISTANE / PHYTANE	=	1.926	
AVG. OEP VALUE (25-35)	=	2.070	(5)

IG47-1-1(440-460 CM)

NO. OF CARBONS	REL. WT. PCNT.	SMOOTH WT. PCNT.	OEP VALUE
15	.810		
16	3.057		
17	6.106	5.155	1.222
18	6.222	6.412	1.207
19	7.923	6.854	1.225
20	6.098	6.699	1.209
21	6.744	6.392	1.166
22	5.708	6.167	1.190
23	6.658	5.954	1.286
24	4.711	5.806	1.403
25	6.899	5.852	1.489
26	4.692	5.970	1.649
27	7.965	5.954	2.020
28	3.193	5.860	2.640
29	9.035	5.564	3.360
30	1.912	4.971	3.495
31	6.425	4.385	2.549
32	3.030		
33	2.810		

ISOPRENOIDS (RELATIVE TO N-ALKANES)

16	0
18	2.870
PRISTANE	9.093
PHYTANE	6.012

RATIOS

N-C-17 / PRISTANE	=	.671	
N-C-18 / PHYTANE	=	1.035	
PRISTANE / PHYTANE	=	1.512	
AVG. OEP VALUE (25-35)	=	2.457	(7)

IG47-1-1(460-480 CM)

NO. OF CARBONS	REL. WT. PCNT.	SMOOTH WT. PCNT.	OEP VALUE
15	1.894		
16	3.906		
17	6.660	5.666	1.165
18	6.563	6.482	1.102
19	6.932	6.555	1.077
20	6.062	6.315	1.071
21	6.129	6.063	1.034
22	5.859	5.777	1.034
23	5.618	5.392	1.138
24	4.228	5.333	1.217
25	6.091	5.965	1.076
26	7.264	6.558	1.044
27	7.306	6.326	1.345
28	3.525	5.754	2.037
29	8.130	5.312	2.915
30	1.903	4.874	3.672
31	7.191	4.304	3.718
32	1.746		
33	2.992		

ISOPRENOIDS (RELATIVE TO N-ALKANES)

16	.512
18	3.569
PRISTANE	10.202
PHYTANE	6.051

RATIOS

N-C-17 / PRISTANE	=	.653
N-C-18 / PHYTANE	=	1.085
PRISTANE / PHYTANE	=	1.686
AVG. OEP VALUE (25-35)	=	2.258 (7)

IG47-1-1(CORE CATCHER)

NO. OF CARBONS	REL. WT. PCNT.	SMOOTH WT. PCNT.	OEP VALUE
15	11.443		
16	11.017		
17	13.829	15.939	.942
18	21.815	20.434	1.116
19	29.277		
20	12.619		

ISOPRENOIDS (RELATIVE TO N-ALKANES)

16	0
18	7.761
PRISTANE	20.196
PHYTANE	8.845

RATIOS

N-C-17 / PRISTANE	=	.685
N-C-18 / PHYTANE	=	2.466
PRISTANE / PHYTANE	=	2.283
AVG. OEP VALUE (25-35)	=	I (0)

IG47-2-2(200-240 CM)

NO. OF CARBONS	REL. WT. PCNT.	SMOOTH WT. PCNT.	OEP VALUE
17	1.014		
18	1.366		
19	1.939	1.839	1.124
20	2.099	2.277	1.143
21	2.918	2.851	1.220
22	3.038	3.610	1.445
23	5.616	4.378	1.768
24	3.289	5.074	2.096
25	8.125	6.028	2.577
26	3.451	7.752	2.995
27	15.121	10.257	2.907
28	7.051	13.043	2.783
29	23.258	14.551	2.536
30	9.409		
31	12.305		

ISOPRENOIDS (RELATIVE TO N-ALKANES)

16	0
18	0
PRISTANE	1.230
PHYTANE	1.926

RATIOS

N-C-17 / PRISTANE	=	.824	
N-C-18 / PHYTANE	=	.709	
PRISTANE / PHYTANE	=	.639	
AVG. OEP VALUE (25-35)	=	2.759	(5)

IG47-2-2(380-400 CM)

NO. OF CARBONS	REL. WT. PCNT.	SMOOTH WT. PCNT.	OEP VALUE
14	4.011		
15	5.991		
16	5.131	5.703	1.305
17	6.925	5.996	1.417
18	4.790	6.504	1.505
19	8.703	7.136	1.289
20	7.679	6.952	.994
21	5.158	6.033	.915
22	4.924	5.478	1.128
23	6.455	5.294	1.381
24	3.971	4.932	1.453
25	5.231	4.669	1.526
26	3.422	4.808	1.868
27	7.295	5.079	2.536
28	2.323	5.342	3.456
29	9.279	5.402	4.213
30	1.822		
31	6.889		

ISOPRENOIDS (RELATIVE TO N-ALKANES)

16	5.009
18	2.145
PRISTANE	10.691
PHYTANE	6.749

RATIOS

N-C-17 / PRISTANE	=	.648	
N-C-18 / PHYTANE	=	.710	
PRISTANE / PHYTANE	=	1.584	
AVG. OEP VALUE (25-35)	=	2.720	(5)

IG47-2-2(530-550 CM)

NO. OF CARBONS	REL. WT. PCNT.	SMOOTH WT. PCNT.	OEP VALUE
15	1.340		
16	3.575		
17	7.778	6.680	1.076
18	9.295	7.788	.950
19	7.397	7.156	1.066
20	4.559	6.260	1.337
21	6.927	6.200	1.302
22	6.216	6.496	1.181
23	7.142	6.492	1.160
24	5.806	6.358	1.072
25	6.012	6.611	.908
26	8.052	6.866	.918
27	7.135	6.251	1.232
28	3.148	5.183	1.878
29	6.393	4.401	2.510
30	1.867	3.755	2.986
31	4.858	2.979	3.606
32	.720		
33	1.779		

ISOPRENOIDS (RELATIVE TO N-ALKANES)

16	0
18	2.800
PRISTANE	8.693
PHYTANE	5.948

RATIOS

N-C-17 / PRISTANE	=	.895	
N-C-18 / PHYTANE	=	1.563	
PRISTANE / PHYTANE	=	1.461	
AVG. OEP VALUE (25-35)	=	2.006	(7)

IG47-2-2(750-770 CM)

NO. OF CARBONS	REL. WT. PCNT.	SMOOTH WT. PCNT.	OEP VALUE
16	1.353		
17	4.430		
18	5.463	5.382	1.145
19	7.063	6.180	1.153
20	6.017	6.235	1.128
21	6.156	6.054	1.134
22	5.332	6.156	1.238
23	7.467	6.446	1.276
24	5.998	6.462	1.245
25	6.867	6.267	1.337
26	4.729	6.247	1.652
27	8.700	6.301	2.132
28	3.318	6.229	2.746
29	9.564	6.021	3.559
30	1.965	5.751	4.321
31	9.116	5.321	4.130
32	2.184		
33	4.279		

ISOPRENOIDS (RELATIVE TO N-ALKANES)

16	0
18	1.375
PRISTANE	5.133
PHYTANE	4.318

RATIOS

N-C-17 / PRISTANE	=	.863	
N-C-18 / PHYTANE	=	1.265	
PRISTANE / PHYTANE	=	1.189	
AVG. OEP VALUE (25-35)	=	2.840	(7)

IG47-2-5(680-700 CM)

NO. OF CARBONS	REL. WT. PCNT.	SMOOTH WT. PCNT.	OEP VALUE
15	3.702		
16	6.797		
17	11.824	8.800	1.457
18	7.530	8.741	1.446
19	8.845	7.633	1.398
20	5.200	6.531	1.383
21	6.315	5.871	1.273
22	5.132	5.513	1.234
23	5.865	5.005	1.321
24	3.495	4.416	1.283
25	4.061	4.409	1.114
26	4.846	5.077	1.183
27	6.944	5.654	1.384
28	4.639	5.658	1.545
29	6.794	5.184	1.754
30	2.892		
31	5.120		

ISOPRENOIDS (RELATIVE TO N-ALKANES)

16	.770
18	5.234
PRISTANE	11.926
PHYTANE	6.726

RATIOS

N-C-17 / PRISTANE	=	.991
N-C-18 / PHYTANE	=	1.120
PRISTANE / PHYTANE	=	1.773
AVG. OEP VALUE (25-35)	=	1.396 (5)

IG47-2-5(850-870 CM)

NO. OF CARBONS	REL. WT. PCNT.	SMOOTH WT. PCNT.	OEP VALUE
15	2.108		
16	3.615		
17	6.068	5.168	1.277
18	5.465	6.137	1.310
19	7.852	6.557	1.268
20	6.098	6.255	1.139
21	5.471	5.612	1.074
22	4.727	5.245	1.163
23	5.809	5.210	1.299
24	4.335	5.308	1.457
25	6.779	5.490	1.689
26	3.830	5.922	1.881
27	8.688	6.711	1.855
28	5.571	7.497	1.872
29	10.860	7.649	2.034
30	4.512		
31	8.210		

ISOPRENOIDS (RELATIVE TO N-ALKANES)

16	.852
18	3.373
PRISTANE	8.961
PHYTANE	5.078

RATIOS

N-C-17 / PRISTANE	=	.677	
N-C-18 / PHYTANE	=	1.076	
PRISTANE / PHYTANE	=	1.765	
AVG. OEP VALUE (25-35)	=	1.866	(5)

IG47-2-7 (0-10 CM)

NO. OF CARBONS	REL. WT. PCNT.	SMOOTH WT. PCNT.	OEP VALUE
15	1.275		
16	1.539		
17	2.926	2.842	1.331
18	3.337	4.142	1.544
19	7.127	5.051	1.580
20	4.492	4.965	1.223
21	3.800	4.753	.915
22	5.436	5.492	.869
23	6.412	7.122	.856
24	9.912	8.618	.940
25	10.289	8.754	1.176
26	6.177	7.705	1.377
27	7.568	6.653	1.407
28	4.880	6.148	1.341
29	6.518	6.297	1.201
30	6.561	6.687	1.243
31	8.306		
32	3.443		

ISOPRENOIDS (RELATIVE TO N-ALKANES)

16	1.010
18	1.460
PRISTANE	2.006
PHYTANE	3.592

RATIOS

N-C-17 / PRISTANE	=	1.459	
N-C-18 / PHYTANE	=	.929	
PRISTANE / PHYTANE	=	.559	
AVG. OEP VALUE (25-35)	=	1.291	(6)

IG47-2-7 (80-120 CM)

NO. OF CARBONS	REL. WT. PCNT.	SMOOTH WT. PCNT.	OEP VALUE
15	2.695		
16	3.399		
17	4.745	4.459	1.229
18	4.601	5.492	1.426
19	8.168	6.208	1.530
20	5.212	6.247	1.379
21	6.314	6.067	1.136
22	6.149	5.859	1.030
23	5.576	5.506	1.154
24	4.078	5.448	1.478
25	7.422	5.780	1.677
26	4.560	6.014	1.729
27	7.820	6.153	1.937
28	3.821	6.698	2.195
29	10.586	7.356	1.977
30	6.063	6.988	1.652
31	6.827		
32	1.964		

ISOPRENOIDS (RELATIVE TO N-ALKANES)

16	1.236
18	3.336
PRISTANE	6.788
PHYTANE	4.248

RATIOS

N-C-17 / PRISTANE	=	.699	
N-C-18 / PHYTANE	=	1.083	
PRISTANE / PHYTANE	=	1.598	
AVG. OEP VALUE (25-35)	=	1.861	(6)

IG47-2-7 (180-210 CM)

NO. OF CARBONS	REL. WT. PCNT.	SMOOTH WT. PCNT.	OEP VALUE
15	2.000		
16	3.508		
17	6.199	5.480	1.189
18	6.504	6.699	1.204
19	8.439	7.040	1.234
20	6.103	6.534	1.122
21	5.381	5.981	.954
22	6.142	5.831	.953
23	5.999	5.717	1.086
24	4.822	5.490	1.261
25	6.247	5.320	1.475
26	3.777	5.368	1.689
27	7.238	5.721	1.780
28	4.454	6.180	1.892
29	8.933	6.284	2.088
30	3.686	5.895	2.145
31	7.149		
32	3.418		

ISOPRENOIDS (RELATIVE TO N-ALKANES)

16	.759
18	4.077
PRISTANE	8.787
PHYTANE	5.760

RATIOS

N-C-17 / PRISTANE	=	.705	
N-C-18 / PHYTANE	=	1.129	
PRISTANE / PHYTANE	=	1.526	
AVG. OEP VALUE (25-35)	=	1.845	(6)

IG47-2-7 (250-310 CM)

NO. OF CARBONS	REL. WT. PCNT.	SMOOTH WT. PCNT.	OEP VALUE
15	2.295		
16	3.823		
17	3.234	3.613	.837
18	4.043	3.987	.976
19	4.641	4.326	1.099
20	4.202	4.599	1.138
21	5.151	4.903	1.096
22	5.155	5.157	1.063
23	5.478	5.597	1.233
24	4.870	6.677	1.727
25	11.437	7.598	2.144
26	4.796	7.626	1.972
27	8.806	7.715	1.529
28	7.408	8.163	1.421
29	10.358	8.062	1.663
30	4.702		
31	9.600		

ISOPRENOIDS (RELATIVE TO N-ALKANES)

16	1.369
18	3.688
PRISTANE	5.375
PHYTANE	3.940

RATIOS

N-C-17 / PRISTANE	=	.602	
N-C-18 / PHYTANE	=	1.026	
PRISTANE / PHYTANE	=	1.364	
AVG. OEP VALUE (25-35)	=	1.746	(5)

IG47-2-7 (450-470 CM)

NO. OF CARBONS	REL. WT. PCNT.	SMOOTH WT. PCNT.	OEP VALUE
15	3.744		
16	4.790		
17	5.254	5.035	1.039
18	5.090	5.257	1.103
19	5.778	5.196	1.131
20	4.662	4.842	1.066
21	4.215	4.564	1.007
22	4.435	4.705	1.082
23	5.564	5.178	1.221
24	4.890	5.779	1.409
25	7.957	6.222	1.619
26	4.614	6.405	1.718
27	8.236	6.649	1.728
28	5.135	7.057	1.829
29	10.015	7.129	1.963
30	4.490	6.390	2.076
31	7.234	4.923	2.483
32	1.163		
33	2.735		

ISOPRENOIDS (RELATIVE TO N-ALKANES)

16	1.684
18	4.032
PRISTANE	8.253
PHYTANE	4.598

RATIOS

N-C-17 / PRISTANE	=	.637	
N-C-18 / PHYTANE	=	1.107	
PRISTANE / PHYTANE	=	1.795	
AVG. OEP VALUE (25-35)	=	1.916	(7)

IG47-2-7 (530-550 CM)

NO. OF CARBONS	REL. WT. PCNT.	SMOOTH WT. PCNT.	OEP VALUE
15	2.738		
16	4.115		
17	4.938	4.760	.950
18	5.650	5.093	.905
19	4.739	4.947	.901
20	4.758	4.733	.886
21	4.153	4.872	.819
22	5.958	5.204	.854
23	5.437	5.327	1.059
24	4.393	5.449	1.342
25	7.054	5.858	1.519
26	4.908	6.416	1.608
27	8.769	7.019	1.691
28	5.524	7.511	1.898
29	10.907	7.430	2.326
30	3.411	6.810	2.680
31	8.933		
32	3.616		

ISOPRENOIDS (RELATIVE TO N-ALKANES)

16	1.459
18	3.558
PRISTANE	6.492
PHYTANE	4.475

RATIOS

N-C-17 / PRISTANE	=	.761	
N-C-18 / PHYTANE	=	1.263	
PRISTANE / PHYTANE	=	1.451	
AVG. OEP VALUE (25-35)	=	1.954	(6)

IG47-2-7 (570-600 CM)

NO. OF CARBONS	REL. WT. PCNT.	SMOOTH WT. PCNT.	OEP VALUE
15	5.086		
16	4.178		
17	4.501	5.244	.822
18	7.337	5.813	.788
19	5.750	5.482	.968
20	3.809	4.649	1.135
21	4.135	4.461	1.108
22	4.657	5.079	1.202
23	6.956	5.841	1.382
24	5.151	6.342	1.521
25	8.350	6.530	1.655
26	4.686	6.529	1.697
27	8.080	6.710	1.642
28	5.472	7.072	1.742
29	9.891	7.033	2.051
30	3.749		
31	8.211		

ISOPRENOIDS (RELATIVE TO N-ALKANES)

16	2.832
18	3.573
PRISTANE	6.602
PHYTANE	4.649

RATIOS

N-C-17 / PRISTANE	=	.682
N-C-18 / PHYTANE	=	1.578
PRISTANE / PHYTANE	=	1.420
AVG. OEP VALUE (25-35)	=	1.757 (5)

IG47-2-7 (750-780 CM)

NO. OF CARBONS	REL. WT. PCNT.	SMOOTH WT. PCNT.	OEP VALUE
14	2.895		
15	4.907		
16	4.761	4.670	1.086
17	4.819	4.843	1.125
18	4.353	5.174	1.388
19	7.211	5.288	1.599
20	3.786	4.865	1.348
21	3.958	4.724	.914
22	6.084	5.023	.827
23	5.136	5.142	1.102
24	3.698	5.377	1.685
25	8.362	5.835	2.128
26	3.763	6.085	2.133
27	8.210	6.382	1.980
28	4.805	6.782	2.119
29	10.221	6.610	2.778
30	2.193	5.777	3.957
31	8.224	4.561	5.354
32	.678		
33	1.934		

ISOPRENOIDS (RELATIVE TO N-ALKANES)

16	3.250
18	5.048
PRISTANE	7.424
PHYTANE	5.163

RATIOS

N-C-17 / PRISTANE	=	.649	
N-C-18 / PHYTANE	=	.843	
PRISTANE / PHYTANE	=	1.438	
AVG. OEP VALUE (25-35)	=	2.921	(7)

APPENDIX III

Plots of Saturated Hydrocarbons

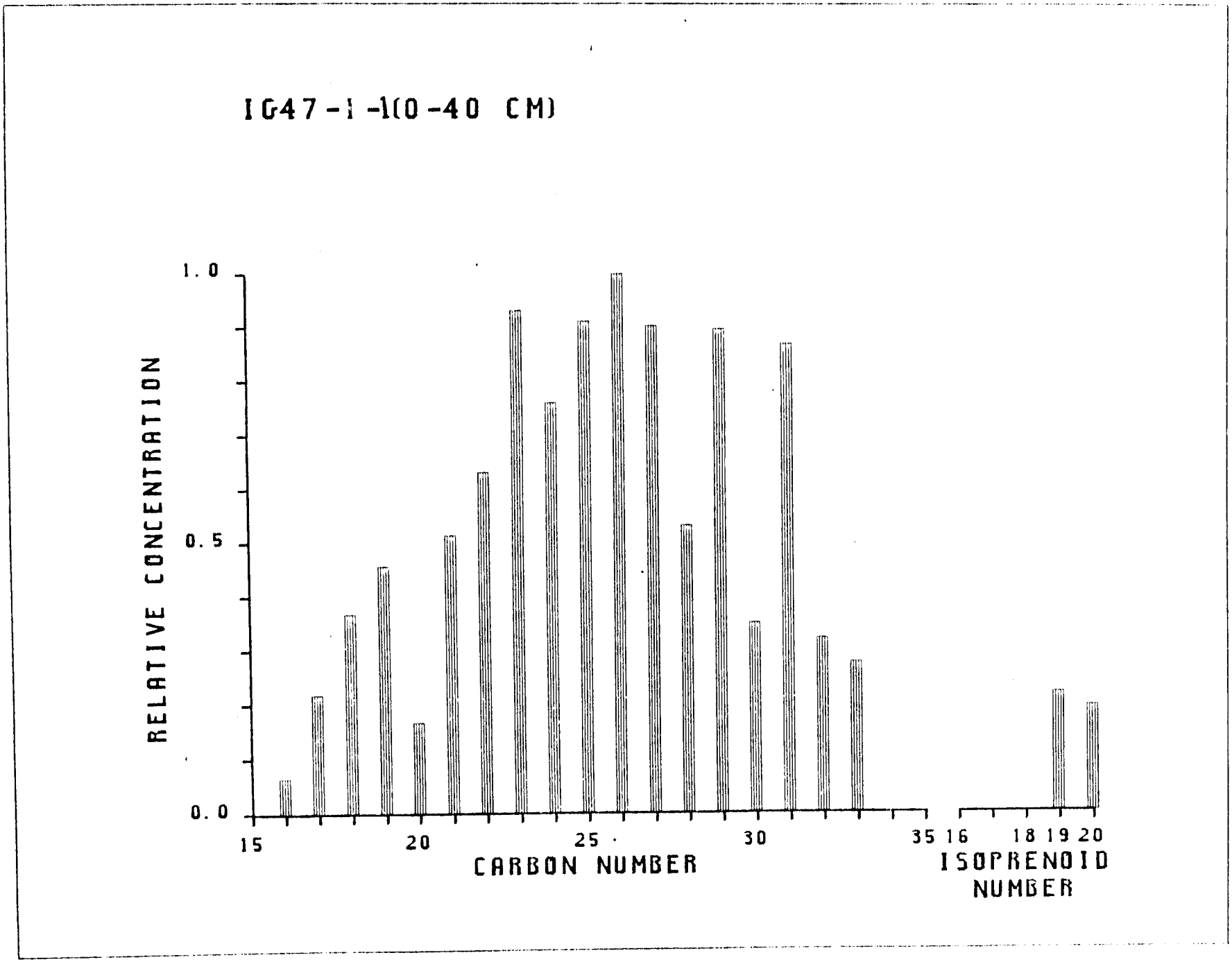
IG47-1-1(0-40 CM)
RELATIVE CONCENTRATION
1.0
0.5
0.0
15
20
25
30
35
CARBON NUMBER
16
18
19
20
ISOPRENOID NUMBER

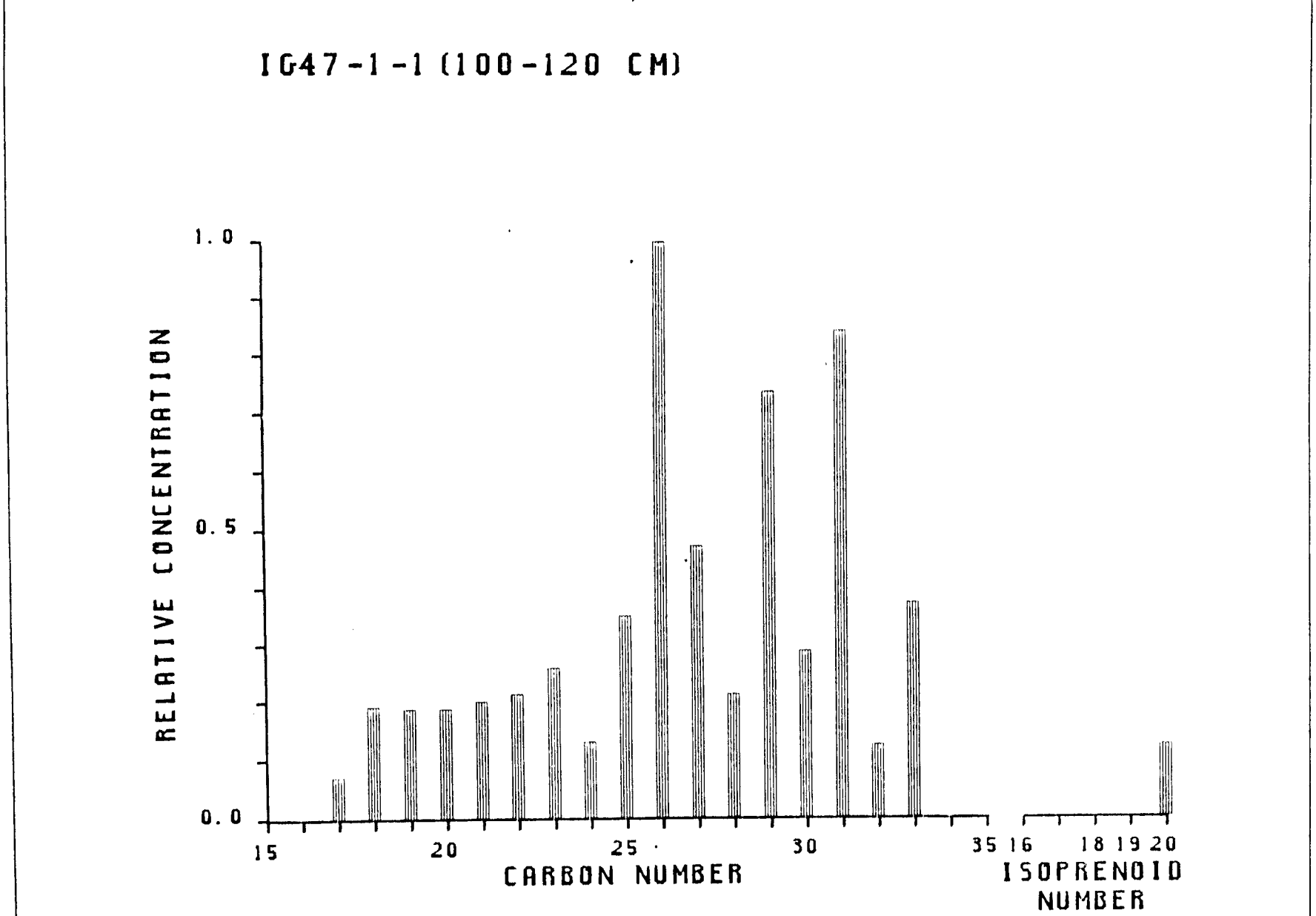
IG47-1-1 (100-120 CM)
1.0
0.5
0.0
RELATIVE CONCENTRATION
15
20
25
30
35
CARBON NUMBER
16
18
19
20
ISOPRENOID NUMBER

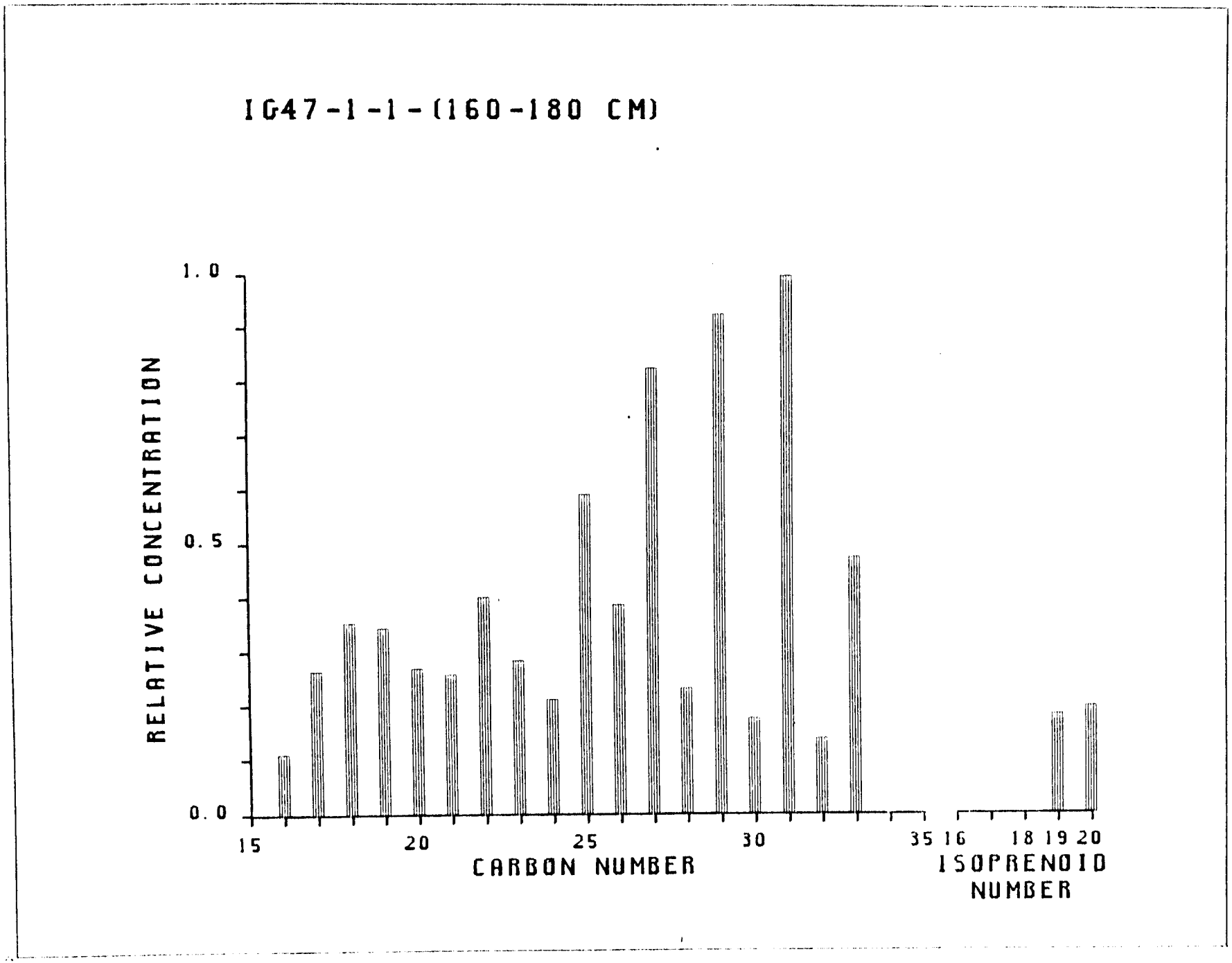
IG47-1-1-(160-180 CM)
1.0
0.5
0.0
RELATIVE CONCENTRATION
15
20
25
30
35
CARBON NUMBER
16
18
19
20
ISOPRENOID NUMBER

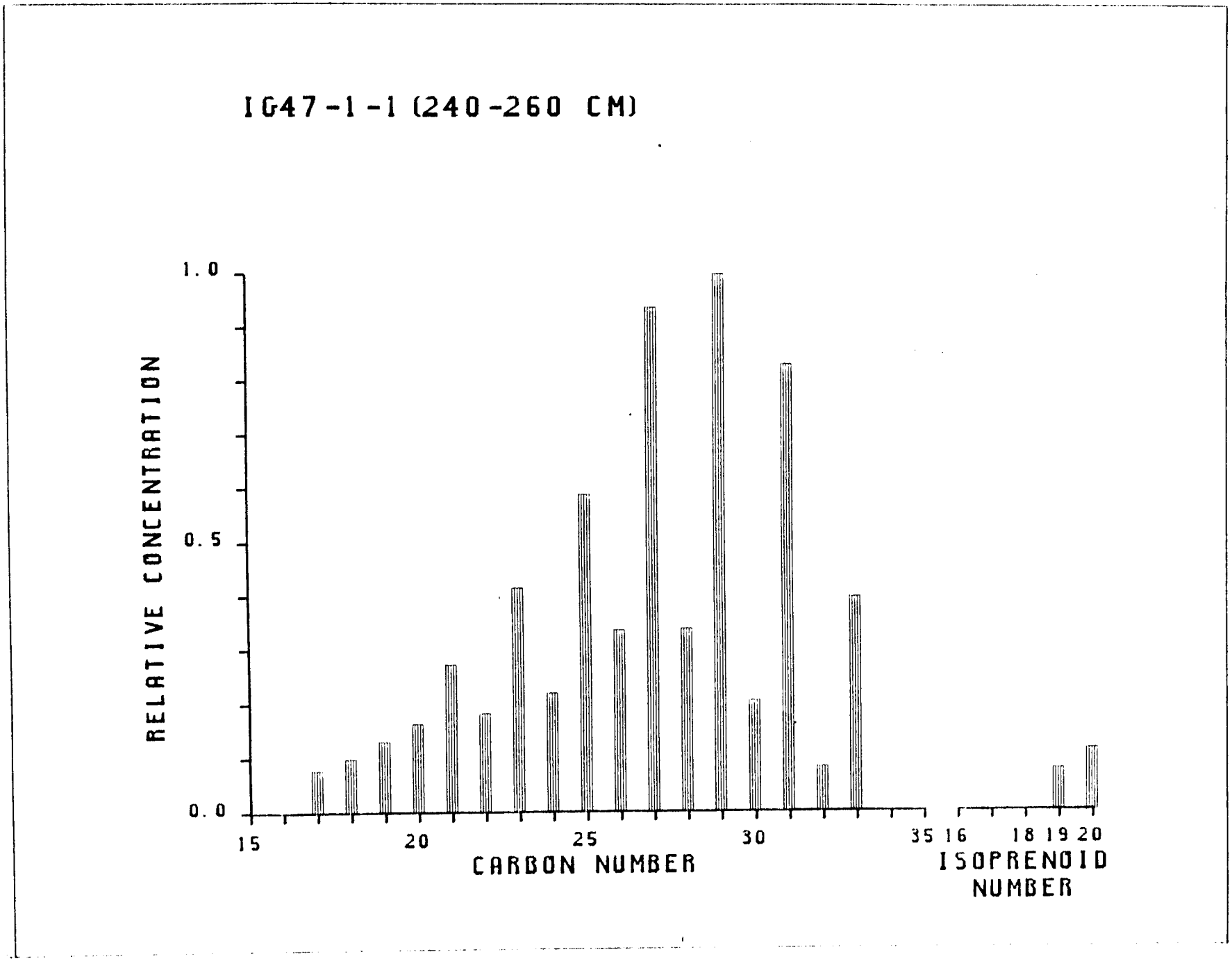
IG47-1-1 (240-260 CM)
1.0
0.5
0.0
RELATIVE CONCENTRATION
15
20
25
30
35
CARBON NUMBER
16
18
19
20
ISOPRENOID NUMBER

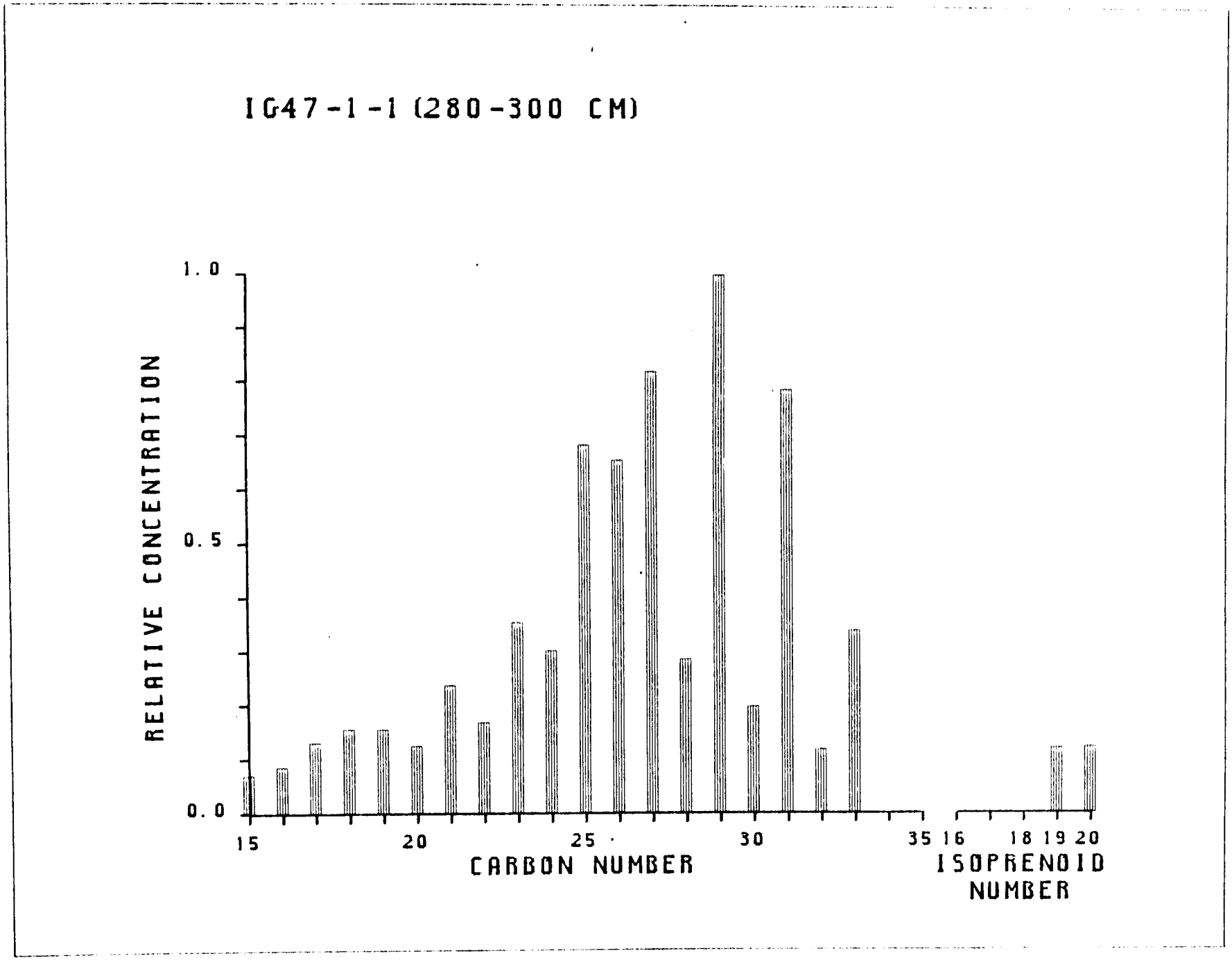
IG47-1-1 (280-300 CM)
1.0
0.5
0.0
RELATIVE CONCENTRATION
15
20
25
30
35
16
18
19
20
CARBON NUMBER
ISOPRENOID NUMBER

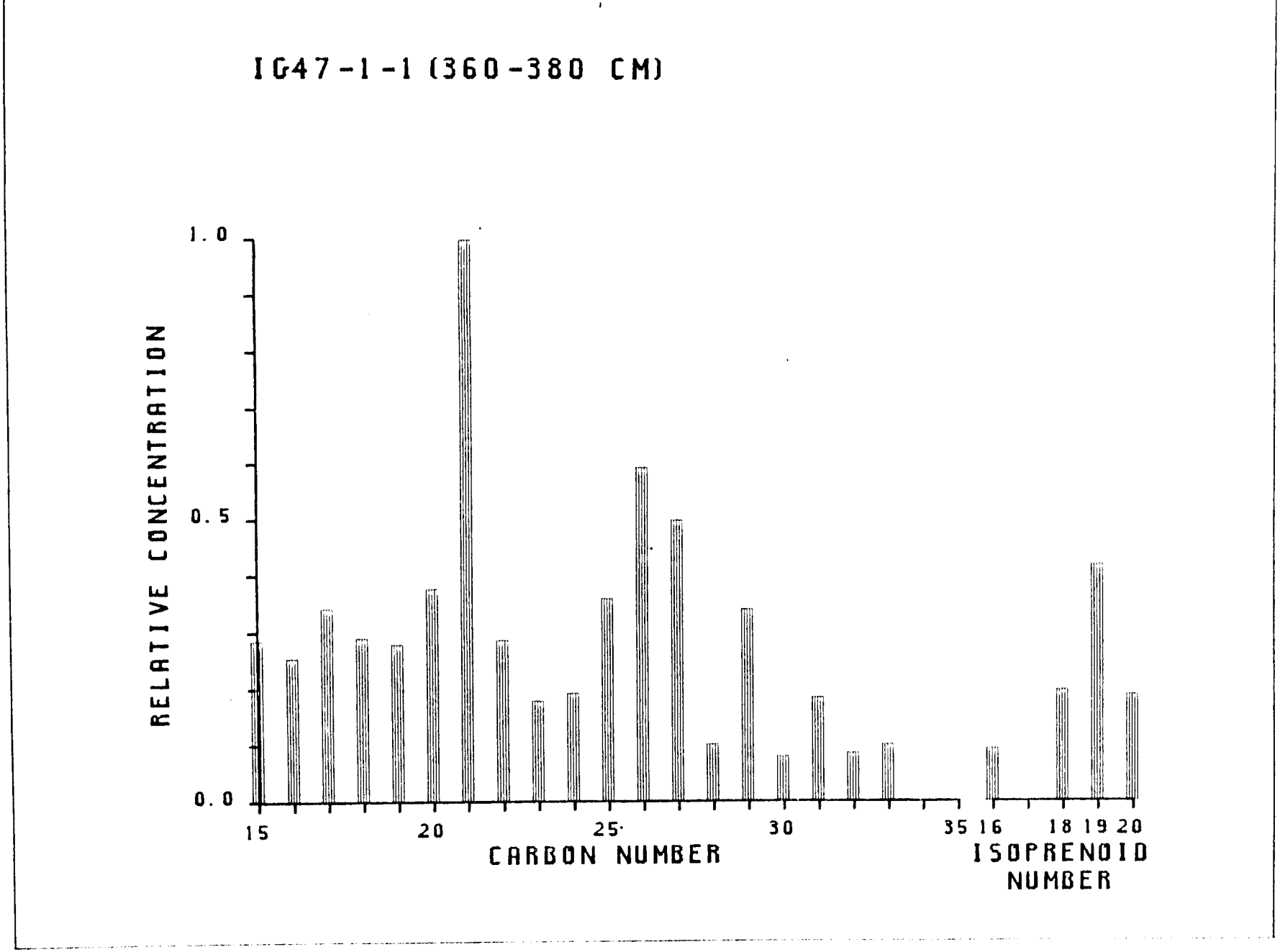
IG47-1-1 (360-380 CM)
RELATIVE CONCENTRATION
1.0
0.5
0.0
15
20
25
30
35
16
18
19
20
CARBON NUMBER
ISOPRENOID NUMBER

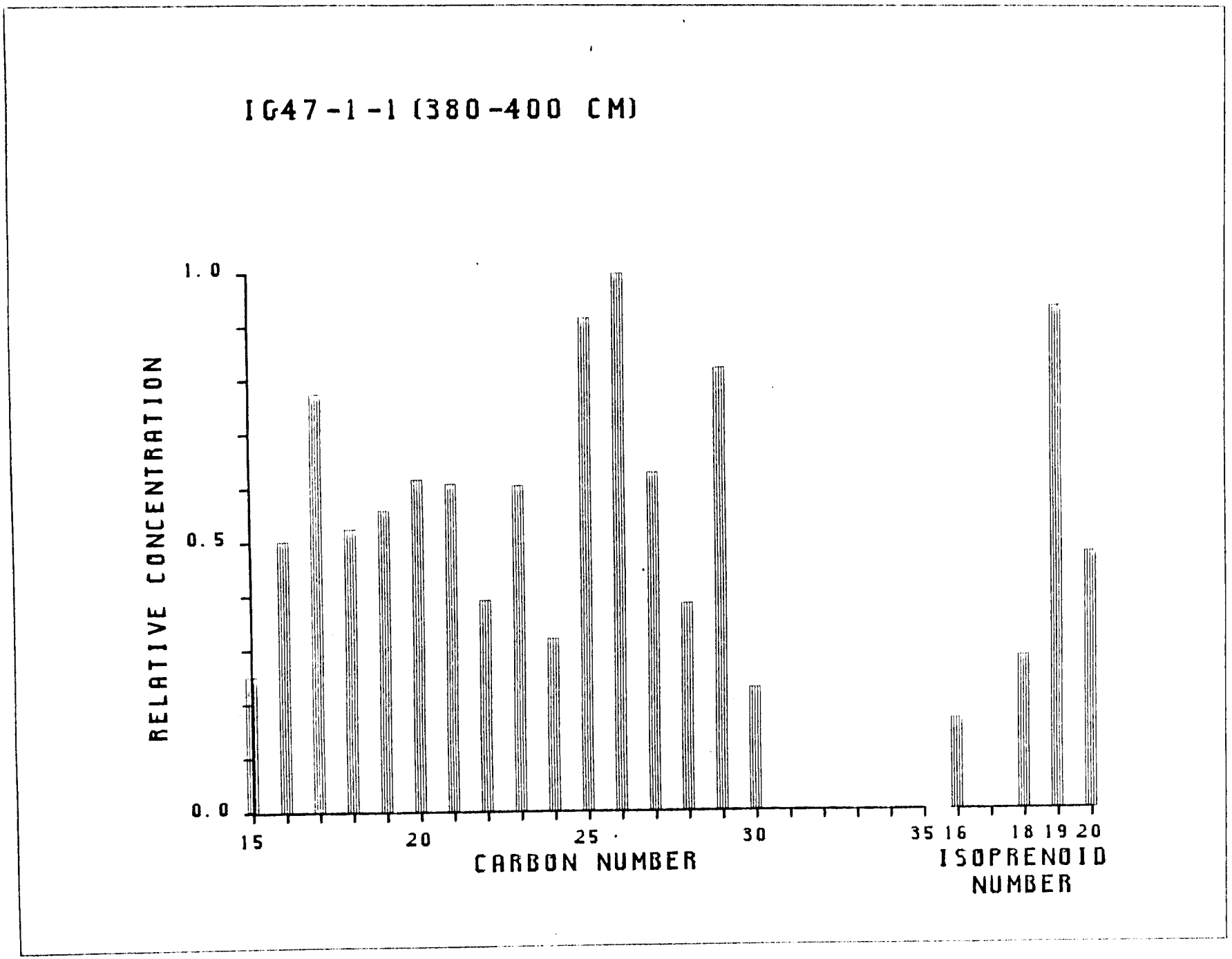
IG47-1-1 (380-400 CM)
1.0
0.5
0.0
RELATIVE CONCENTRATION
15
20
25
30
35
CARBON NUMBER
16
18
19
20
ISOPRENOID NUMBER

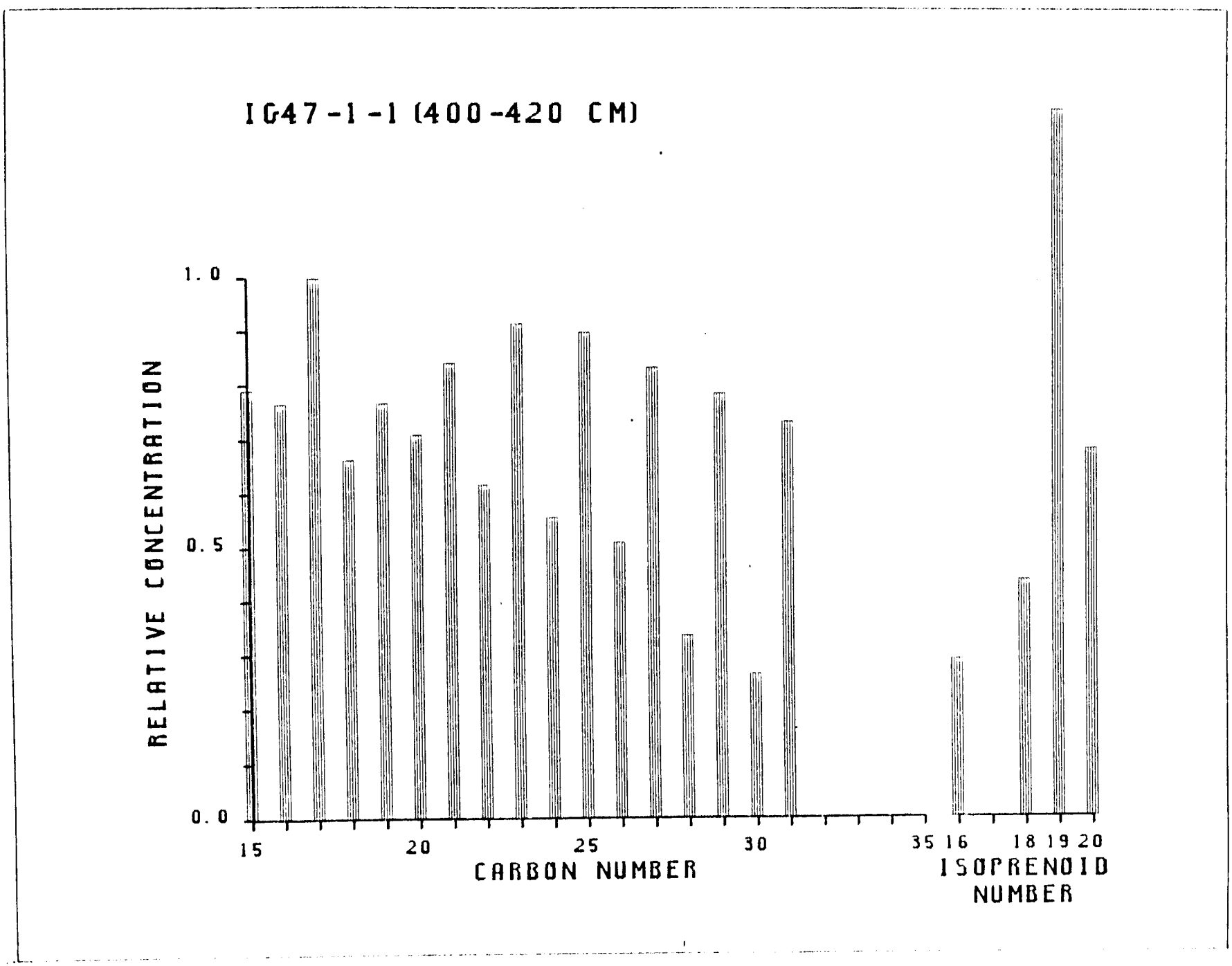
IG47-1-1 (400-420 CM)
RELATIVE CONCENTRATION
1.0
0.5
0.0
15
20
25
30
35
CARBON NUMBER
16
18
19
20
ISOPRENOID NUMBER

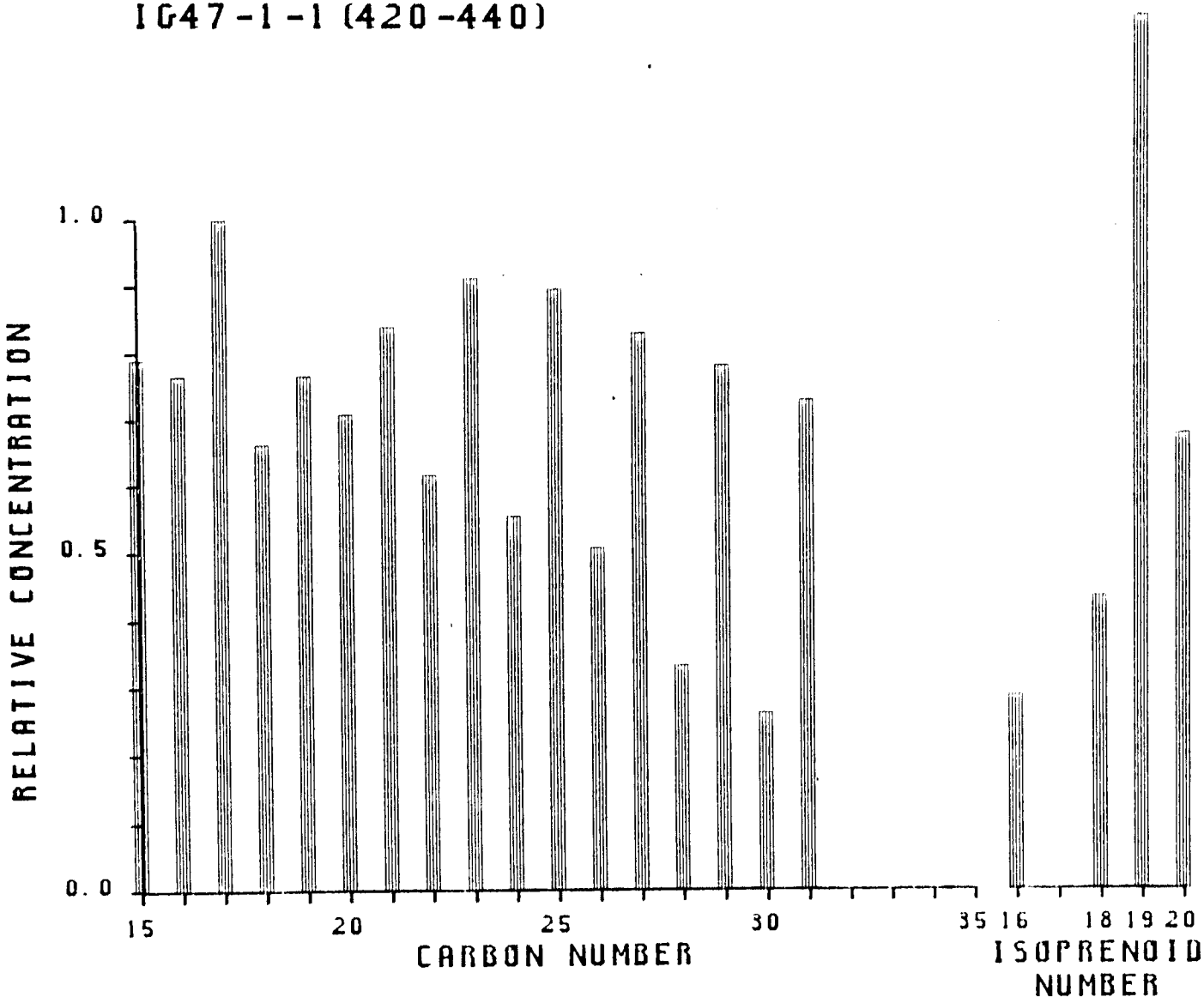
IG47-1-1 (420-440)
1.0
0.5
0.0
RELATIVE CONCENTRATION
15
20
25
30
35
16
18
19
20
CARBON NUMBER
ISOPRENOID NUMBER

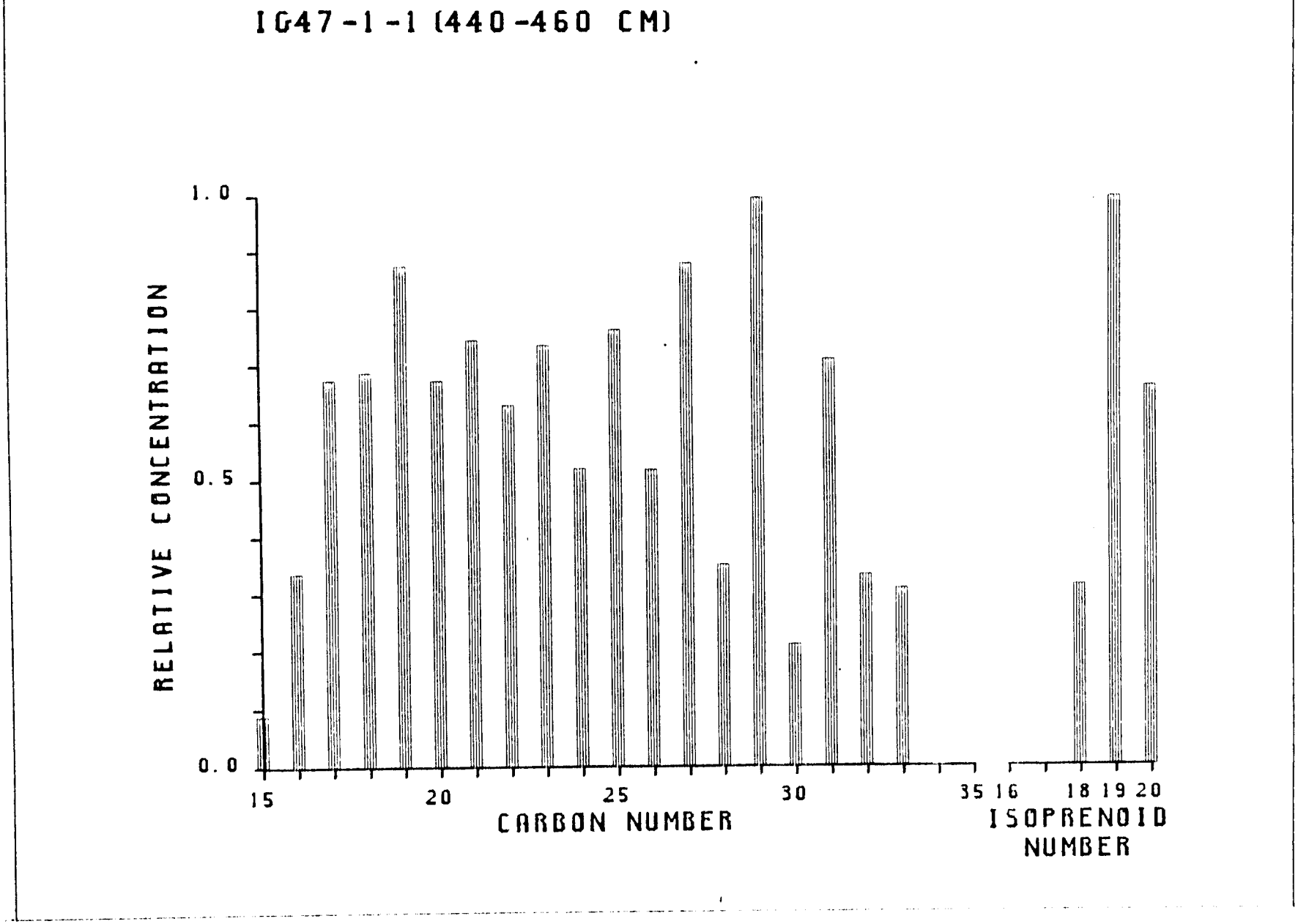
IG47-1-1 (440-460 CM)
1.0
0.5
0.0
RELATIVE CONCENTRATION
15
20
25
30
35
CARBON NUMBER
16
18
19
20
ISOPRENOID NUMBER

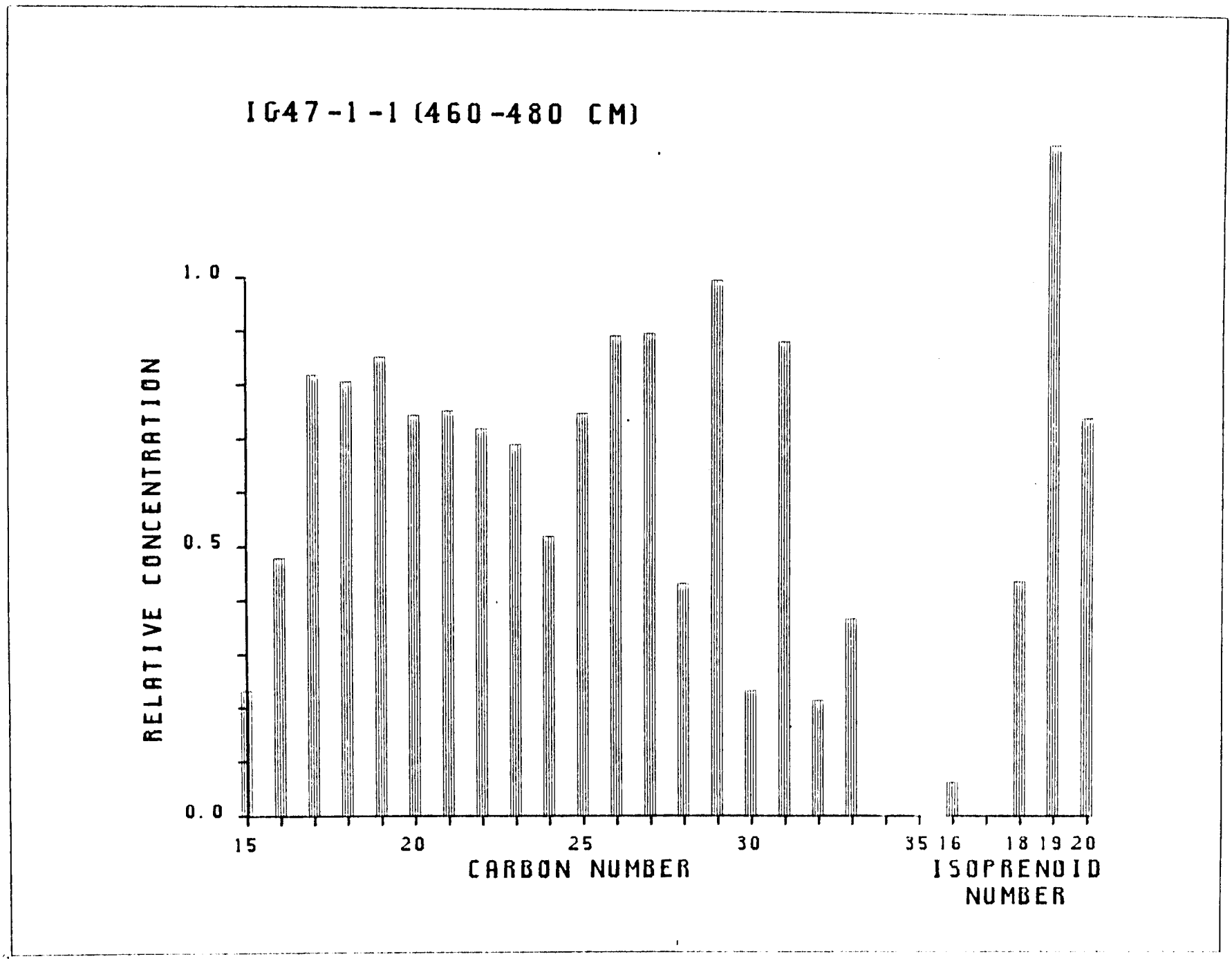
IG47-1-1 (460-480 CM)
RELATIVE CONCENTRATION
1.0
0.5
0.0
15
20
25
30
35
16
18
19
20
CARBON NUMBER
ISOPRENOID NUMBER

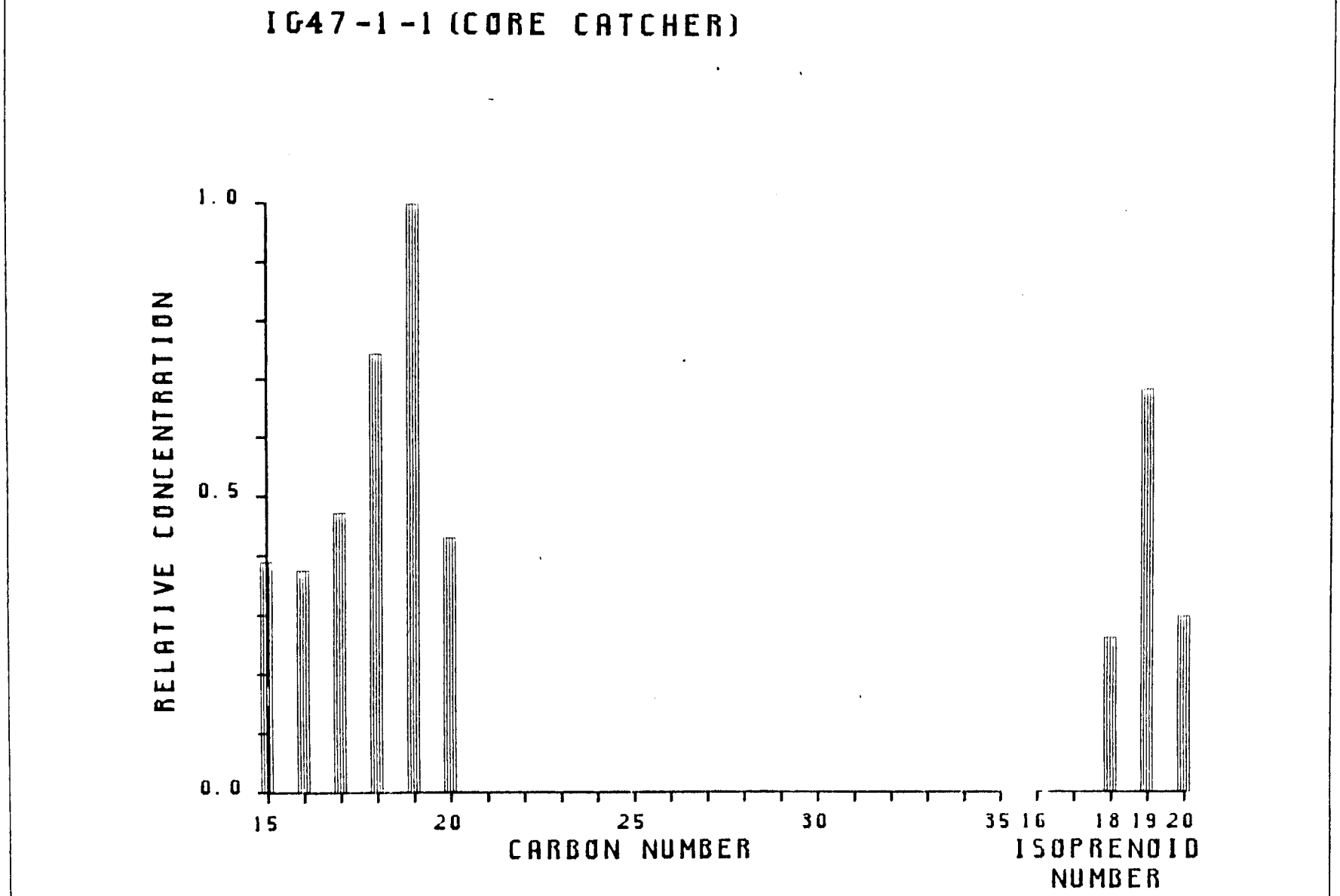
IG47-1-1 (CORE CATCHER)
RELATIVE CONCENTRATION
1.0
0.5
0.0
15
20
25
30
35
CARBON NUMBER
16
18
19
20
ISOPRENOID NUMBER

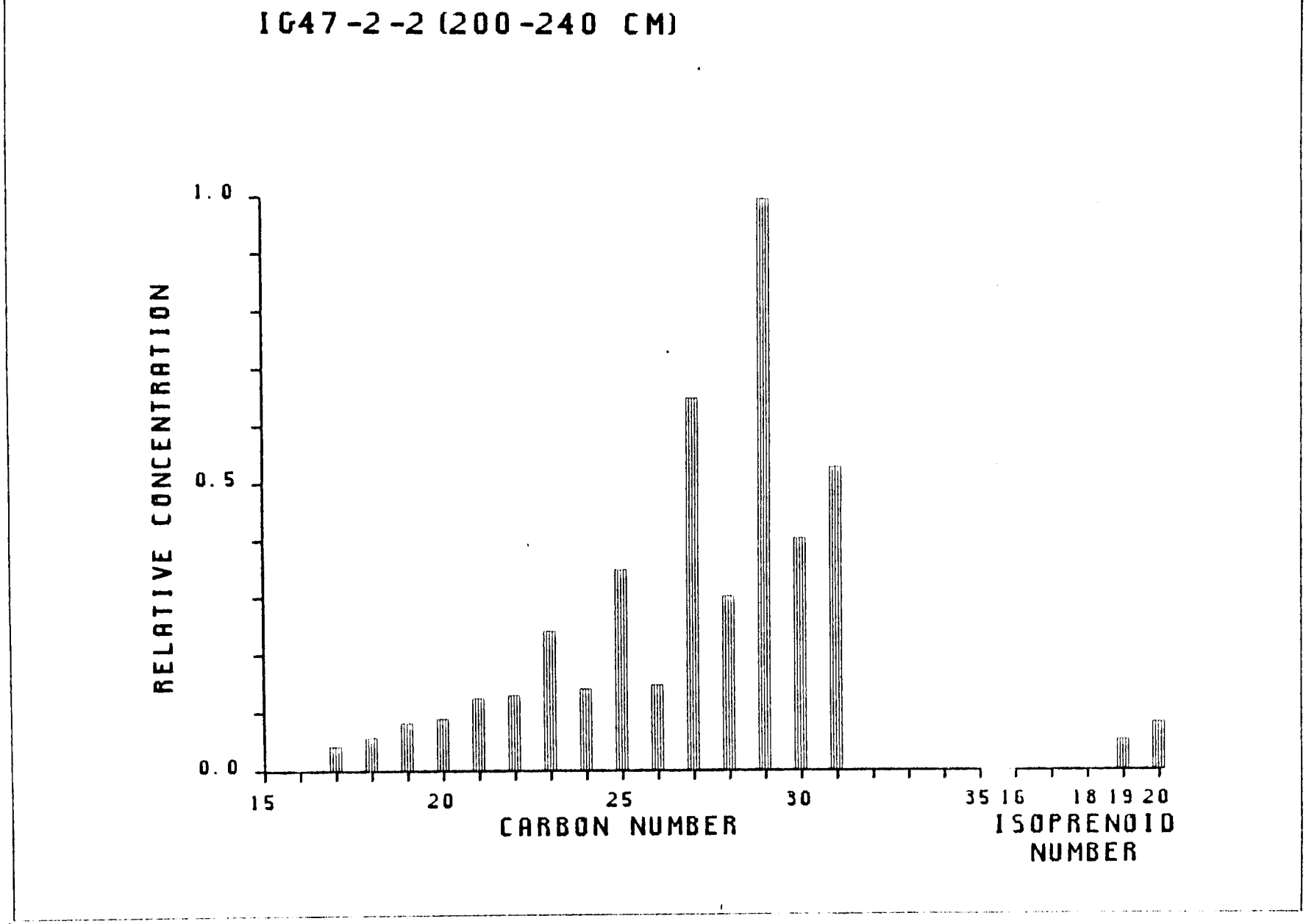
IG47-2-2 (200-240 CM)
1.0
0.5
0.0
RELATIVE CONCENTRATION
15
20
25
30
35
CARBON NUMBER
16
18
19
20
ISOPRENOID NUMBER

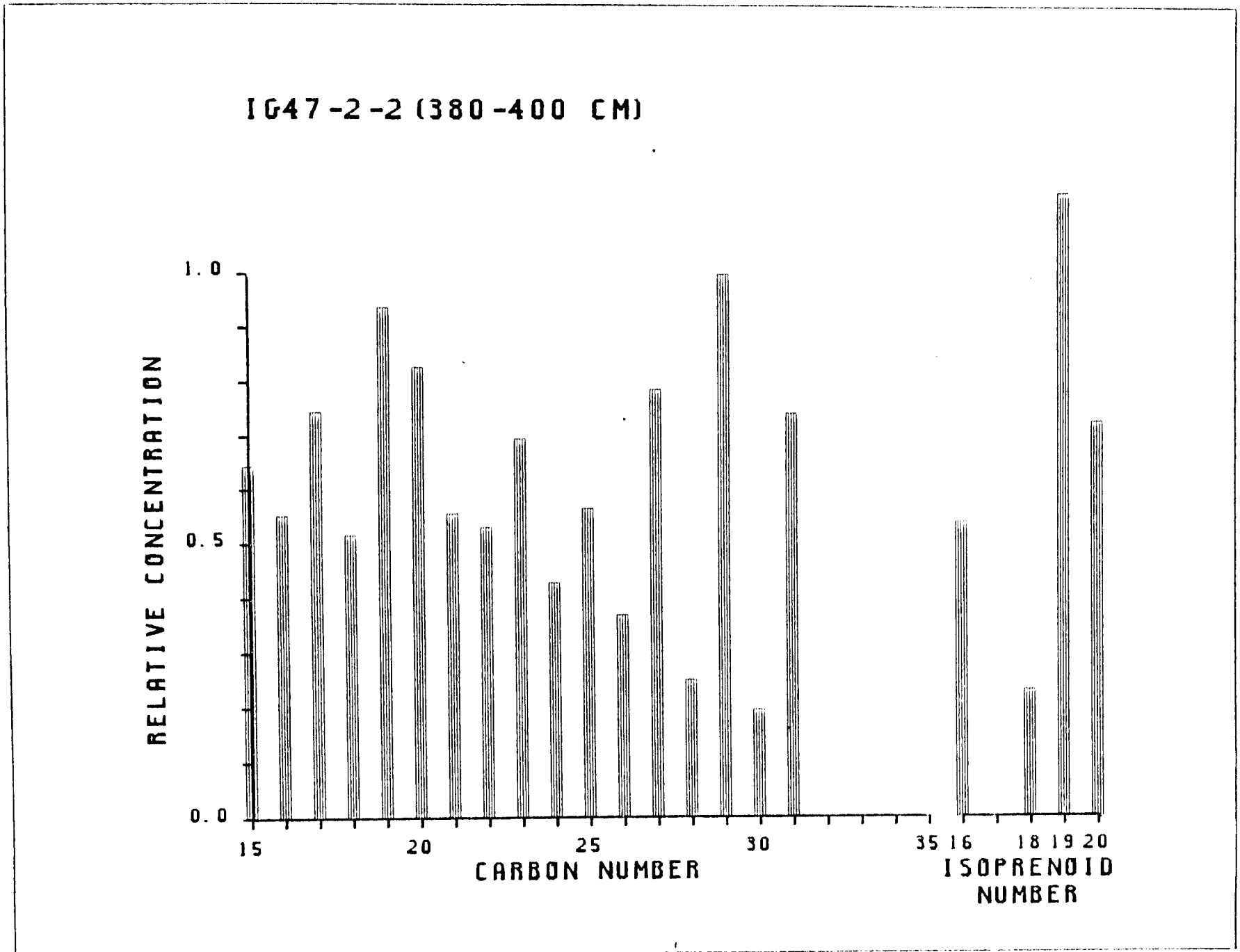
IG47-2-2 (380-400 CM)
1.0
0.5
0.0
RELATIVE CONCENTRATION
15
20
25
30
35
CARBON NUMBER
16
18
19
20
ISOPRENOID NUMBER

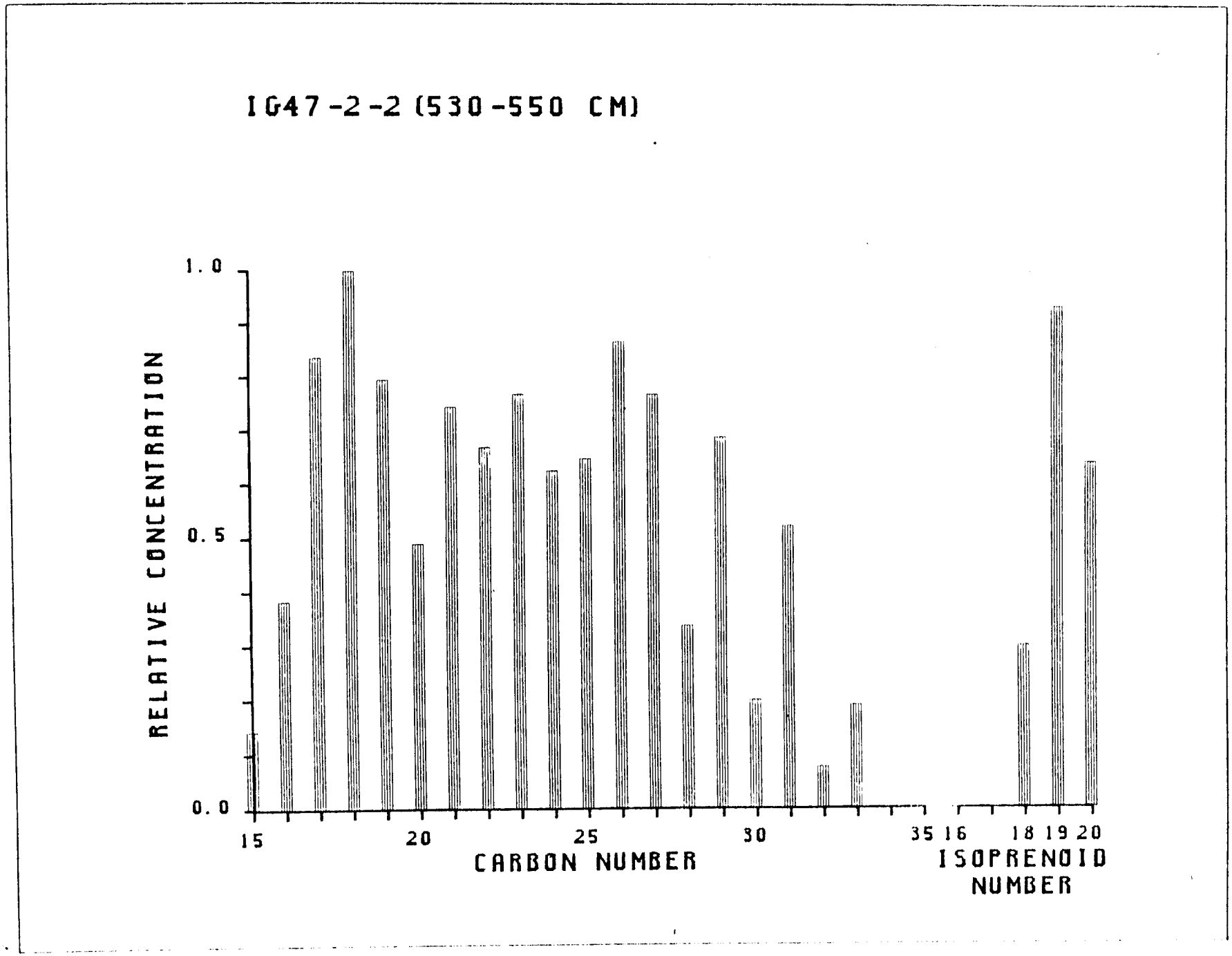
IG47-2-2 (530-550 CM)
1.0
0.5
0.0
RELATIVE CONCENTRATION
15
20
25
30
35
16
18
19
20
CARBON NUMBER
ISOPRENOID NUMBER

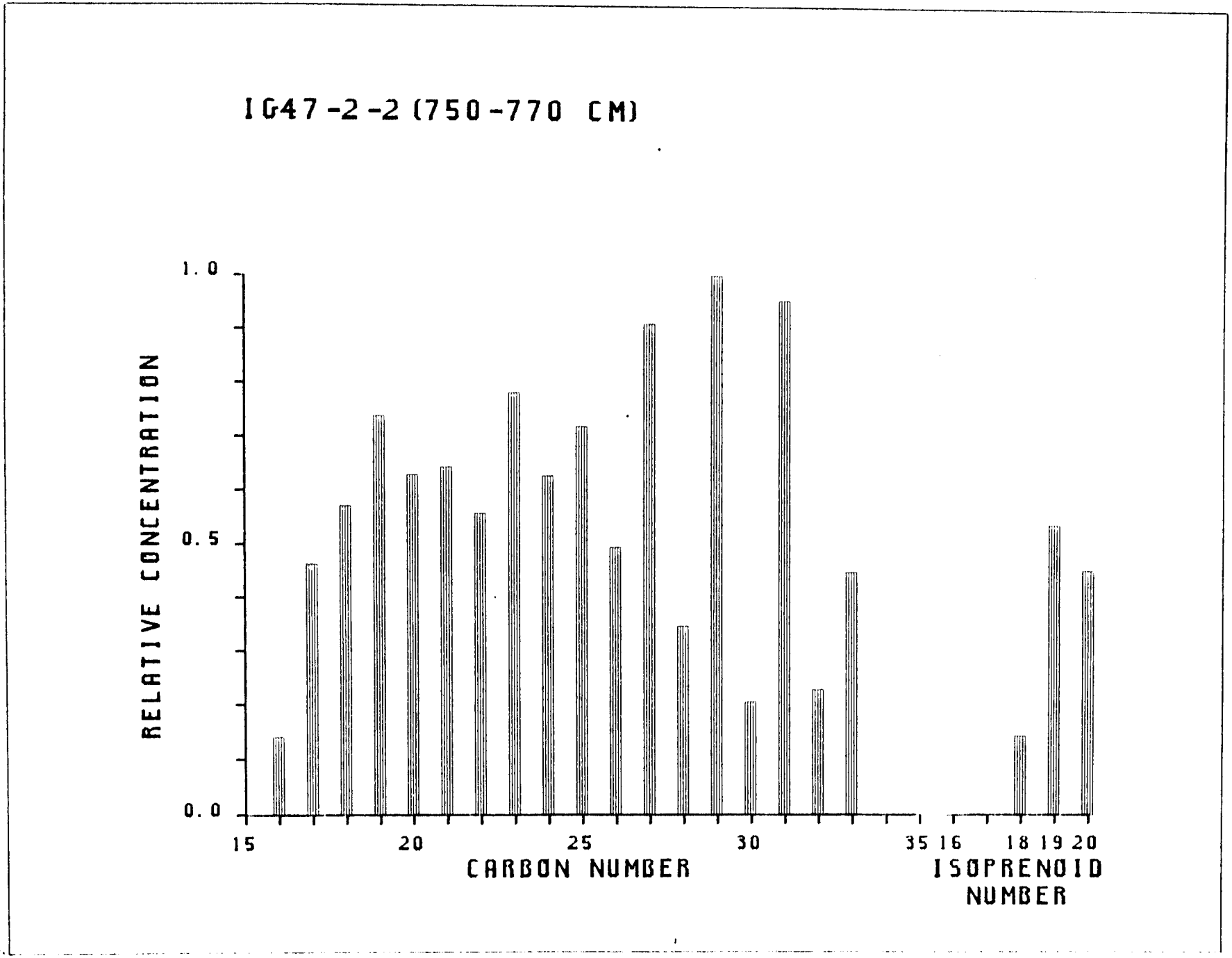
IG47-2-2 (750-770 CM)
RELATIVE CONCENTRATION
1.0
0.5
0.0
15
20
25
30
35
16
18
19
20
CARBON NUMBER
ISOPRENOID NUMBER

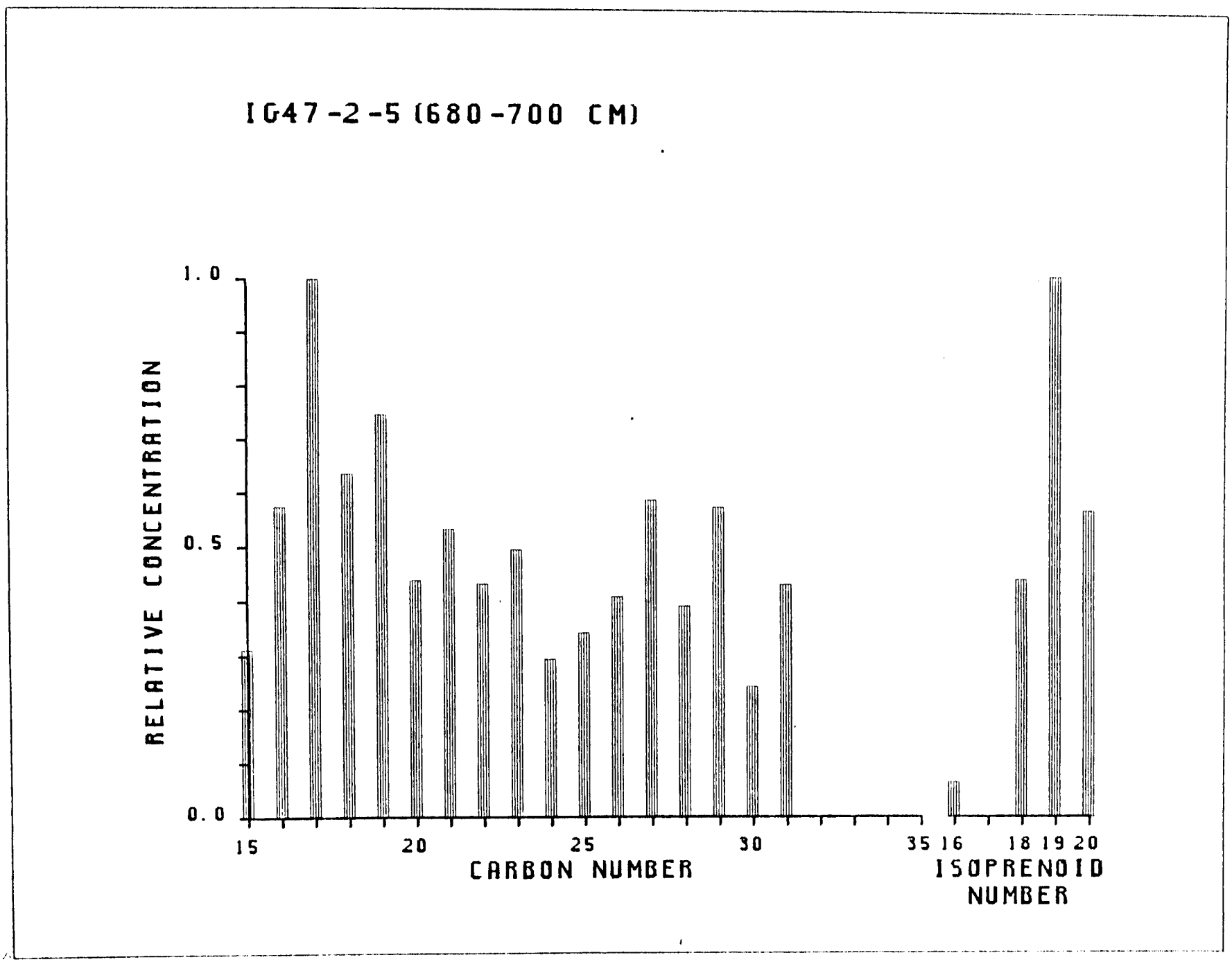
IG47-2-5 (680-700 CM)
1.0
0.5
0.0
RELATIVE CONCENTRATION
15
20
25
30
35
CARBON NUMBER
16
18
19
20
ISOPRENOID NUMBER

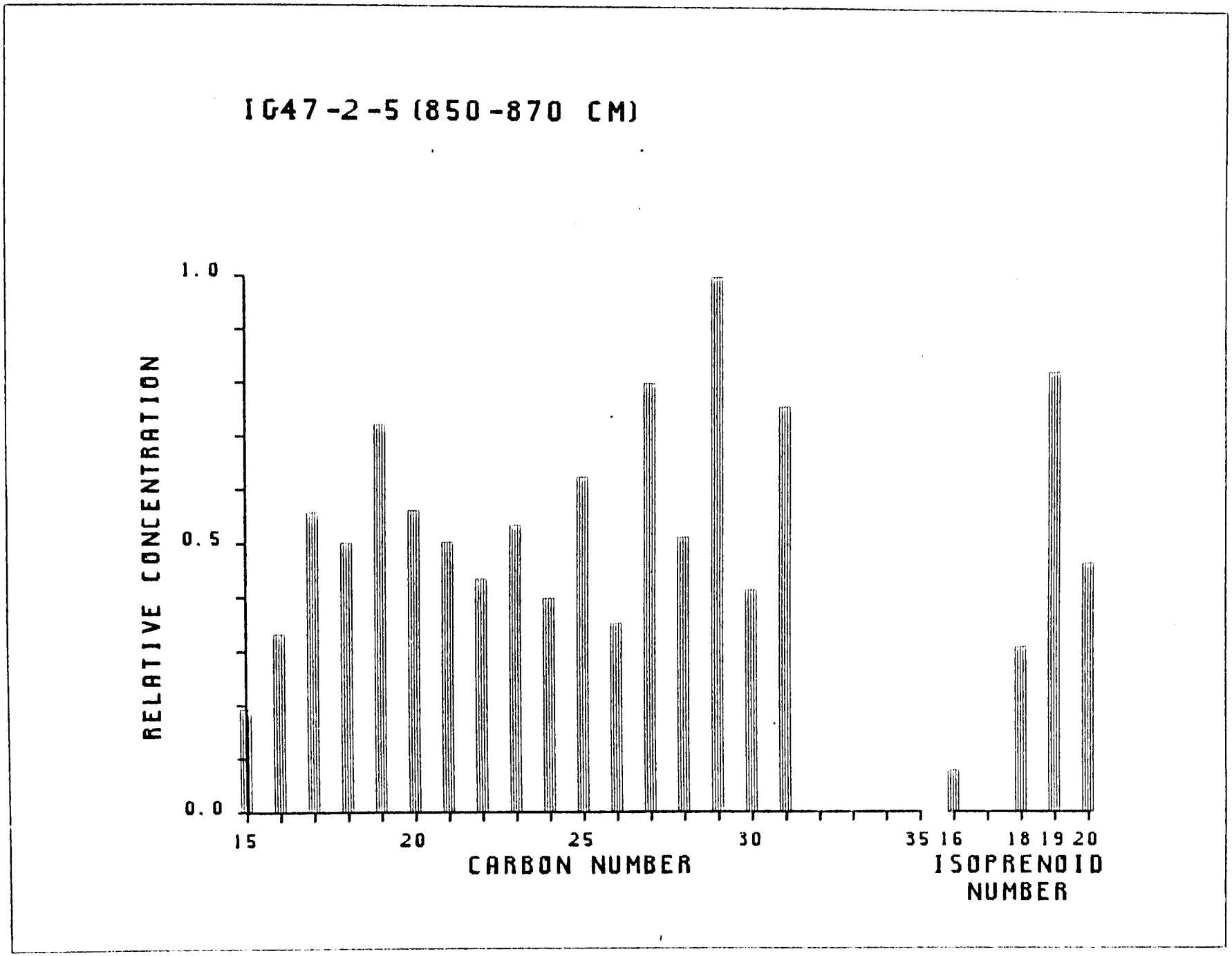
IG47-2-5 (850-870 CM)
RELATIVE CONCENTRATION
1.0
0.5
0.0
15
20
25
30
35
CARBON NUMBER
16
18
19
20
ISOPRENOID NUMBER

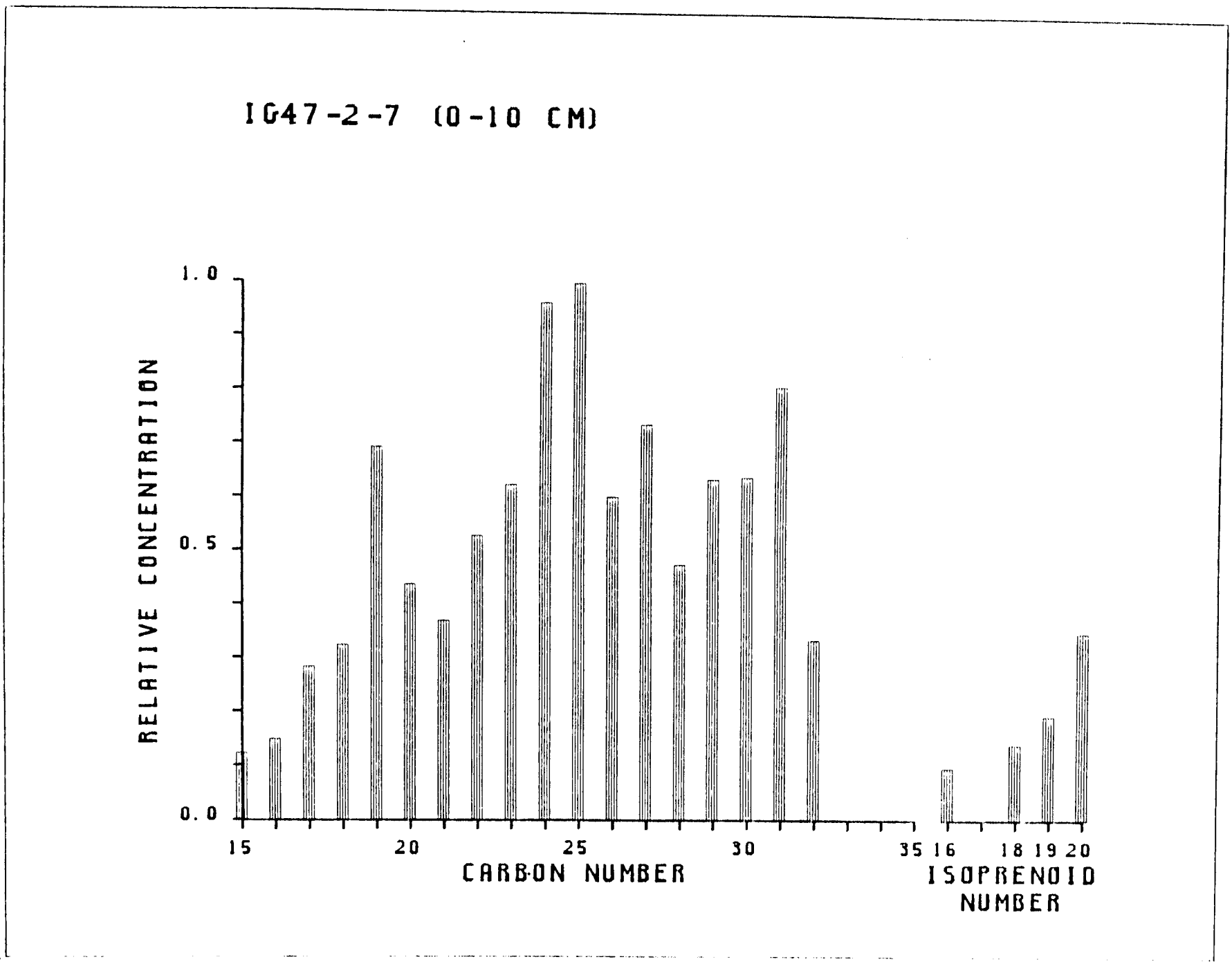
IG47-2-7 (0-10 CM)
1.0
0.5
0.0
RELATIVE CONCENTRATION
15
20
25
30
35
CARBON NUMBER
16
18
19
20
ISOPRENOID NUMBER

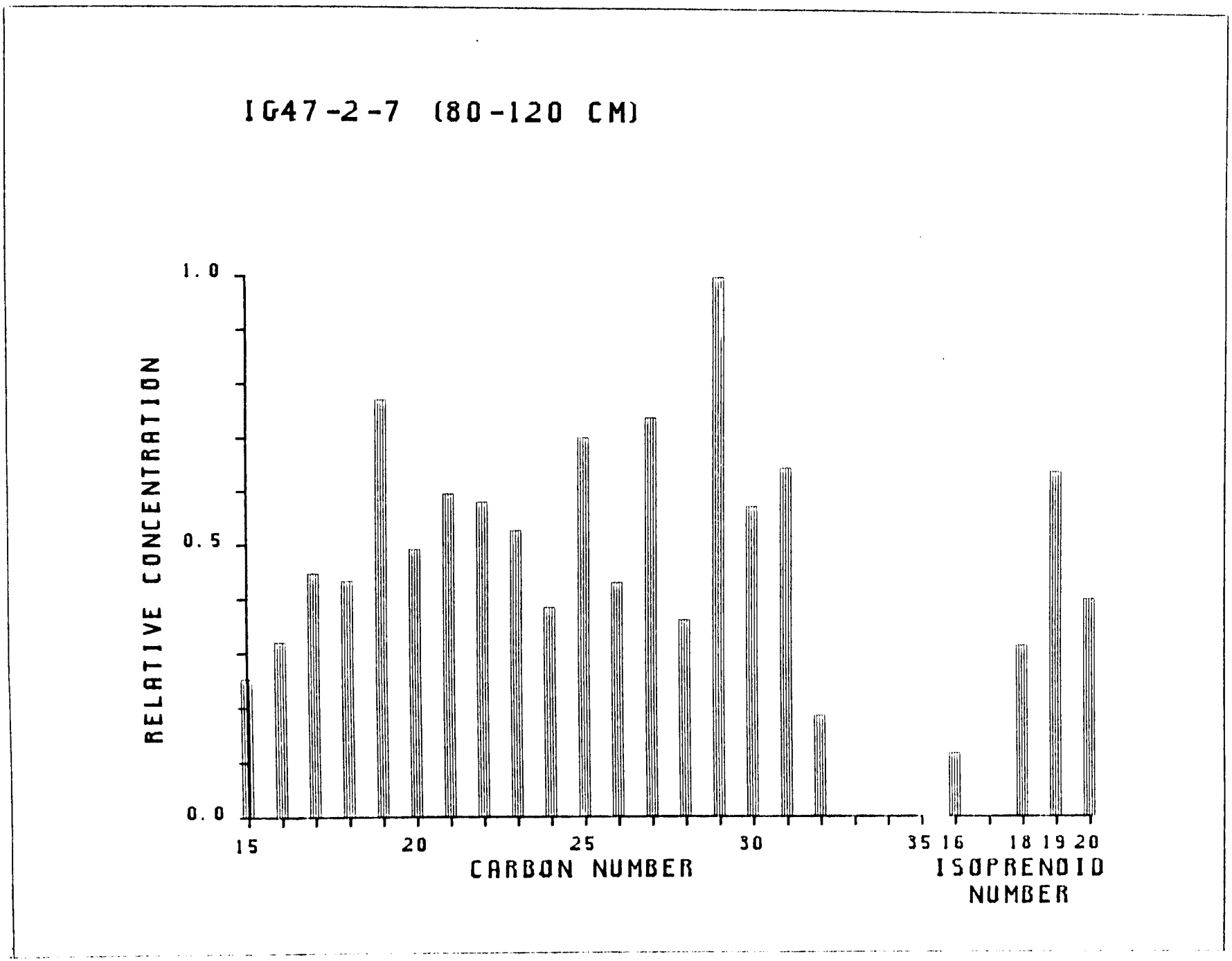
IG47-2-7 (80-120 CM)
RELATIVE CONCENTRATION
1.0
0.5
0.0
15
20
25
30
35
CARBON NUMBER
16
18
19
20
ISOPRENOID NUMBER

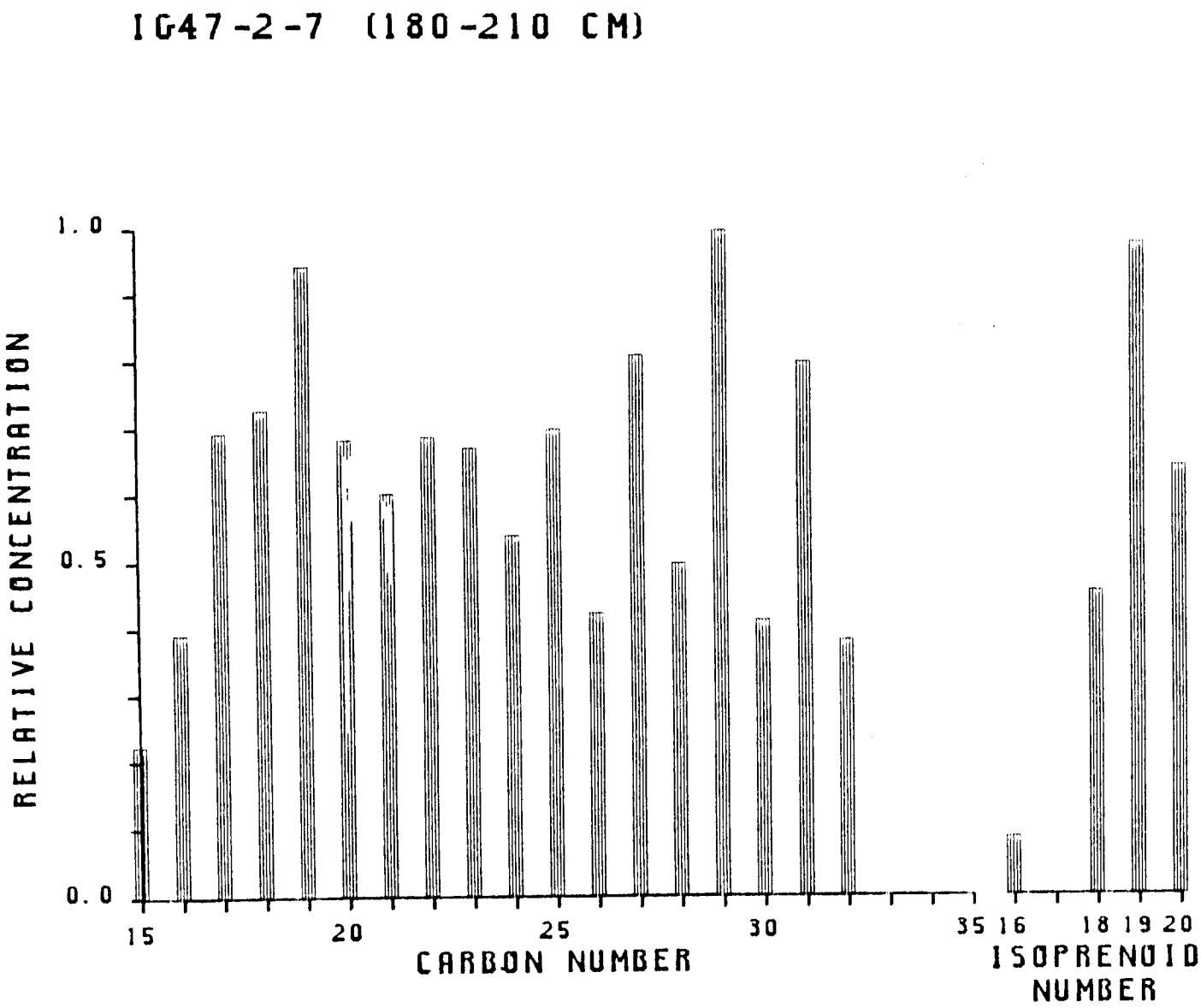
IG47-2-7 (180-210 CM)
1.0
0.5
0.0
RELATIVE CONCENTRATION
15
20
25
30
35
CARBON NUMBER
16
18
19
20
ISOPRENOID NUMBER

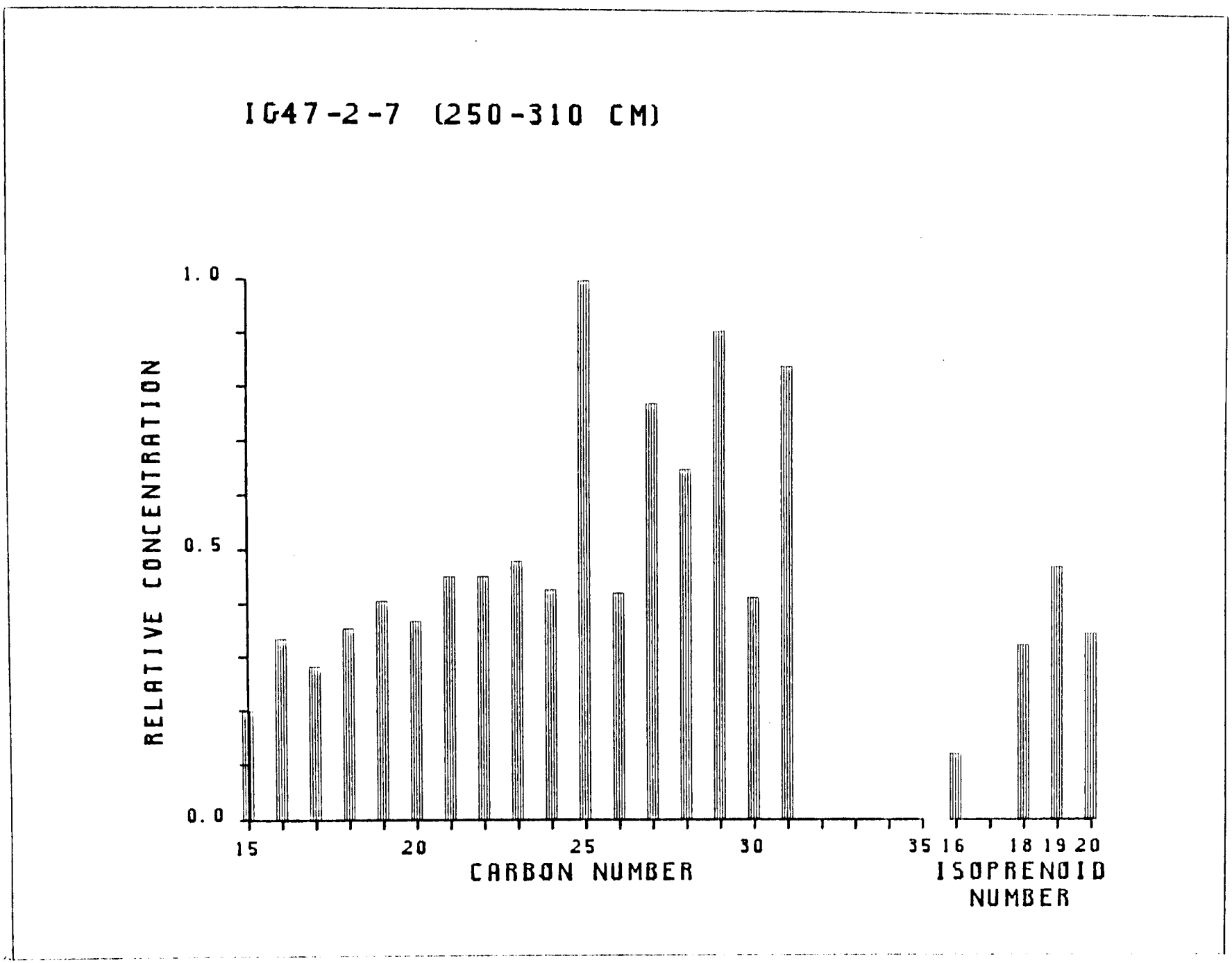
IG47-2-7 (250-310 CM)
1.0
0.5
0.0
RELATIVE CONCENTRATION
15
20
25
30
35
CARBON NUMBER
16
18
19
20
ISOPRENOID NUMBER

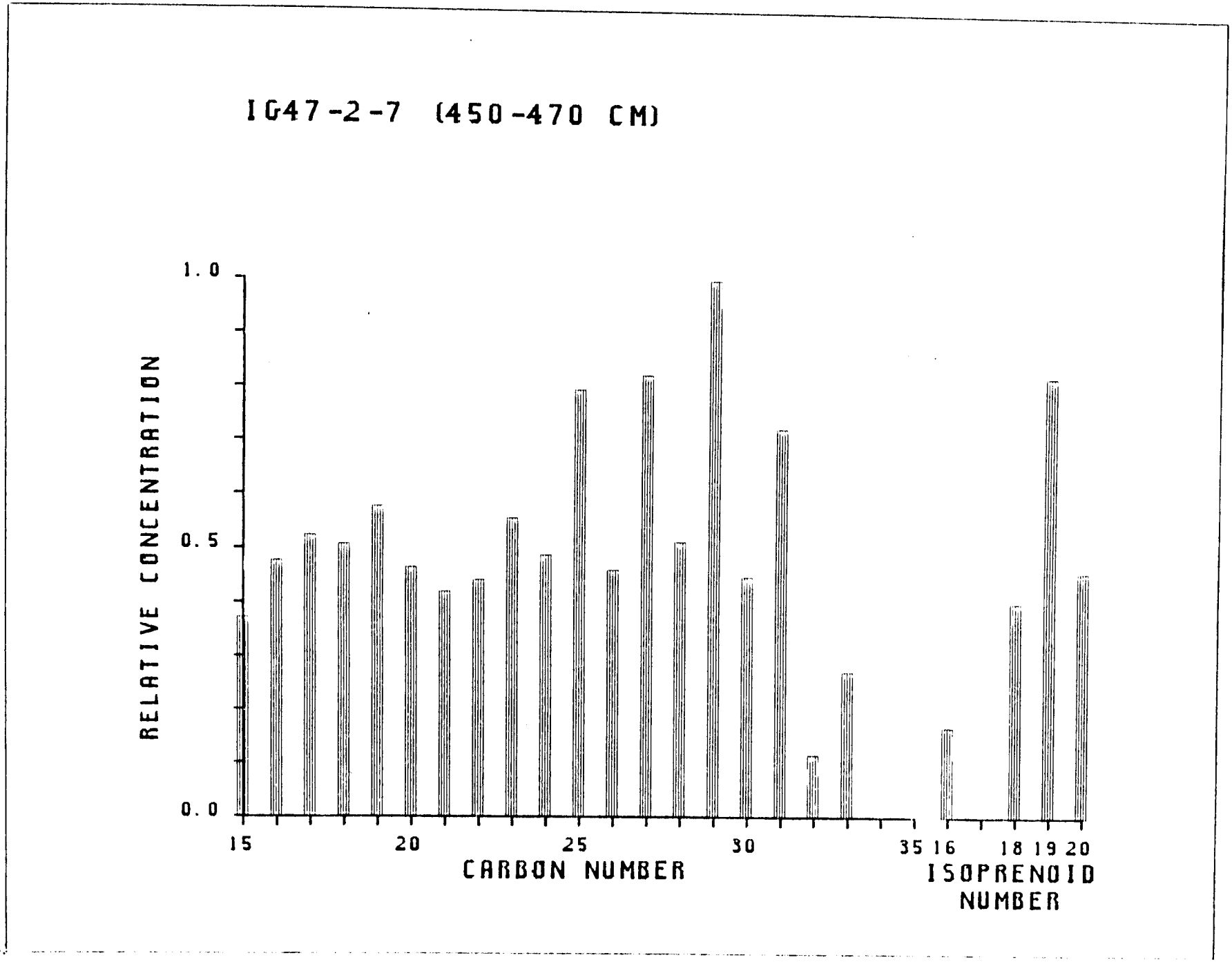
IG47-2-7 (450-470 CM)
RELATIVE CONCENTRATION
1.0
0.5
0.0
15
20
25
30
35
16
18
19
20
CARBON NUMBER
ISOPRENOID NUMBER

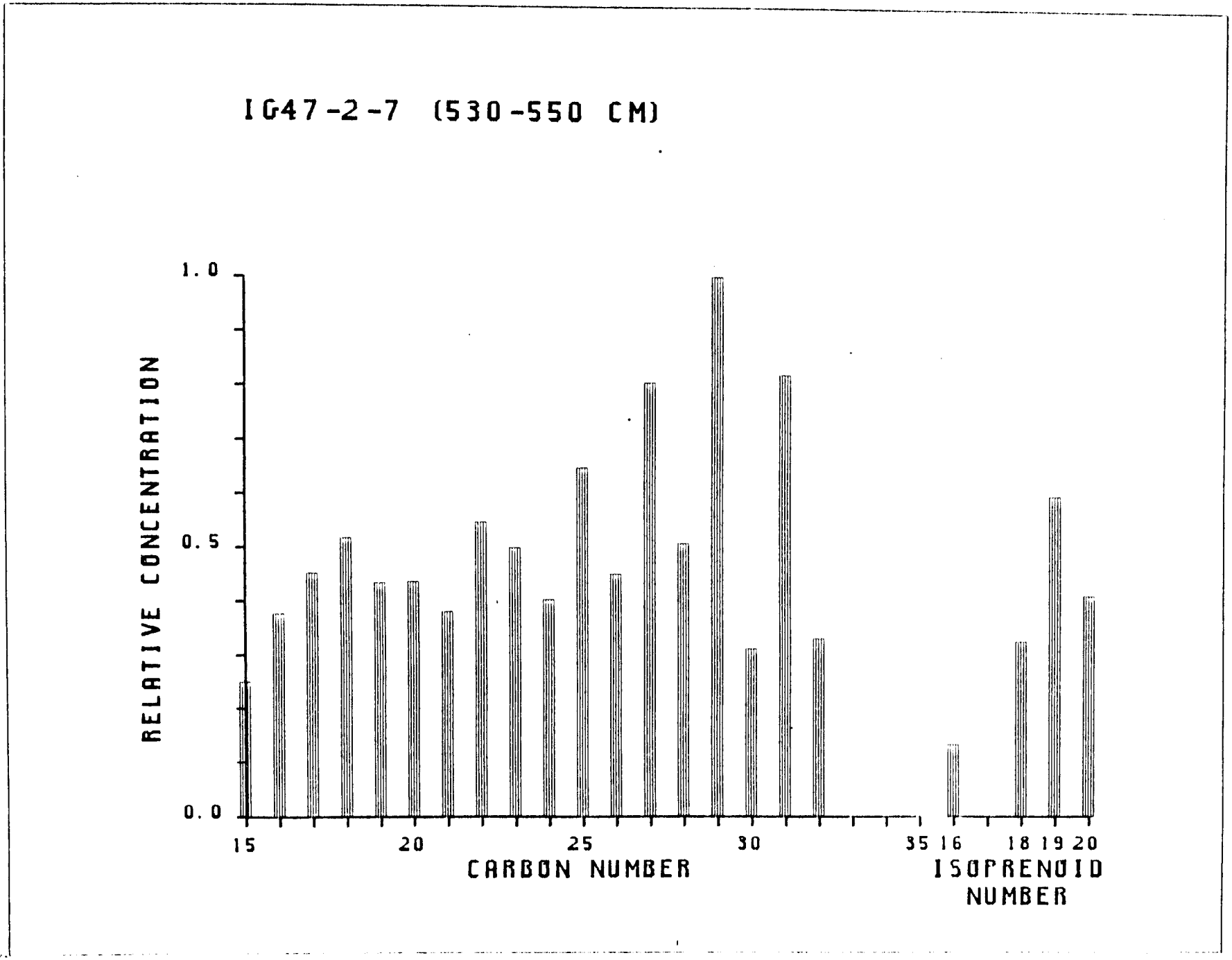
IG47-2-7 (530-550 CM)
1.0
0.5
0.0
RELATIVE CONCENTRATION
15
20
25
30
35
16
18
19
20
CARBON NUMBER
ISOPRENOID NUMBER

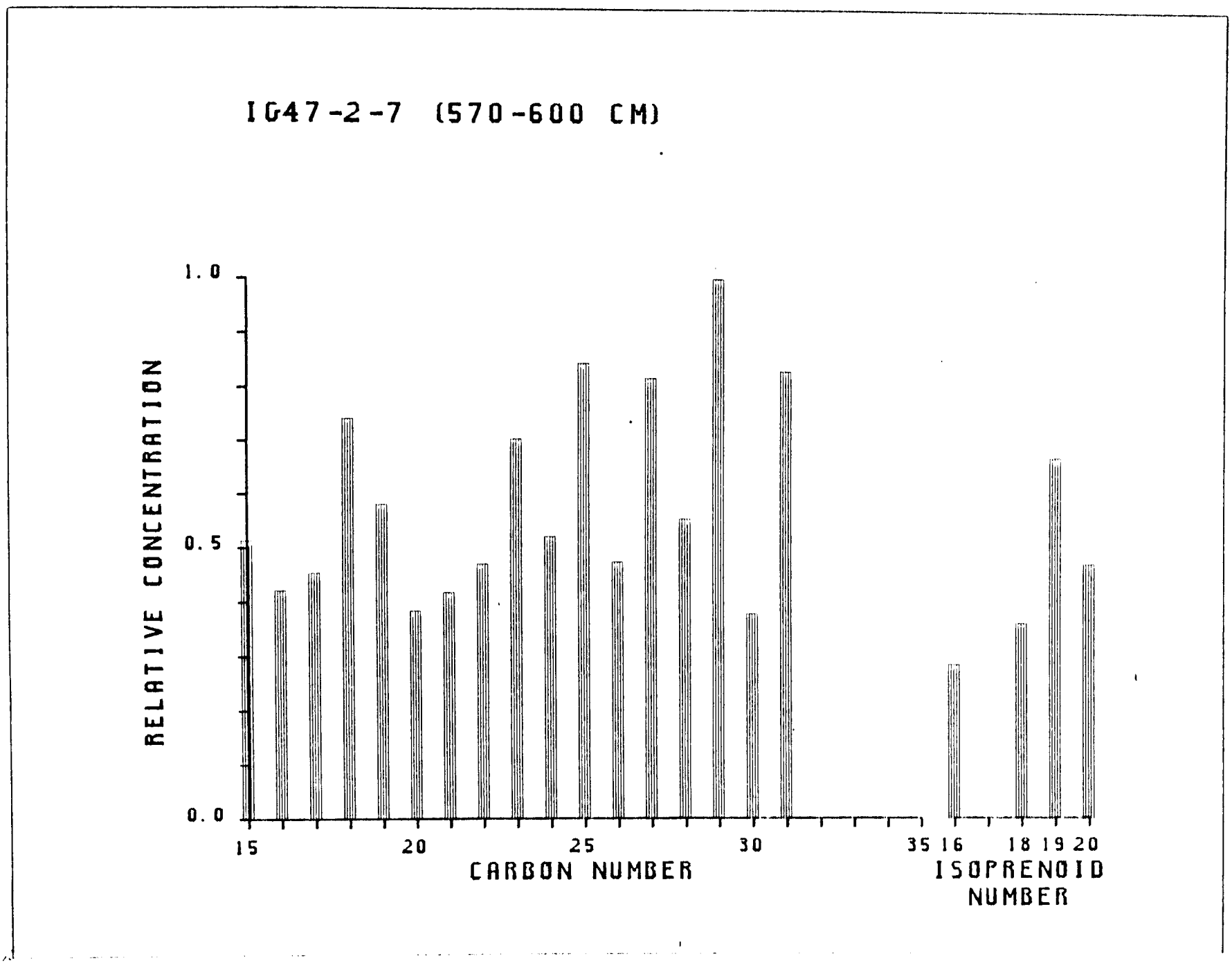
IG47-2-7 (570-600 CM)
1.0
0.5
0.0
RELATIVE CONCENTRATION
15
20
25
30
35
CARBON NUMBER
16
18
19
20
ISOPRENOID NUMBER

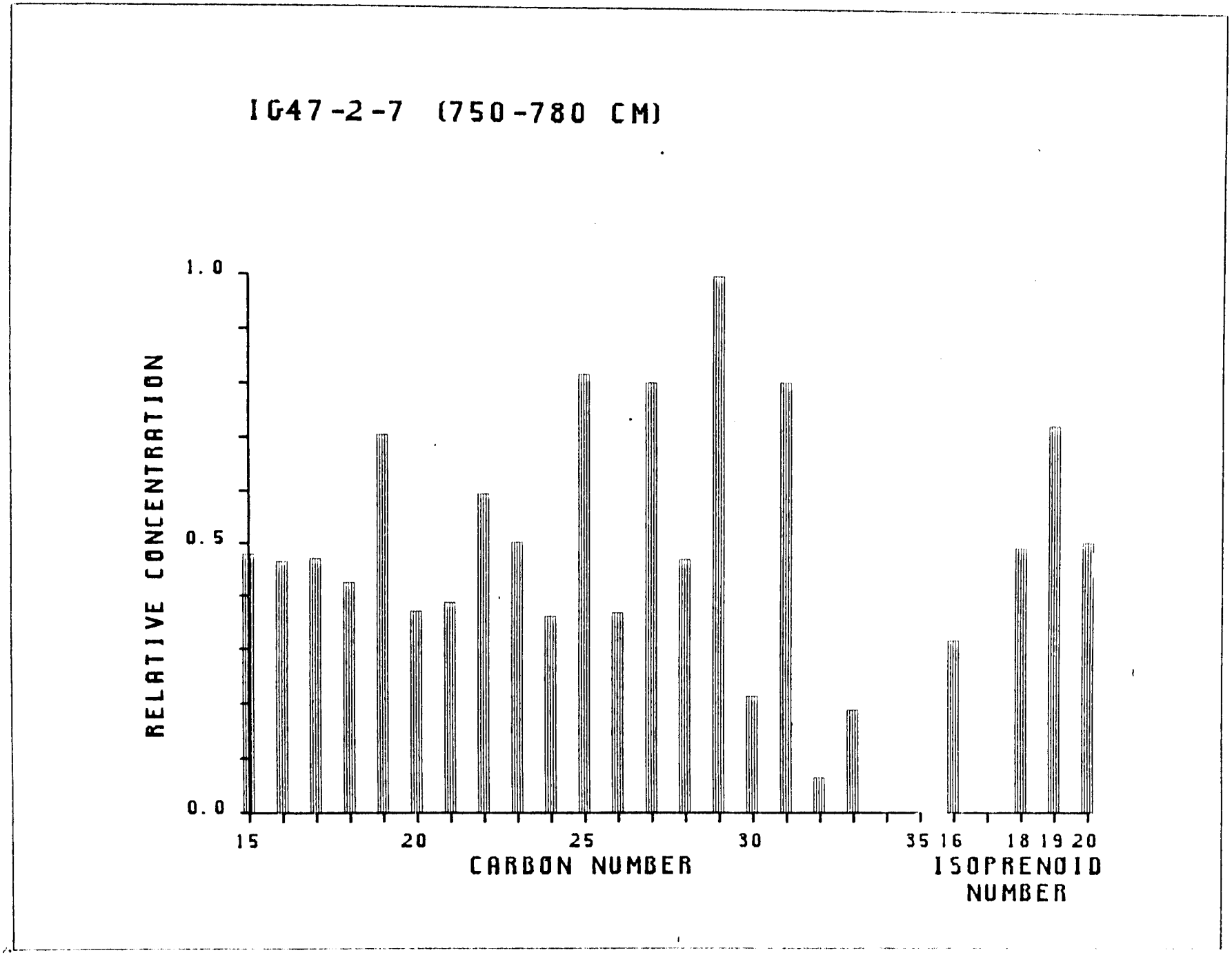
IG47-2-7 (750-780 CM)
RELATIVE CONCENTRATION
1.0
0.5
0.0
15
20
25
30
35
16
18
19
20
CARBON NUMBER
ISOPRENOID NUMBER